ISSN: 2146-1414

MIRT

Molecular Imaging and Radionuclide Therapy

February 2018 Volume 27 Issue 1 www.tsnm.org

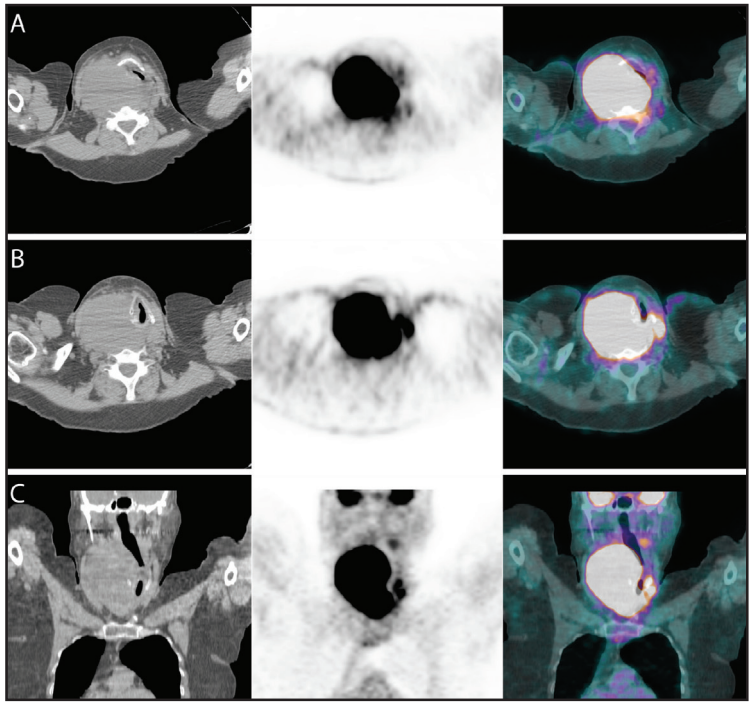

"Official Journal of the Turkish Society of Nuclear Medicine"

galenos yayinevi

TURKISH SOCIETY OF NUCLEAR MEDICINE 1975

MIRT

Molecular Imaging and Radionuclide Therapy

MIRT

Molecular Imaging and Radionuclide Therapy

Turkish Society of Nuclear Medicine
Cinnah Caddesi Pilot Sokak No: 10/12 Çankaya 06650 Ankara, Turkey **Phone:** +90 312 441 00 45 **Fax:** +90 312 441 12 95 **Web:** www.tsnm.org **E-mail:** dernekmerkezi@tsnm.org
"Formerly Turkish Journal of Nuclear Medicine"

The paper used to print this journal conforms to ISO 9706: 1994 standard (Requirements for Permanence). The National Library of Medicine suggests that biomedical publications be printed on acid-free paper (alkaline paper). Reviewing the articles' conformity to the publishing standards of the Journal, typesetting, reviewing and editing the manuscripts and abstracts in English, creating links to source data, and publishing process are realized by Galenos.

Galenos Publishing House Owner and Publisher
Erkan Mor

Publication Director
Nesrin Çolak

Web Coordinators
Soner Yıldırım
Turgay Akpınar

Web Assistant
Büşra Başak Yılmaz

Graphics Department
Ayda Alaca
Çiğdem Birinci

Project Coordinators
Eda Kolukısa
Hatice Balta
Lütfiye Ayhan İrtem
Melis Kuru
Zeynep Altındağ

Project Assistants
Esra Semerci
Günay Selimoğlu
Sedanur Sert

Finance Coordinator
Sevinç Çakmak

Research&Development
Denis Sleptsov

Publisher Contact
Address: Molla Gürani Mah. Kaçamak Sk. No: 21/1
34093 İstanbul, Turkey
Phone: +90 (212) 621 99 25 **Fax:** +90 (212) 621 99 27
E-mail: info@galenos.com.tr/yayin@galenos.com.tr
Web: www.galenos.com.tr

Printing at: Creative Basım Ltd. Şti.
Litros Yolu 2. Matbaacılar Sitesi ZD1 Topkapı, İstanbul, Turkey
Phone: +90 (212) 709 75 25
Printing Date: January 2018
ISSN: 2146-1414 **E-ISSN:** 2147-1959
International scientific journal published quarterly.

MIRT

Molecular Imaging and Radionuclide Therapy

ABOUT US

Molecular Imaging and Radionuclide Therapy (formerly Turkish Journal of Nuclear Medicine) is the official publication of Turkish Society of Nuclear Medicine.

Focus and Scope

Molecular Imaging and Radionuclide Therapy (Mol Imaging Radionucl Ther, MIRT) is a double-blind peer-review journal published in English language. It publishes original research articles, reviews, editorials, short communications, letters, consensus statements, guidelines and case reports with a literature review on the topic, interesting images in the field of molecular imaging, multimodality imaging, nuclear medicine, radionuclide therapy, radiopharmacy, medical physics, dosimetry and radiobiology. MIRT is published three times a year (February, June, October). Audience: Nuclear medicine physicians, medical physicists, radiopharmaceutical scientists, radiobiologists.

The editorial policies are based on the "Recommendations for the Conduct, Reporting, Editing, and Publication of Scholarly Work in Medical Journals (ICMJE Recommendations)" by the International Committee of Medical Journal Editors (2016, archived at http://www.icmje.org/) rules.

Open Access Policy

This journal provides immediate open access to its content on the principle that making research freely available to the public supports a greater global exchange of knowledge.

Open Access Policy is based on rules of Budapest Open Access Initiative (BOAI) (http://www.budapestopenaccessinitiative.org/). By "open access" to [peer-reviewed research literature], we mean its free availability on the public internet, permitting any users to read, download, copy, distribute, print, search, or link to the full texts of these articles, crawl them for indexing, pass them as data to software, or use them for any other lawful purpose, without financial, legal, or technical barriers other than those inseparable from gaining access to the internet itself. The only constraint on reproduction and distribution, and the only role for copyright in this domain, should be to give authors control over the integrity of their work and the right to be properly acknowledged and cited.

Permission Requests

Instructions for Authors

Instructions for authors are published in the journal and on the website http://mirt.tsnmjournals.org

Manuscripts can only be submitted electronically through the Journal Agent website (http://www.journalagent.com/mirt/?plng=eng) after creating an account. This system allows online submission and review.

All published volumes in full text can be reached free of charge through the website http://mirt.tsnmjournals.org

Material Disclaimer

Scientific and legal responsibilities pertaining to the papers belong to the authors. Contents of the manuscripts and accuracy of references are also the author's responsibility. The Turkish Society of Nuclear Medicine, the Editor, the Editorial Board or the publisher do not accept any responsibility for opinions expressed in articles.

Financial expenses of the journal are covered by Turkish Society of Nuclear Medicine.

Correspondence Address

Editor-in-Chief, Prof. Zehra Özcan, MD,

Ege University, Medical School, Department of Nuclear Medicine, İzmir, Turkey

Phone: +90 312 441 00 45

Fax: +90 312 441 12 97

E-mail: editor@tsnmjournals.org

Web page: http://mirt.tsnmjournals.org

Publisher Corresponding Address

Galenos Yayınevi Tic. Ltd. Şti.

Address: Molla Gürani Mah. Kaçamak Sk. No: 21/1 34093

Fındıkzade, İstanbul, Turkey

Phone: +90 212 621 99 25

Fax: +90 212 621 99 27

E-mail: info@galenos.com.tr

The journal is printed on an acid-free paper.

MIRT

Molecular Imaging and Radionuclide Therapy

INSTRUCTIONS TO AUTHORS

Molecular Imaging and Radionuclide Therapy (Mol Imaging Radionucl Ther, MIRT) publishes original research articles, short communications, reviews, editorials, case reports with a literature review on the topic, interesting images, consensus statements, guidelines, letters in the field of molecular imaging, multimodality imaging, nuclear medicine, radionuclide therapy, radiopharmacy, medical physics, dosimetry and radiobiology. MIRT is published by the Turkish Society of Nuclear Medicine three times a year (February, June, October). The journal is printed on an acid-free paper.

Molecular Imaging and Radionuclide Therapy does not charge any article submission or processing fees.

GENERAL INFORMATION

MIRT commits to rigorous peer review, and stipulates freedom from commercial influence, and promotion of the highest ethical and scientific standards in published articles. Neither the Editor(s) nor the publisher guarantees, warrants or endorses any product or service advertised in this publication. All articles are subject to review by the editors and peer reviewers. If the article is accepted for publication, it may be subjected to editorial revisions to aid clarity and understanding without changing the data presented.

Manuscripts must be written in English and must meet the requirements of the journal. The journal is in compliance with the uniform requirements for manuscripts submitted to biomedical journals published by the International Committee of Medical Journal Editors (NEJM 1997; 336:309-315, updated 2016). Manuscripts that do not meet these requirements will be returned to the author for necessary revision before the review. Authors of manuscripts requiring modifications have a maximum of two months to resubmit the revised text. Manuscripts returned after this deadline will be treated as new submissions.

It is the authors' responsibility to prepare a manuscript that meets ethical criteria. The Journal adheres to the principles set forth in the Helsinki Declaration October 2013 (https://www.wma.net/policies-post/wma-declaration-of-helsinki-ethical-principles-for-medical-research-involving-human-subjects/) and holds that all reported research involving "Human beings" conducted in accordance with such principles.

Reports describing data obtained from research conducted in human participants must contain a statement in the MATERIALS AND METHODS section indicating approval by the ethical review board (including the approval number) and affirmation that INFORMED CONSENT was obtained from each participant.

All manuscripts reporting experiments using animals must include a statement in the MATERIALS AND METHODS section giving assurance that all animals have received humane care in compliance with the Guide for the Care and Use of Laboratory Animals (www.nap.edu) and indicating approval by the ethical review board.

If the study should have ethical approval, authors asked to provide ethical approval in order to proceed the review process. If they provide approval, review of the manuscript will continue.

In case report(s) and interesting image(s) a statement regarding the informed consent of the patients should be included in the manuscript and the identity of the patient(s) should be hidden.

Subjects must be identified only by number or letter, not by initials or names. Photographs of patients' faces should be included only if scientifically relevant. Authors must obtain written consent from the patient for use of such photographs.

In cases of image media usage that potentially expose patients' identity requires obtaining permission for publication from the patients or their parents/guardians.

If the proposed publication concerns any commercial product, the author must include in the cover letter a statement indicating that the author(s) has (have) no financial or other interest with the product or explaining the nature of any relations (including consultancies) between the author(s) and editor the manufacturer or distributor of the product.

All submissions will be screened by Crossref Smilarity Check powered by "iThenticate". Manuscripts with an overall similarity index of greater than 25%, or duplication rate at or higher than 5% with a single source will be returned back to authors.

MANUSCRIPT CATEGORIES

1. Original Articles

2. Short Communications are short descriptions of focused studies with important, but very straightforward results.

3. Reviews address important topics in the field. Authors considering the submission of uninvited reviews should contact the editor in advance to determine if the topic that they propose is of current potential interest to the Journal. Reviews will be considered for publication only if they are written by authors who have at least three published manuscripts in the international peer reviewed journals and these studies should be cited in the review. Otherwise only invited reviews will be considered for peer review from qualified experts in the area.

4. Editorials are usually written by invitation of the editor by the editors on current topics or by the reviewers involved in the evaluation of a submitted manuscript and published concurrently with that manuscript.

5. Case Report and Literature Reviews are descriptions of a case or small number of cases revealing a previously undocumented disease process, a unique unreported manifestation or treatment of a known disease process, unique unreported complications of treatment regimens or novel and important insights into a condition's pathogenesis, presentation, and/or management. The journal's policy is to accept case reports only if it is accompanied by a review of the literature on the related topic. They should include an adequate number of images and figures.

6. Interesting Image

One of the regular parts of Molecular Imaging and Radionuclide Therapy is a section devoted to interesting images. Interesting image(s) should describe case(s) which are unique and include interesting findings adding insights into the interpretation of patient images, a condition's pathogenesis, presentation, and/or management.

7. Consensus Statements or Guidelines may be submitted by professional societies. All such submissions will be subjected to peer review, must be modifiable in response to criticisms, and will be published only if they meet the Journal's usual editorial standards.

8. Letters to the Editor may be submitted in response to work that has been published in the Journal. Letters should be short commentaries related to specific points of agreement or disagreement with the published work.

Note on Prior Publication

Articles are accepted for publication on the condition that they are original, are not under consideration by another journal, or have not been previously

MIRT
Molecular Imaging and Radionuclide Therapy

published. Direct quotations, tables, or illustrations that have appeared in copyrighted material must be accompanied by written permission for their use from the copyright owner and authors. Materials previously published in whole or in part shall not be considered for publication. At the time of submission, authors must report that the manuscript has not been published elsewhere. Abstracts or posters displayed at scientific meetings need not be reported.

MANUSCRIPT SUBMISSION PROCEDURES

MIRT only accepts electronic manuscript submission at the web site http://www.journalagent.com/mirt/. After logging on to the website Click the 'online manuscript submission' icon. All corresponding authors should be provided with a password and a username after entering the information required. If you already have an account from a previous submission, enter your username and password to submit a new or revised manuscript. If you have forgotten your username and/or password, please send an e-mail to the editorial office for assistance. After logging on to the article submission system please read carefully the directions of the system to give all needed information and attach the manuscript, tables and figures and additional documents.

All Submissions Must Include:

1. Completed Copyright Assignment & Disclosure of Potential Conflict of Interest Form; This form should be downloaded from the website (provided in the author section), filled in thoroughly and uploaded to the website during the submission.
2. All manuscripts describing data obtained from research conducted in human participants must be accompanied with an approval document by the ethical review board.
3. All manuscripts reporting experiments using animals must include approval document by the animal ethical review board.
4. All submissions must include the authorship contribution form which is signed by all authors.

Authors must complete all online submission forms. If you are unable to successfully upload the files please contact the editorial office by e-mail.

MANUSCRIPT PREPARATION

General Format

The Journal requires that all submissions be submitted according to these guidelines:

- Text should be double spaced with 2.5 cm margins on both sides using 12-point type in Times Roman font.
- All tables and figures must be placed after the text and must be labeled.
- Each section (abstract, text, references, tables, figures) should start on a separate page.
- Manuscripts should be prepared as a word document (*.doc) or rich text format (*.rtf).
- Please make the tables using the table function in Word.
- Abbreviations should be defined in parenthesis where the word is first mentioned and used consistently thereafter.
- Results should be expressed in metric units. Statistical analysis should be done accurately and with precision. Please consult a statistician if necessary.
- Authors' names and institutions should not be included in the manuscript text and should be written only in the title page.

Title Page

The title page should be a separate form from the main text and should include the following:

- Full title (in English and in Turkish). Turkish title will be provided by the editorial office for the authors who are not Turkish speakers.
- Authors' names and institutions.
- Short title of not more than 40 characters for page headings.
- At least three and maximum eight keywords. (in English and in Turkish). Do not use abbreviations in the keywords. Turkish keywords will be provided by the editorial office for the authors who are not Turkish speakers. If you are not a native Turkish speaker, please reenter your English keywords to the area provided for the Turkish keywords. English keywords should be provided from http://www.nlm.nih.gov/mesh (Medical Subject Headings) while Turkish keywords should be provided from http://www.bilimterimleri.com.
- Word count (excluding abstract, figure legends and references).
- Corresponding author's e-mail and address, telephone and fax numbers.
- Name and address of person to whom reprint requests should be addressed.

Original Articles

Authors are required to state in their manuscripts that ethical approval from an appropriate committee and informed consents of the patients were obtained.

Original Articles should be submitted with a structured abstract of no more than 250 words. All information reported in the abstract must appear in the manuscript. The abstract should not include references. Please use complete sentences for all sections of the abstract. Structured abstract should include background, objective, methods, results and conclusions. Turkish abstract will be provided by the editorial office for the authors who are not Turkish speakers. If you are not a native Turkish speaker, please reenter your English abstract to the area provided for the Turkish abstract.

- Introduction
- Materials and Methods
- Results
- Discussion
- Study Limitations
- Conclusion

May be given for contributors who are not listed as authors, or for grant support of the research.

References should be cited in numerical order (in parentheses) in the text and listed in the same numerical order at the end of the manuscript on a separate page or pages. The author is responsible for the accuracy of references. Examples of the reference style are given below. Further examples will be found in the articles describing the Uniform Requirements for Manuscripts Submitted to Biomedical Journals (Ann Intern Med.1988; 208:258-265, Br Med J. 1988; 296:401-405). The titles of journals should be abbreviated according to the style used in the Index Medicus. Journal Articles and Abstracts: Surnames and initials of author's name, title of the article, journal name, date, volume number, and pages. All authors should be listed regardless of number. The citation of unpublished papers, observations or personal communications is not permitted. Citing an abstract is

not recommended. Books: Surnames and initials of author's names, chapter title, editor's name, book title, edition, city, publisher, date and pages.

Sample References

Journal Article: Sayit E, Söylev M, Capa G, Durak I, Ada E, Yilmaz M. The role of technetium-99m-HMPAO-labeled WBC scintigraphy in the diagnosis of orbital cellulitis. Ann Nucl Med 2001;15:41-44.

Erselcan T, Hasbek Z, Tandogan I, Gumus C, Akkurt I. Modification of Diet in Renal Disease equation in the risk stratification of contrast induced acute kidney injury in hospital inpatients. Nefrologia 2009 doi: 10.3265/Nefrologia.2009.29.5.5449.en.full.

Article in a journal published ahead of print: Ludbrook J. Musculovenous pumps in the human lower limb. Am Heart J 2009;00:1-6. (accessed 20 February 2009).

Lang TF, Duryea J. Peripheral Bone Mineral Assessment of the Axial Skeleton: Technical Aspects. In: Orwoll ES, Bliziotes M (eds). Osteoporosis: Pathophsiology and Clinical Management. New Jersey, Humana Pres Inc, 2003;83-104.

Books: Greenspan A. Orthopaedic Radiology a Pratical Approach. 3th ed. Philadelphia, Lippincott Williams Wilkins 2000, 295-330.

Website: Smith JR. 'Choosing Your Reference Style', Online Referencing 2(3), http://orj.sagepub.com (2003, accessed October 2008).

- Tables

Tables must be constructed as simply as possible. Each table must have a concise heading and should be submitted on a separate page. Tables must not simply duplicate the text or figures. Number all tables in the order of their citation in the text. Include a title for each table (a brief phrase, preferably no longer than 10 to 15 words). Include all tables in a single file following the manuscript.

– Figure Legends

Figure legends should be submitted on a separate page and should be clear and informative.

– Figures

Number all figures (graphs, charts, photographs, and illustrations) in the order of their citation in the text. At submission, the following file formats are acceptable: AI, EMF, EPS, JPG, PDF, PPT, PSD, TIF. Figures may be embedded at the end of the manuscript text file or loaded as separate files for submission. All images MUST be at or above intended display size, with the following image resolutions: Line Art 800 dpi, Combination (Line Art + Halftone) 600 dpi, Halftone 300 dpi. Image files also must be cropped as close to the actual image as possible.

Short Communications:

Short communications should be submitted with a structured abstract of no more than 200 words. These manuscripts should be no longer than 2000 words, and include no more than two figures and tables and 20 references. Other rules which the authors are required to prepare and submit their manuscripts are the same as described above for the original articles.

Review Articles:

- Title page (see above)
- Abstract: Maximum 250 words; without structural divisions; in English and in Turkish . Turkish abstract will be provided by the editorial office for the authors who are not Turkish speakers. If you are not a native Turkish speaker, please reenter your English abstract to the area provided for the Turkish abstract.
- Text
- Conclusion
- Acknowledgements (if any)
- References

Editorial:

- Title page (see above)
- Abstract: Maximum 250 words; without structural divisions; in English and in Turkish. Turkish abstract will be provided by the editorial office for the authors who are not Turkish speakers. If you are not a native Turkish speaker, please re enter your English abstract to the area provided for the Turkish abstract.
- Text
- References

Case Report and Literature Review

- Title page (see above)
- Abstract: Approximately 100-150 words; without structural divisions; in English and in Turkish. Turkish abstract will be provided by the editorial office for the authors who are not Turkish speakers. If you are not a native Turkish speaker, please re-enter your English abstract to the area provided for the Turkish abstract.
- Introduction
- Case report
- Literature Review and Discussion
- References

Interesting Image:

No manuscript text is required. Interesting Image submissions must include the following:

Title Page: (see Original article section)

Abstract: Approximately 100-150 words; without structural divisions; in English and in Turkish. Turkish abstract will be provided by the editorial office for the authors who are not Turkish speakers. If you are not a native Turkish speaker, please re-enter your English abstract to the area provided for the Turkish abstract.

Image(s): The number of images is left to the discretion of the author. (See Original article section)

Figure Legend: Reference citations should appear in the legends, not in the abstract. Since there is no manuscript text, the legends for illustrations should be prepared in considerable detail but should be no more than 500 words total. The case should be presented and discussed in the Figure legend section.

References: Maximum eight references (see original article section).

Letters to the Editor:

- Title page (see above)
- Short comment to a published work, no longer than 500 words, no figures or tables.
- References no more than five.

Consensus Statements or Guidelines: These manuscripts should typically be no longer than 4000 words and include no more than six figures and tables and 120 references.

MIRT
Molecular Imaging and Radionuclide Therapy

INSTRUCTIONS TO AUTHORS

Proofs and Reprints

Proofs and a reprint orders are sent to the corresponding author. The author should designate by footnote on the title page of the manuscript the name and address of the person to whom reprint requests should be directed. The manuscript when published will become the property of the journal.

Archiving

The editorial office will retain all manuscripts and related documentation (correspondence, reviews, etc.) for 12 months following the date of publication or rejection.

Submission Preparation Checklist

As part of the submission process, authors are required to check off their submission's compliance with all of the following items, and submissions may be returned to authors that do not adhere to these guidelines.

1. The submission has not been previously published, nor is it before another journal for consideration (or an explanation has been provided in Comments to the Editor).
2. The submission file is in Microsoft Word, RTF, or WordPerfect document file format. The text is double-spaced; uses a 12-point font; employs italics, rather than underlining (except with URL addresses); and the location for all illustrations, figures, and tables should be marked within the text at the appropriate points.
3. Where available, URLs for the references will be provided.
4. All authors should be listed in the references, regardless of the number.
5. The text adheres to the stylistic and bibliographic requirements outlined in the Author Guidelines, which is found in About the Journal.
6. English keywords should be provided from http://www.nlm.nih.gov/mesh(Medical Subject Headings), while Turkish keywords should be provided fromhttp://www.bilimterimleri.com
7. The title page should be a separate document from the main text and should be uploaded separately.
8. The "Affirmation of Originality and Assignment of Copyright/The Disclosure Form for Potential Conflicts of Interest Form" and Authorship Contribution Form should be downloaded from the website, filled thoroughly and uploaded during the submission of the manuscript.

TO AUTHORS

Copyright Notice

The author(s) hereby affirms that the manuscript submitted is original, that all statement asserted as facts are based on author(s) careful investigation and research for accuracy, that the manuscript does not, in whole or part, infringe any copyright, that it has not been published in total or in part and is not being submitted or considered for publication in total or in part elsewhere. Completed Copyright Assignment & Affirmation of Originality Form will be uploaded during submission. By signing this form;

1. Each author acknowledges that he/she participated in the work in a substantive way and is prepared to take public responsibility for the work.
2. Each author further affirms that he or she has read and understands the "Ethical Guidelines for Publication of Research".
3. The author(s), in consideration of the acceptance of the manuscript for publication, does hereby assign and transfer to the Molecular Imaging and Radionuclide Therapy all of the rights and interest in and the copyright of the work in its current form and in any form subsequently revised for publication and/or electronic dissemination.

Privacy Statement

The names and email addresses entered in this journal site will be used exclusively for the stated purposes of this journal and will not be made available for any other purpose or to any other party.

Peer Review Process

1. The manuscript is assigned to an editor, who reviews the manuscript and makes an initial decision based on manuscript quality and editorial priorities.
2. For those manuscripts sent for external peer review, the editor assigns at least two reviewers to the manuscript.
3. The reviewers review the manuscript.
4. The editor makes a final decision based on editorial priorities, manuscript quality, and reviewer recommendations.
5. The decision letter is sent to the author.

Contact Address

All correspondence should be directed to the Editorial Office:
Cinnah Caddesi Pilot Sokak No:10/12 06650 Çankaya / Ankara, Turkey
Phone: +90 312 441 00 45
Fax: +90 312 441 12 97
E-mail: info@tsnmjournals.org

MIRT
Molecular Imaging and Radionuclide Therapy

CONTENTS

MIRT
Molecular Imaging and Radionuclide Therapy

CONTENTS

Türkiye
Nükleer Tıp
Derneği

30 yıl
KARARLI ve BİRLİKTE

ULUSAL NÜKLEER TIP KONGRESİ

Gloria Kongre Merkezi
Belek, Antalya

11 - 15 Nisan 2018

BİLİMSEL SEKRETERYA

Türkiye Nükleer Tıp Derneği
Cinnah Cad. Pilot Sok. No:10/12
06690 Çankaya - ANKARA
T: 0 (312) 441 00 45
GSM: 0 535 047 20 73
F: 0 (312) 441 12 97
E-posta:dernekmerkezi@tsnm.org
Web: www.tsnm.org

SERENAS ULUSLARARASI TURİZM KONGRE ORGANİZASYON A.Ş.
Hilal Mh. Cezayir Cd.
No:13, 06550 Yıldız,
Çankaya - ANKARA
T: +90 (312) 440 50 11
F: +90 (312) 441 45 64
E-posta: info@untk2018.org
Web: www.serenas.com.tr

Editorial
Mol Imaging Radionucl Ther 2018;27:1-2 DOI:10.4274/mirt.30502

The Evolving Role of Nuclear Medicine and Molecular Imaging: Theranostics and Personalized Therapeutic Applications

Nükleer Tıp ve Moleküler Görüntülemenin Gelişen Rolü: Teranostikler ve Kişiselleştirilmiş Tedavi Uygulamaları

M. Fani Bozkurt[1], Zehra Özcan[2]
[1]Hacettepe University Medical School, Department of Nuclear Medicine, Ankara, Turkey
[2]Ege University Medical School, Department of Nuclear Medicine, İzmir, Turkey

During the last decade, there have been excellent and very rapid advances in "Nuclear Medicine and Molecular Imaging" throughout the world. The developments in radiopharmaceuticals induced evolution of nuclear medicine from imaging certain biologic features to targeted drug delivery designed for the specific characteristics of an individual patient's disease. While the use of therapeutic radioisotopes was an important but minor component of the therapeutic oncology in the past, now with the development of "Theranostic" applications, intelligent options for targeted internal radionuclide treatments became possible in a variety of tumors and Theranostics started to give rise to a paradigm shift in oncology.

"Theranostic" concept in nuclear medicine represent both diagnostic and therapeutic function in one drug formulation and while bridging these two goals. The term "Theranostic" is generated from 'therapy' and 'diagnostics/diagnosis' (1). Actually Iodine-131 is the oldest and the most common isotope in theranostic applications. In this case, the same radioisotope Iodine-131 serves for both diagnostic and therapeutic purpose on the basis of using the same target, although Iodine-123 which is the pure gamma emitter isotope of Iodine can take part as the diagnostic agent. Theranostic approach also includes the use of different radioistopes but again depending on the principle of using the same target for both diagnosis and therapy Recently, there have been new "theranostics" agents in clinical practice, which are good examples for theranostic approach with two different radioisotopes. For instance, somatostatin receptors on the surface of the neuroendocrine neoplasia have been used as targets for radionuclide imaging and treatment on the basis of "theranostic" approach. PET Imaging with positron emitter Ga-68 labelled peptides which show affinity to somatostatin receptors and treatment with beta emitter Y-90/Lu-177 labelled peptides targeting these receptors gained wide acceptance in the field (2,3).

There has been a growing interest also for the use theranostic approach in prostate cancer which affects a great number of males. The presence of prostate specific membrane antigen (PSMA) expression in prostate cancer served as a basis for the idea of targeting these receptors for PET imaging using Ga-68 labelled PSMA and consequently treating with Lu-177 labelled PSMA (4,5). The potential for drug delivery system using theranostic basis also enables us to administer therapy according to the individual requirements of the patient. As the tumor nature is heterogenous, a specific drug indicating a certain characteristic will be a therapeutic option only for a subset of tumors. So the treatment will be customized for only patients whose tumor contains very specific proteins or receptors, which will eventually result with a more "precise" therapy.

Recently, Radium 223 which is a calcium mimicking radioisotope has been introduced as an effective treatment in metastatic castration resistant prostate cancer patients with bone involvement only (6). While delivering alpha emission to the metastatic deposits detected by bone imaging tracers, Ra-223 provides improvement in patient survival and skeletal related events. Therefore, Ra-233 treatment became available in all over the world and

Address for Correspondence: Zehra Özcan MD, Ege University Medical School, Department of Nuclear Medicine, İzmir, Turkey
E-mail: zehra.ozcan@yahoo.com ORCID ID: orcid.org/0000-0002-6942-4704
Received: 15.01.2018 **Accepted:** 15.01.2018

covered in most European countries (7). Being recently licensed in Turkey, it is believed that this new targeted radionuclide treatment will also be available in our patients and alpha emitting radionuclides will open a new era in therapeutic nuclear medicine.

It is clear that nuclear medicine and molecular imaging will enlarge its role in the early diagnosis and treatment of cancer and also will be a driving force in personalized medicine using theranostic concepts. Finally, while completing a successful year and starting a new year, we, the editors of MIRT, hope that scientific researches in our field will expand more and MIRT will be a leading publication for all these new ideas and researches promoting diagnostic and therapeutic Nuclear Medicine applications.

References

1. Durak H. Onkolojide Kişiselleştirilmiş Tedavi ve Teranostik Yaklaşımlar. Nucl Med Sem 2015;1:80-84.
2. Bozkurt MF, Virgolini I, Balogova S, Beheshti M, Rubello D, Decristoforo C, Ambrosini V, Kjaer A, Delgado-Bolton R, Kunikowska J, Oyen WJG, Chiti A, Giammarile F, Fanti S. Guideline for PET/CT imaging of neuroendocrine neoplasms with 68Ga-DOTA-conjugated somatostatin receptor targeting peptides and 18F-DOPA. Eur J Nucl Med Mol Imaging 2017;44:1588-1601.
3. Strosberg J, El-Haddad G, Wolin E, Hendifar A, Yao J, Chasen B, Mittra E, Kunz PL, Kulke MH, Jacene H, Bushnell D, O'Dorisio TM, Baum RP, Kulkarni HR, Caplin M, Lebtahi R, Hobday T, Delpassand E, Van Cutsem E, Benson A, Srirajaskanthan R, Pavel M, Mora J, Berlin J, Grande E, Reed N, Seregni E, Öberg K, Lopera Sierra M, Santoro P, Thevenet T, Erion JL, Ruszniewski P, Kwekkeboom D, Krenning E; NETTER-1 Trial Investigators. Phase 3 Trial of 177Lu-Dotatate for Midgut Neuroendocrine Tumors. N Engl J Med 2017;376:125-135.
4. Afshar-Oromieh A, Hetzheim H, Kratochwil C, Benesova M, Eder M, Neels OC, Eisenhut M, Kübler W, Holland-Letz T, Giesel FL, Mier W, Kopka K, Haberkorn U. The Theranostic PSMA Ligand PSMA-617 in the Diagnosis of Prostate Cancer by PET/CT: Biodistribution in Humans, Radiation Dosimetry, and First Evaluation of Tumor Lesions. J Nucl Med 2015;56:1697-1705.
5. Kabasakal L, Toklu T, Yeyin N, Demirci E, Abuqbeitah M, Ocak M, Aygün A, Karayel E, Pehlivanoğlu H, Alan Selçuk N. Lu-177-PSMA-617 Prostate-Specific Membrane Antigen Inhibitor Therapy in Patients with Castration-Resistant Prostate Cancer: Stability, Bio-distribution and Dosimetry. Mol Imaging Radionucl Ther 2017;26:62-68.
6. Hoskin P, Sartor O, O'Sullivan JM, Johannessen DC, Helle SI, Logue J, Bottomley D, Nilsson S, Vogelzang NJ, Fang F, Wahba M, Aksnes AK, Parker C. Efficacy and safety of radium-223 dichloride in patients with castration-resistant prostate cancer and symptomatic bone metastases, with or without previous docetaxel use: a prespecified subgroup analysis from the randomised, double-blind, phase 3 ALSYMPCA trial. Lancet Oncol 2014;15:1397-1406.
7. Poeppel TD, Handkiewicz-Junak D, Andreeff M, Becherer A, Bockisch A, Fricke E, Geworski L, Heinzel A, Krause BJ, Krause T, Mitterhauser M, Sonnenschein W, Bodei L, Delgado-Bolton RC, Gabriel M. EANM guideline for radionuclide therapy with radium-223 of metastatic castration-resistant prostate cancer Eur J Nucl Med Mol Imaging 2017. doi: 10.1007/s00259-017-3900-4.

Original Article
Mol Imaging Radionucl Ther 2018;27:3-9 DOI:10.4274/mirt.74436

The Role of ^{18}F-FDG PET/CT in Evaluating Elevated Levels of Tumor Markers in Breast Cancer

Meme Kanseri Tanısı ile Takip Edilmekte Olan Hastalarda Saptanan Tümör Belirteç Yüksekliğinin Değerlendirilmesinde ^{18}F-FDG PET/BT'nin Rolü

İnan Göktaş, Hakan Cayvarlı
Ordu State Hospital, Clinic of Nuclear Medicine, Ordu, Turkey

Abstract

Objective: Our aim was to assess the diagnostic performance of integrated positron emission tomography/computed tomography (PET/CT) in the follow-up of breast cancer patients, who underwent a PET/CT scan due to a suspicion of recurrence based on elevated levels of serum tumor markers.

Methods: Seventy-seven consecutive patients were included in this study. PET/CT scan results were compared with the final diagnoses that were obtained from histopathological sampling or a minimum 6 months of radiological follow-up. The sensitivity, specificity, positive predictive value (PPV), negative predictive value (NPV) and the diagnostic accuracy of PET/CT for detecting recurrence were calculated.

Results: All 77 patients had increased serum cancer antigen 15-3 levels while 37 had increased serum carcinoembryonic antigen levels. According to PET/CT scan results, 59 of 77 patients (PET/CT positive) had local recurrence and/or distant metastasis while there was no pathological finding in 18 patients (PET/CT negative). In a follow-up of minimum 6 months, tumor recurrence was confirmed in 58 of "PET/CT positive" patients while no tumor recurrence was detected in 16 of "PET/CT negative" patients. According to these results the sensitivity, specificity, PPV, NPV and the diagnostic accuracy of PET/CT for detecting recurrence on a per-person basis were calculated as 98%, 88%, 96%, 94% and 96%, respectively.

Conclusion: In case of elevated levels of serum tumor markers, PET/CT has a high diagnostic accuracy in detecting tumor recurrence in patients with breast cancer, and it is an effective modality that can be used in addition to conventional imaging techniques.

Keywords: ^{18}F-FDG PET/CT scan, breast cancer, biochemical tumor markers

Öz

Amaç: Bu çalışmada meme kanseri tanısı ile takip edilmekte iken tümör belirteçlerinde [kanser antijeni (CA) 15-3 ve karsinoembriyonik antijen (CEA)] yükselme saptanan ve bu sebeple nüks şüphesiyle yeniden evreleme amacıyla ^{18}F-FDG pozitron emisyon tomografi/bilgisayarlı tomografi (PET/BT) çekilen hastalarda PET/BT'nin tanısal etkinliği araştırıldı.

Yöntem: Çalışmaya 77 hasta dahil edildi. Hastaların PET/BT sonuçları ile çalışma sonrası minimum 6 aylık takip döneminde elde edilen histopatolojik ve radyolojik veriler karşılaştırıldı. Bu sonuçlara göre PET/BT'nin duyarlılığı, özgüllüğü, pozitif prediktif değerleri (PPV) ve negatif prediktif değerleri (NPV) ile tanısal doğruluğu hesaplandı.

Bulgular: Çalışmaya dahil edilen hastaların tamamında CA 15-3 düzeyi yüksek iken, CEA düzeyi 37 hastada yüksek idi. PET/BT sonuçlarına göre 77 hastanın 59 tanesinde lokal nüks ve/veya uzak metastaz şüpheli lezyon saptanırken, 18 hastada

Address for Correspondence: Hakan Cayvarlı MD, Ordu State Hospital, Clinic of Nuclear Medicine, Ordu, Turkey
Phone: +90 452 234 32 32 E-mail: hakancayvarli@hotmail.com ORCID ID: orcid.org/0000-0003-3225-8711
Received: 10.04.2017 **Accepted:** 10.08.2017

Öz

herhangi bir patolojik bulguya rastlanmadı. Minimum 6 aylık takip neticesinde PET/BT'de şüpheli lezyon saptanan 59 hastanın 58 tanesinde lokal nüks ve/veya uzak metastaz varlığı doğrulanırken, PET/BT'de patolojik bulgu saptanmayan 18 hastanın 16 tanesinde takipleri süresince lokal nüks ve/veya uzak metastaz gelişmedi. Bu sonuçlara göre çalışmamızda PET/BT'nin hasta bazında duyarlılığı %96, özgüllüğü %94, PPV %98, NPV %88 ve tanısal doğruluğu %96 olarak bulundu.

Sonuç: ^{18}F-FDG PET/BT, meme kanseri tanısı ile takip edilmekte iken tümör belirteç yüksekliği saptanan hastalarda lokal nüks ve/veya uzak metastazın araştırılması için tanısal etkinliği yüksek non-invaziv ve konvansiyonel görüntüleme yöntemlerine ek olarak kullanılabilecek etkili bir görüntüleme yöntemidir.

Anahtar kelimeler: ^{18}F-FDG PET/BT, meme kanseri, biyokimyasal tümör belirteçleri

Introduction

Breast cancer is the most common cancer among females. It is also the leading cause of cancer related death among females worldwide, with an estimated 1,7 million new cases and 521.900 deaths in 2012 (1).

Recurrence in breast cancer can occur even after 15 years following primary therapy, thus requiring life-long routine follow-up (2). Early detection of tumor recurrence improves long-term survival rates as well as quality of life.

Cancer antigen 15-3 (CA 15-3) and carcinoembryonic antigen (CEA) are two frequently used tumor markers in the follow-up of breast cancer (3,4). However, the results of many studies about these tumor markers in follow-up of breast cancer are inconsistent, even conflicting with each other. Previous studies have been conducted to quantitatively evaluate the serum levels of these two tumor markers and some found no significant correlation between increased tumor marker levels and recurrence while some found a significant correlation between them (5,6,7).

Although the definitive diagnostic method of breast cancer recurrence is histopathologic confirmation, it is not always easy to perform due to deep location or being very small in size or being too close to organs or great vessels making sampling either difficult or risky. Morphological imaging studies or tumor markers can be used to evaluate breast cancer recurrence. Currently, the most commonly used morphological imaging methods for detecting breast cancer recurrence include mammography, ultrasound (US), computed tomography (CT) and magnetic resonance imaging (MRI). However, both tumor markers and morphological imaging studies have some limitations. For instance, tumor markers can neither localize the recurrence site nor differentiate loco-regional recurrence from distant metastasis. Even though morphological imaging studies can detect both loco-regional recurrence and distant metastasis, it is not always easy to discriminate post-operational changes from loco-regional recurrence. In addition, they also cannot evaluate the viability of the tumor tissue or small lesions since their diagnostic criteria depends on size measurement and morphological changes.

Integrated positron emission tomography (PET)/CT scan is a functional imaging modality that can measure increased glucose metabolism in tumor cells by using ^{18}F-fluorodeoxyglucose (^{18}F-FDG) as a radiopharmaceutical agent. Recently this imaging modality is also frequently performed for evaluating breast cancer, like many other types of cancers (8,9). However, the data on the value of ^{18}F-FDG PET/CT in evaluating breast cancer recurrence in case of elevated levels of tumor markers is limited and not clear (10).

In clinical practice, during the follow-up of breast cancer, it is difficult to manage treatment when serum tumor marker levels increase without any morphological imaging finding or when suspicious morphological imaging findings are found in terms of breast cancer recurrence but histopathological confirmation is not convenient. In such circumstances, PET/CT scan can be used for evaluating recurrence (11,12).

That is why, in this study we aimed to assess the diagnostic performance of ^{18}F-FDG PET/CT in evaluating recurrence in case of elevated levels of serum tumor markers (CA 15-3 and CEA) during follow-up of breast cancer, and to find the optimal cut-off values of serum tumor markers that can be used in discrimination of tumor recurrence when reporting PET/CT.

Materials and Methods

Seventy-seven consecutive patients who were followed-up for breast cancer and who underwent ^{18}F-FDG PET/CT scan due to suspicion of recurrence based on elevated levels of serum tumor markers (CA 15-3 and CEA) were included in this study. Elevated serum tumor marker levels were accepted as >25 U/mL for CA 15-3, and >3.8 ng/mL for CEA. PET/CT scan results were compared with the final diagnoses that were obtained from histopathologic sampling or at least 6 months of radiological follow-up.

^{18}F-FDG PET/CT Imaging

All scans were performed by using an integrated PET/CT system (Discovery 600; GE Healthcare, Milwaukee, USA) that consisted of a full-ring high-resolution bismuth germanate oxide PET and a 16-slice CT. Patients were fasted for at least 6 hours before imaging. Blood glucose levels were checked to be less than 200 mg/dL before injection of 10 to 15 mCi of ^{18}F-FDG. 500 mL of oral contrast was administered and

intravenous injection of ^{18}F-FDG was followed by a period of approximately 60 minutes. The images were obtained from the vertex of the head to mid-thigh.

Image Analysis

Two experienced nuclear medicine physicians interpreted PET/CT images. The readers were blinded to the results of previous imaging studies and to the follow-up data. For the purpose of statistical analysis, patients who have at least one positive PET lesion compatible with recurrence on PET/CT were categorized as "PET/CT positive" and all others as "PET/CT negative". Then, the PET/CT data were compared with the follow-up data. If a patient has both loco-regional recurrence and distant metastasis but the PET/CT detected only one component (i.e. PET/CT detected the loco-regional recurrence but not the distant metastasis or vice versa) then PET/CT scan result was classified as false negative. The golden standard in this study was either radiological follow-up (in most of the patients) or histopathologic confirmation. Radiologically confirmed recurrence was defined as detection of recurrence by conventional imaging modalities (mammography, US, CT or MRI) within 6 months of PET/CT scan. When a suspicious lesion showed interval increment in size during follow-up or interval decrement in size after radio/chemotherapy it was accepted as a radiologically confirmed recurrence. A patient was accepted as free of recurrence after a negative radiological follow-up within at least 6 months of PET/CT scan. Recurrence detected after this period was interpreted as a new recurrence.

Statistical Analysis

A retrospective analysis of prospectively collected archive data was performed. The Statistical Package for Social Sciences version 22.0 (SPSS Inc,; Chicago, IL, USA) was used for statistical analysis. Tests with a p value less than 0.05 were considered as statistically significant. Patient based sensitivity, specificity, positive predictive value (PPV), negative predictive value (NPV) and diagnostic accuracy of PET/CT were calculated. Receiver operating characteristic analysis was used to detect the optimal cut-off serum tumor marker levels that can be used in interpreting PET/CT. Kappa coefficient was used in the measurement of agreement analysis. Written informed consent was obtained from each patient included in this study.

Results

Seventy-seven consecutive patients were included in this study. The mean age of patients was 50.9, ranging from 27 to 78. Of all 77 patients, all of them had increased (>25 U/mL) serum CA 15-3 levels while 37 of them had increased (>3.8 ng/mL) serum CEA levels. In terms of histopathologic classifying; 66 patients had invasive ductal carcinoma, 6 had invasive lobular carcinoma and 5 had other type of tumors. According to TNM staging; 2 patients were classified as stage 1, 17 as stage 2, 24 as stage 3 and 34 had stage 4 disease. Patient characteristics are summarized in Table 1.

According to PET/CT scan results, 59 of 77 patients (PET/CT positive) had local recurrence and/or distant metastasis (57 were reported as having distant metastasis and 2 were reported as having loco-regional recurrence) while 18 were reported as having no pathological finding (PET/CT negative).

Bone metastasis was reported in 48 patients while liver metastasis was reported in 14, lung metastasis in 3, plural metastasis in 4, brain metastasis in 3, adrenal gland metastasis in 2, peritoneal metastasis in 1, spleen metastasis in 1, regional lymph node metastasis in 8, and extra-regional lymph node metastasis in 15 patients.

Of all 77 patients evaluated in this study; 58 of "PET/CT positive" patients and 2 of "PET/CT negative" patients were confirmed to have tumor recurrence, and 1 of "PET/CT positive" patients and 16 of "PET/CT negative" patients were accepted as negative for tumor recurrence finally. PET/CT scan results were false positive in 1 patient and false negative in 2 patients. In the follow-up, one patient who has been reported as having distant metastasis in PET/CT (false positive) was diagnosed as having mediastinal granulomatous disease finally. On the other hand, out of the 2 patients who have been reported as having no pathological findings in PET/CT (false negative) one was diagnosed with bone and pleural metastasis 5 months after the PET/CT scan, while bone metastasis in addition to neck and mediastinal lymph node metastasis was detected 12 months after the PET/CT scan in another patient.

Final diagnoses were obtained by histopathologic sampling in 23 (30%) of 77 patients and by radiological follow-up in the remaining 54 (70%). Histopathologic confirmation was obtained in 2 of 2 loco-regional recurrence site, 6 of 8 regional lymph node metastasis site, 6 of 15 extra-regional lymph node metastasis site, 4 of 48 bone metastasis site, 2 of 4 pleural metastasis site, 1 of 3 lung metastasis site and 2 of 14 liver metastasis site. Other sites of recurrence were confirmed by radiological follow-up. PET/CT scan results and correlation of PET/CT with final diagnosis are listed in Table 1.

Based on these results, on a per-person basis, there was a statistically significant correlation between PET/CT scan results and final diagnosis (kappa: 0.89, p=0.000 <0.05) with a sensitivity, specificity, PPV, NPV and diagnostic accuracy of 96%, 94%, 98%, 88% and 96% respectively.

There was no statistically significant correlation between elevated serum CA 15-3 levels (>25 U/mL) and final diagnosis (kappa: 0.0, p=1.0 >0.05). Nevertheless, a statistically significant correlation was detected if an optimal cut-off value of 40 U/mL was used to discriminate tumor recurrence when reporting a PET/CT scan (kappa: 0.35, p=0.001 <0.05) with a sensitivity, specificity, PPV and NPV of 76%, 64%, 88% and 44%, respectively. There was

Table 1. Patient characteristics and positron emission tomography/computed tomography scan results

No	Age	Histological subtype	Disease stage	CA 15-3 (u/mL)	CEA (ng/mL)	PET/CT scan report	PET/CT correlation with final diagnosis
1	59	IDCA	4	31	12.4	BM, LNM	+
2	29	IDCA	3	41	3	BM, VM	+
3	36	OTHER (1)	3	83.3	79.3	BM	+
4	38	ILCA	4	85.5	4.8	BM, LNM	+
5	48	IDCA	2	35.6	1.9	NPF	+
6	39	IDCA	4	75.9	1.6	BM	+
7	47	IDCA	4	55.2	5.1	BM, VM	+
8	27	ILCA	2	74.4	3.7	VM	+
9	65	IDCA	4	27.4	1.7	BM	+
10	58	IDCA	3	25.9	1.1	LNM	+
11	36	IDCA	4	53.3	1.1	BM, VM	+
12	58	IDCA	2	46.6	11.3	NPF	+
13	45	ILCA	3	115.3	2.5	BM	+
14	47	IDCA	2	517.9	0.5	VM	+
15	63	IDCA	3	34.5	20.3	BM, VM	+
16	35	IDCA	4	241.2	21.4	BM	+
17	34	ILCA	3	40.9	33.6	BM, VM	+
18	67	IDCA	3	175.1	2.9	BM, LNM	+
19	58	IDCA	3	705.3	24.3	BM, VM, LNM	+
20	35	IDCA	4	299.7	25.5	BM	+
21	36	IDCA	4	85.2	2.6	BM	+
22	72	IDCA	3	43.6	9	LNM	+
23	62	IDCA	2	51.9	1.7	NPF	+
24	46	IDCA	3	49.4	1	BM	+
25	56	IDCA	4	140.6	3.7	BM, VM	+
26	34	IDCA	4	25.2	2.3	BM, VM, LNM	+
27	38	OTHER (2)	3	26.6	4.7	NPF	+
28	70	IDCA	3	47.9	3.3	LNM	+
29	51	IDCA	3	32.5	2.9	NPF	+
30	42	IDCA	3	52.1	7.2	BM, LNM	+
31	49	IDCA	4	33.1	7.1	VM	+
32	60	IDCA	3	41	2.2	BM, LNM	+
33	49	IDCA	3	45.4	1.9	NPF	+
34	68	IDCA	4	31.6	1.8	BM, VM	+
35	66	IDCA	4	53.3	62.8	BM	+
36	61	IDCA	3	33.9	5.9	LNM	+
37	52	IDCA	2	29.8	7.7	NPF	- (6)
38	61	IDCA	2	37.1	4.6	NPF	+
39	52	OTHER (3)	4	61.4	6.8	BM, VM	+
40	45	IDCA	2	27.1	2.6	NPF	+
41	36	IDCA	4	101.1	0.3	BM, VM	+

Table 1. Continued.

No	Age	Histological subtype	Disease stage	CA 15-3 (u/mL)	CEA (ng/mL)	PET/CT scan report	PET/CT correlation with final diagnosis
42	43	IDCA	2	37.6	0.9	BM	+
43	57	OTHER (4)	4	74.4	4	BM, LNM	+
44	52	IDCA	2	41.1	13.8	BM, VM	+
45	28	IDCA	4	41.1	5.7	BM, LNM	+
46	42	IDCA	4	69.5	7.8	BM, VM	+
47	70	IDCA	2	26.6	2	NPF	+
48	76	IDCA	2	37.8	2.2	LRR	+
49	63	IDCA	4	725.5	5.2	BM, VM	+
50	42	IDCA	4	187	69	BM, VM	+
51	35	IDCA	2	32.3	3.1	LNM	- (7)
52	35	IDCA	4	85.6	30.5	BM	+
53	48	IDCA	2	25.5	49.1	NPF	+
54	56	OTHER (5)	4	78.9	429.8	BM, VM	+
55	35	IDCA	4	83.3	2.6	BM	+
56	72	ILCA	4	483.1	4.2	BM, VM, LNM	+
57	48	IDCA	4	1507	1183	BM	+
58	74	IDCA	4	51.6	2.3	BM	+
59	45	IDCA	4	41.1	2.1	BM	+
60	45	IDCA	3	41	5.3	NPF	- (8)
61	63	IDCA	4	30	1.9	BM	+
62	45	IDCA	3	99	3.6	VM, LNM	+
63	54	IDCA	4	527	3.7	BM, LNM	+
64	64	IDCA	2	30.2	1	NPF	+
65	58	IDCA	4	94.1	26.6	BM, VM, LNM	+
66	73	IDCA	1	28.7	0.9	NPF	+
67	54	IDCA	4	527.6	3.7	BM, VM	+
68	37	IDCA	3	57.8	0.6	NPF	+
69	59	IDCA	1	31.8	2.4	NPF	+
70	56	ILCA	3	32.1	49.1	BM	+
71	58	IDCA	4	195.4	95	BM, VM, LNM	+
72	46	IDCA	4	76.1	2.3	BM	+
73	46	IDCA	2	53.1	2.3	NPF	+
74	78	IDCA	3	963.9	130	BM, VM	+
75	49	IDCA	2	61.1	9.4	NPF	+
76	41	IDCA	3	30.8	1.4	LRR	+
77	42	IDCA	3	103.9	11.9	BM, VM	+

Elevated serum tumor marker levels are defined as >25 U/mL for CA 15-3 and >3.8 ng/mL for CEA, CA 15-3: Cancer antigen 15-3, PET/CT: Positron emission tomography/computed tomography, CEA: Carcinoembryonic antigen, IDCA: Invasive ductal carcinoma, ILCA: Invasive lobular carcinoma, LRR: Loco-regional recurrence, BM: Bone metastasis, VM: Visceral metastasis, LNM: Lymph node metastasis, NPF: No pathological finding. Other: (1) Mix invasive mucinous and invasive ductal carcinoma, (2) mix invasive lobular and invasive ductal carcinoma, (3) mix mucinous carcinoma and invasive micropapillary carcinoma, (4) inflammatory breast carcinoma and (5) tubulolobular carcinoma, (6) finally diagnosed as having bone and pleural metastasis after 5 months of PET/CT scan, (7) finally diagnosed as having mediastinal granulomatous disease, (8) finally diagnosed as having bone metastasis in addition to neck and mediastinal lymph node metastasis after 12 months of PET/CT scan

no statistically significant correlation between elevated serum CEA levels (>3.8 ng/mL) and final diagnosis (kappa: 0.16, p=0.081 >0.05). However, when reporting the PET/CT scan, if an optimal cut-off value of 4.8 ng/mL was used to differentiate tumor recurrence, a statistically significant correlation was detected (kappa: 0.21, p=0.017 <0.05) with a sensitivity, specificity, PPV and NPV of 50%, 82%, 90% and 31%, respectively.

Discussion

One of the major problems in breast cancer follow-up is detecting loco-regional recurrence and/or distant metastasis since the 80% 5-year survival rate in early disease is decreased to 15% in advanced stages, and since a considerable amount of patients are diagnosed at advanced stages. Moreover, the recurrence rate is very high -nearly 30% in early stage disease, and it can occur even 15 years after primary therapy. The 5- and 10-year recurrence rates after primary therapy are reported as 6 and 12% in stage 1-2 disease, respectively (2,13). Patients who have tumor recurrence occurring after primary therapy have a chance of curative treatment. Therefore, early detection of recurrence and restaging is important for planning the optimal treatment regimen and selecting the patients who can be curatively treated.

In the follow-up of breast cancer, an increase in tumor marker levels usually indicates recurrence, but its sensitivity is low and the sensitivity spreads in a wide range in different studies. An elevated tumor marker level is not always related to a recurrence. Moreover, tumor markers cannot localize the recurrence and cannot show if the disease is widespread or not.

In a study of Lumachi et al. (14), they found the sensitivity of CEA and CA 15-3 as 38.1% and 61.1% and the specificity of both tumor markers as 98.8% and 91.2%, respectively, in detecting breast cancer recurrence. In another study, Guadagni et al. (15) reported the sensitivity of CEA as 41.3% and the sensitivity of CA 15-3 as 80.8% in recurrent disease.

Some studies showed that the tumor marker levels increase before clinical or radiological findings of recurrence (16,17). In a study by Nicolini et al. (11), patients were divided into two groups; the first group of patients who received medical therapy in case of negative conventional imaging findings but significant increase in one or more components of CEA-TPA-CA 15-3 tumor marker panel ("tumor marker guided" treatment) and the second group of patients who were treated only after radiologically confirmed recurrence (conventional treatment). As a result of this study, "tumor marker guided" treatment prolonged disease-free and overall survival rates significantly (11).

Gallowitsch et al. (18) evaluated the role of ^{18}F-FDG PET in the follow-up of breast cancer in case of clinical suspicion of recurrence and/or tumor marker increase in correlation with conventional imaging modalities and reported on the advantages of ^{18}F-FDG PET in the diagnosis of metastases when compared with conventional imaging modalities. In patients with clinical suspicion of tumor recurrence but not increased tumor marker levels, ^{18}F-FDG PET was found to be a reliable imaging modality for detecting recurrence (18).

In parallel with the aforementioned study, in the study investigating the diagnostic accuracy of FDG PET/CT, CT and bone scintigraphy in patients with suspected breast cancer recurrence, Hildebrandt et al. (19) found that PET/CT was accurate in detecting recurrence and ruling out distant metastasis. They suggested that PET/CT had higher accuracy as compared to conventional imaging modalities in this patient group (19).

In the study by Liu et al. (20) evaluating the impact of FDG PET on detecting breast cancer recurrence based on asymptomatically elevated tumor marker levels, FDG PET correctly detected recurrence in 35/38 sites in 25/28 patients, and they reported the sensitivity and accuracy of FDG PET as 96% and 90%, respectively (20). Similarly, Lonneux et al. (21) found that FDG PET detected recurrence in 37/39 sites in 31/33 patients in their study evaluating the role of ^{18}F-FDG PET imaging in patients with a suspicion of breast cancer recurrence due to tumor marker increase, and they concluded that FDG PET is highly sensitive for detecting distant metastasis despite a low specificity (21). The higher specificity rate detected in our study as compared to these two studies can be attributed to the usefulness of CT integration to PET devices, making discrimination of degenerative changes or physiological uptakes from pathological ones easier. In addition, both the high number of patients and the lower levels of serum tumor markers in our study as compared to those of Liu et al. (20) further confirm the high efficacy of PET/CT, and increase the importance of our study.

PET/CT is a highly sensitive and effective modality for evaluating breast cancer recurrence in case of an increase in tumor marker levels in asymptomatic patients. However, patient management should not be based only on PET/CT results due to its low specificity, and additional radiologic or histopathologic confirmations are required.

In our study, all 77 patients had increased CA 15-3 levels. In 60 of these patient's tumor recurrence was confirmed. According to this data, CA 15-3 had a PPV of 77%. In 37 patient's, serum CEA levels were increased. Thirty-two of these patients had confirmed recurrent disease. Therefore, the PPV of CEA in detecting tumor recurrence was 86%. Nevertheless, it must be remembered that 37 patients had elevated levels of both serum CEA and CA 15-3, so high PPV of CEA is not an unexpected result if both serum tumor markers are used together.

In our study, PET/CT correctly detected 58 of 60 patients who had confirmed tumor recurrence, and 16 of 17 patients who were confirmed as negative for tumor recurrence

yielding a diagnostic accuracy of 96%. We found that in case of elevated levels of serum tumor markers, PET/CT has a high diagnostic accuracy in detecting tumor recurrence in patients with breast cancer.

In conclusion, this study provides significant evidence about the value of PET/CT in evaluating breast cancer recurrence in case of elevated levels of serum tumor markers during follow-up. Moreover, our results demonstrate that PET/CT can allow optimization of the treatment planning and might be considered in clinical decision-making process.

Study Limitations

There are several limitations to our study. First, histopathologic confirmation of recurrence was not provided in most cases. In addition, the majority of included patients had advanced staged disease that increased the possibility of recurrence.

Further well-designed clinical studies are required to analyze the value of PET/CT in evaluating breast cancer recurrence. Also, the role of PET/CT in different histological subgroups of breast cancer should be evaluated.

Conclusion

^{18}F-FDG PET/CT is a noninvasive imaging modality that enables whole body scanning at once. In case of elevated levels of serum tumor markers, ^{18}F-FDG PET/CT has a high diagnostic accuracy in detecting breast cancer recurrence and it is an effective modality that can be used in addition to conventional imaging techniques.

Ethics

Ethics Committee Approval: A retrospective analysis of prospectively collected archive data was performed.

Informed Consent: Written informed consent was obtained from each patient included in this study.

Peer-review: Externally and internally peer-reviewed.

Authorship Contributions

Concept: İ.G., Design: İ.G., Data Collection or Processing: İ.G., H.C., Analysis or Interpretation: İ.G., H.C., Literature Search: İ.G., H.C., Writing: İ.G., H.C.

Conflict of Interest: No conflict of interest was declared by the authors.

Financial Disclosure: The authors declared that this study received no financial support.

References

1. Torre LA, Bray F, Siegel RL, Ferlay J, Lortet-Tieulent J, Jemal A. Global Cancer Statistics, 2012. CA Cancer J Clin 2015;65:87-108.
2. Hayat MA. Methods of Cancer Diagnosis, Therapy, and Prognosis Volume 1, Breast Carcinoma. Springer; 2008.
3. Uehara M, Kinoshita T, Hojo T, Akashi-Tanaka S, Iwamoto E, Fukutomi T. Long-term prognostic study of carcinoembryonic antigen (CEA) and carbohydrate antigen 15-3 (CA 15-3) in breast cancer. Int J Clin Oncol 2008;13:447-451.
4. O'Hanlon DM, Kerin MJ, Kent P, Maher D, Grimes H, Given HF. An evaluation of preoperative CA 15-3 measurement in primary breast carcinoma. Br J Cancer 1995;71:1288-1291.
5. Samy N, Ragab HM, El Maksoud NA, Shaalan M. Prognostic significance of serum Her2/neu, BCL2, CA15-3 and CEA in breast cancer patients: A short follow-up. Cancer Biomark 2010;6:63-72.
6. Thriveni K, Krishnamoorthy L, Ramaswamy G. Correlation study of Carcino Embryonic Antigen & Cancer Antigen 15.3 in pretreated female breast cancer patients. Indian J Clin Biochem 2007;22:57-60.
7. Fu Y, Li H. Assessing Clinical Significance of Serum CA15-3 and Carcinoembryonic Antigen (CEA) Levels in Breast Cancer Patients: A Meta-Analysis. Med Sci Monit 2016;22:3154-3162.
8. Ratib O, Phelps ME, Huang SC, Henze E, Selin CE, Schelbert HR. Positron tomography with deoxyglucose for estimating local myocardial glucose metabolism. J Nucl Med 1982;23:577-586.
9. Kostakoglu L, Agress H Jr, Goldsmith SJ. Clinical role of FDG PET in evaluation of cancer patients. Radiographics 2003;23:315-340.
10. Lei L, Wang X, Chen Z. PET/CT Imaging for Monitoring Recurrence and Evaluating Response to Treatment in Breast Cancer. Adv Clin Exp Med 2016;25:377-382.
11. Nicolini A, Carpi A, Michelassi C, Spinelli C, Conte M, Miccoli P, Fini M, Giardino R. "Tumor marker guided" salvage treatment prolongs survival of breast cancer patients: final report of a 7-year study. Biomed Pharmacother 2003;57:452-459.
12. Xiao Y, Wang L, Jiang X, She W, He L, Hu G. Diagnostic efficacy of 18F-FDG-PET or PET/CT in breast cancer with suspected recurrence: a systematic review and meta-analysis. Nucl Med Commun 2016;37:1180-1188.
13. Howlader N, Noone AM, Krapcho M, Garshell J, Miller D, Altekruse SF, et al. (eds). SEER Cancer Statistics Review, 1975-2012, National Cancer Institute. Bethesda, MD. Available from: http://seer.cancer.gov/csr/1975_2012/
14. Lumachi F, Brandes AA, Boccagni P, Polistina F, Favia G, D'Amico DF. Long-term follow-up study in breast cancer patients using serum tumor markers CEA and CA 15-3. Anticancer Res 1999;19:4485-4489.
15. Guadagni F, Ferroni P, Carlini S, Mariotti S, Spila A, Aloe S, D'Alessandro R, Carone MD, Cicchetti A, Ricciotti A, Venturo I, Perri P, Di Filippo F, Cognetti F, Botti C, Roselli M. A re-evaluation of carcinoembryonic antigen (CEA) as a serum marker for breast cancer: a prospective longitudinal study. Clin Cancer Res 2001;7:2357-2362.
16. Cheung KL, Graves CR, Robertson JF. Tumour marker measurements in the diagnosis and monitoring of breast cancer. Cancer Treat Rev 2000;26:91-102.
17. Nicolini A, Carpi A. Postoperative follow-up of breast cancer patients: overview and progress in the use of tumor markers. Tumour Biol 2000;21:235-248.
18. Gallowitsch HJ, Kresnik E, Gasser J, Kumnig G, Igerc I, Mikosch P, Lind P. F-18 fluorodeoxyglucose positron-emission tomography in the diagnosis of tumor recurrence and metastases in the follow-up of patients with breast carcinoma: a comparison to conventional imaging. Invest Radiol 2003;38:250-256.
19. Hildebrandt MG, Gerke O, Baun C, Falch K, Hansen JA, Farahani ZA, Petersen H, Larsen LB, Duvnjak S, Buskevica I, Bektas S, Søe K, Jylling AM, Ewertz M, Alavi A, Høilund-Carlsen PF. [18F] Fluorodeoxyglucose (FDG)-Positron Emission Tomography (PET)/Computed Tomography (CT) in Suspected Recurrent Breast Cancer: A Prospective Comparative Study of Dual-Time-point FDG-PET/CT, Contrast-Enhanced CT, and Bone Scintigraphy. J Clin Oncol 2016;34:1889-1897.
20. Liu CS, Shen YY, Lin CC, Yen RF, Kao CH. Clinical impact of [(18)F] FDG-PET in patients with suspected recurrent breast cancer based on asymptomatically elevated tumor marker serum levels: a preliminary report. Jpn J Clin Oncol 2002;32:244-247.
21. Lonneux M, Borbath II, Berlière M, Kirkove C, Pauwels S. The Place of Whole-Body PET FDG for the Diagnosis of Distant Recurrence of Breast Cancer. Clin Positron Imaging 2000;3:45-49.

Original Article
Mol Imaging Radionucl Ther 2018;27:10-18 DOI:10.4274/mirt.97659

Evaluation of PET Scanner Performance in PET/MR and PET/CT Systems: NEMA Tests

PET/MR ve PET/BT Sistemlerinde PET Tarayıcının Performanslarının Değerlendirilmesi: NEMA Testleri

Mustafa Demir[1], Türkay Toklu[2], Mohammad Abuqbeitah[1], Hüseyin Çetin[3], H. Sezer Sezgin[3], Nami Yeyin[1], Kerim Sönmezoğlu[1]

[1]İstanbul University Cerrahpaşa Faculty of Medicine, Department of Nuclear Medicine, İstanbul, Turkey
[2]Yeditepe University Faculty of Medicine, Department of Nuclear Medicine, İstanbul, Turkey
[3]Epsilon Landauer Company, İstanbul, Turkey

Abstract

Objective: The aim of the present study was to compare the performance of positron emission tomography (PET) component of PET/computed tomography (CT) with new emerging PET/magnetic resonance (MR) of the same vendor.

Methods: According to National Electrical Manufacturers Association NU2-07, five separate experimental tests were performed to evaluate the performance of PET scanner of General Electric GE company; SIGNA™ model PET/MR and GE Discovery 710 model PET/CT. The main investigated aspects were spatial resolution, sensitivity, scatter fraction, count rate performance, image quality, count loss and random events correction accuracy.

Results: The findings of this study demonstrated superior sensitivity (~ 4 folds) of PET scanner in PET/MR compared to PET/CT system. Image quality test exhibited higher contrast in PET/MR (~ 9%) compared with PET/CT. The scatter fraction of PET/MR was 43.4% at noise equivalent count rate (NECR) peak of 218 kcps and the corresponding activity concentration was 17.7 kBq/cc. Whereas the scatter fraction of PET/CT was found as 39.2% at NECR peak of 72 kcps and activity concentration of 24.3 kBq/cc. The percentage error of the random event correction accuracy was 3.4% and 3.1% in PET/MR and PET/CT, respectively.

Conclusion: It was concluded that PET/MR system is about 4 times more sensitive than PET/CT, and the contrast of hot lesions in PET/MR was ~ 9% higher than PET/CT. These outcomes also emphasize the possibility to achieve excellent clinical PET images with low administered dose and/or a short acquisition time in PET/MR.

Keywords: PET/MR, PET/CT, NEMA tests, quality control

Öz

Amaç: Bu çalışmada son yıllarda nükleer tıpta rutin uygulamaya giren pozitron emisyon tomografisi/manyetik rezonans (PET/MR) görüntüleme sistemi ile PET/bilgisayarlı tomografi (BT) görüntüleme sistemlerinde 'National Electrical Manufacturers Association' (NEMA) testlerinin yapılması ve sonuçların karşılaştırılması amaçlandı.

Yöntem: NEMA NU2-07 testlerinden uzaysal ayırma gücü, hassasiyet, saçılma fraksiyonu kayıp sayımlar ve rastgele olay ölçümleri, görüntü kalitesi, sayım kayıpları rastgele olay düzeltme doğruluğu olmak üzere beş ayrı deneysel çalışma yapıldı.

Address for Correspondence: Mustafa Demir MD, İstanbul University Cerrahpaşa Faculty of Medicine, Department of Nuclear Medicine, İstanbul, Turkey
Phone: +90 533 665 69 79 E-mail: demirm@istanbul.edu.tr ORCID ID: orcid.org/0000-0002-9813-1628
Received: 22.06.2017 **Accepted:** 08.11.2017

Öz

Bulgular: Sensitivite testi sonuçları değerlendirildiğinde PET/MR sisteminin PET/BT sistemine göre yaklaşık 4 kat daha üstün olduğu bulundu. Görüntü kalitesi test sonuçlarından sıcak lezyon kontrastının PET/MR'da %9 daha yüksek olduğu bulundu. PET/MR scatter oranı gürültü eşdeğeri sayım hızı (NECR) 218 kcts ve aktivite konsantrasyonunun 17,7 kcts/cc olduğu durumda %43,4 bulundu. Buna karşılık PET/BT scatter oranı NECR 72 kcts ve aktivite konsantrasyonunun 24,3 kcts/cc olduğu durumda %39,2 bulundu. Tesadüfi hataları düzeltme doğruluğu PET/MR'da 3,4 ve PET/BT'de 3,1 bulundu.

Sonuç: PET/MR'da sensitivite değerinin PET/BT'ye göre yaklaşık 4 kat daha yüksek olduğu, PET/MR'da sıcak lezyon kontrastının PET/BT'ye göre %9 daha yüksek olduğu ayrıca PET/MR'da PET görüntülerinin daha az aktivite miktarı/veya daha kısa çekim süresinde elde edilebileceği sonucuna varıldı.

Anahtar kelimeler: PET/MR, PET/BT, NEMA testleri, kalite kontrol

Introduction

Positron emission tomography/magnetic resonance (PET/MR) has been increasingly considered the cutting edge technology in nuclear medicine. The merger of two different scanner technologies, PET and magnetic resonance imaging (MRI), presented more advanced and reliable means of cancer diagnosis. The advent of innovative labeling molecules promotes this marvel of novelty to be an ideal technology joining best of the nuclear and radiological hybrid imaging modalities for tumor detection and treatment. PET/computed tomography (CT) combination has been used in oncological investigations with long-standing experience and knowledge. Such premium changes in PET scanner design rendered PET/MR technology more versatile and promising evidenced by the enhanced tissue contrast and absence of radiation hazards (1).

Generally, the magnetic field has great influence on the ferromagnetic materials such as iron and nickel. Therefore, the conventionally used metallic photon multiplier tubes (PMTs) in PET/CT are not applicable for PET/MR configuration. Instead, silicon photo multipliers (SiPM) and avalanche photodiodes have been introduced as PET/MR compatible photodetectors (2). Accordingly, one of the most important differences between PET/MR and PET/CT equipment is attributed to the photomultiplier's structure and properties. Semi-conductor detectors are mostly superior to the normal PMTs in terms of quantum efficiency and signal quality (3). Nowadays, the providers might start to replace the classical PMTs by SiPM in the new generations of PET/CT devices (4).

Attenuation correction of PET/CT images is made by using attenuation coefficients (μ) derived from CT map (5). In contrast, attenuation correction of PET images in PET/MR is accomplished via variable algorithms that are not as precise as CT. MR image-based atlas and segmentation methods are the most common algorithms, where the attenuation coefficients obtained from CT images are no longer available in PET/MR (6).

National Electrical Manufacturers Association (NEMA) tests of PET scanners has been firstly introduced as NU 2-1994 for performance assessment. It was published by Society of Nuclear Medicine working group in 1991. Meanwhile, similar standards were being conducted in Europe. However, NEMA and ICE are different standards dedicated for the same purpose. Currently, NEMA standards have been updated through new version (NU2-07). The new update is so far similar to ICR standards that renewed in 2002 and 2007. NEMA tests are performed and recorded prior to accepting new devices. NEMA criteria substantially provides appropriate methods to carry out the performance tests, but never specifies any reference limit. The manufacturer should undertake informing the installation site about the reference values and whether the device is sensitive to possible faults and changes in the ambient conditions such as temperature, humidity, etc. In case of inconsistence between the reference values and quality control results, calibration of the machine ought to be performed and thereafter repeating the quality control tests to evaluate the performance again (7). Three performance parameters are forming the baseline of image quality including spatial resolution, contrast and noise (8). Moreover, different standard phantoms were developed for performing NEMA tests and acquiring PET images. All required algorithms to explore the image quality are available, and the conformity of the images obtained from the device is compared to the global standards. The reference values are saved to be used in the upcoming quality control tests of the equipment (9).

The aim of this study was to evaluate the PET scanner's performance of PET/MR and PET/CT systems, which are provided by the same vendor with variation due to different PET scanner design, PMT type, and attenuation correction algorithms.

Materials and Methods

In the current study, NEMA tests (NEMA NU2-07) were performed on PET/CT and PET/MR systems. Both products belong to the same company and supplied with time of flight (TOF) technology: PET/MR General Electric GE Company (SIGNA^{TM} model) and PET/CT GE (Discovery 710 model). The properties of the PET scanner of PET/MR system are outlined as axial field of view (FOV) 25 cm, crystal size 4×5.3×25 mm, LYSO scintillator, trans-axial

FOV 60 cm and SiPMTs. While these for the PET/CT were designed as: axial FOV 15.7 cm, crystal size 4.7×6.3×25 mm, LYSO scintillator, trans-axial FOV 70 cm and metallic PMTs. the varied technical aspects of PET scanner in both PET/MR and PET/CT might arise the difference on the performance.

An ethical consent was not obtained since the study was performed on body phantoms.

NEMA Tests (NEMA NU2-07)

Spatial Resolution

This test set the capability of the PET system to localize the position of a point source after image reconstruction and to measure the tomographic spatial resolution of the device in air (non-scattering medium) with ^{18}F radioisotope. The spatial resolution of the PET system represents the potential of separation between two points after reconstruction in three-dimensional views. Point spread function is often used to reflect the spatial resolution after reconstruction by measuring the photo-peak full width at half maximum (FWHM) and the full width at tenth maximum (FWTM) of 10%.

Measurement Method

Point sources were obtained from 5 mCi ^{18}F solution, then inserted into three capillaries with an inner diameter ≤1 mm and outer diameter ≤2 mm. The sources were placed on the transverse and axial axis at t 1 cm from the center and 10 cm radial offset (Figure 1). 100 000 counts were acquired and filtered back projection was used for multidimensional image reconstruction.

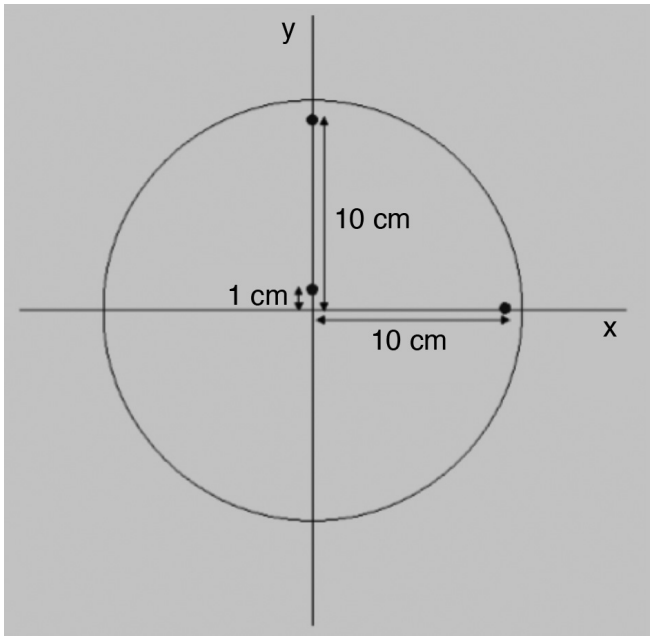

Figure 1. Sources positioning for spatial resolution test

Sensitivity

The detector sensitivity of PET device is defined as the count per unit time of the source activity. The purpose of this test is to measure the ability of the scanner system to detect the annihilations resulting from positrons interaction. The measurements were obtained by using specific phantom made up of 5 aluminum sleeves (tubes) that can be inserted in each other. The internal diameters of the bars are between 3.9 mm - 16.6 mm and the external diameters are between 6.4 mm - 19.1 mm. The thickness of the five aluminum sleeves is equal to 1.25 mm and the length is fixed as 700 mm (Figure 2).

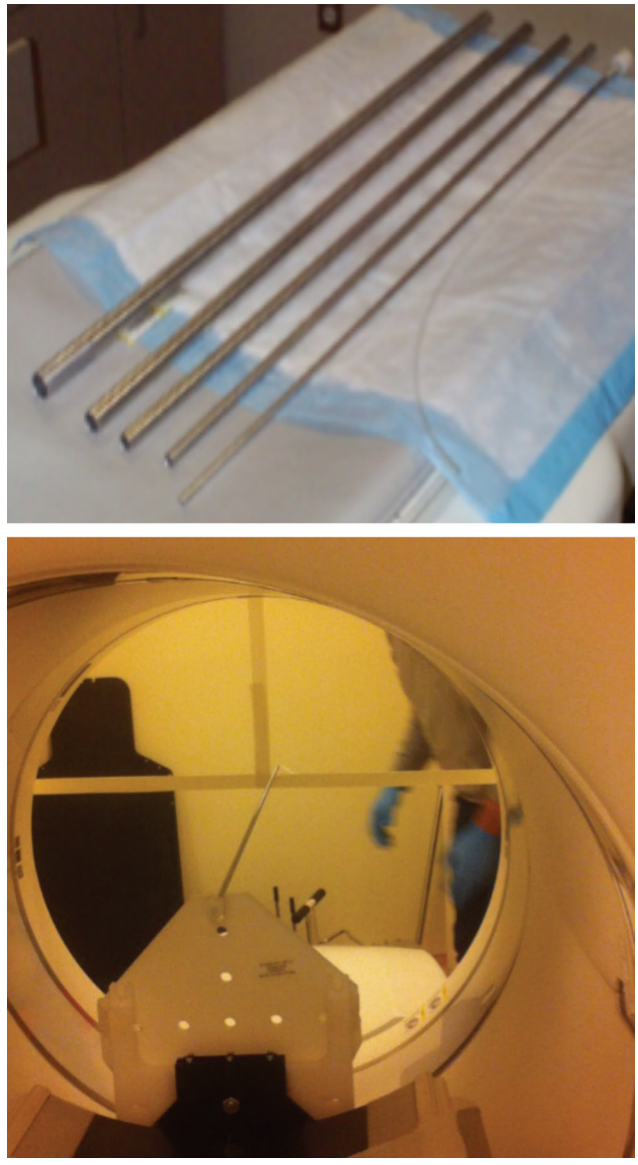

Figure 2. National Electrical Manufacturers Association sensitivity phantom on the (up), centering the source on the (right)

Measurement Method

A low-activity (~ 135 μCi, 5 MBq) of ^{18}F was prepared to measure sensitivity values. A portion of the 700±5 mm plastic tube was filled by ^{18}F mixed with water, then the tube was closed at the two ends. The phantom was positioned trans-axially at the center of FOV, so that a supporting device was required to keep it outside the imaging field. At least 10000 true counts per slice were acquired. This experiment was repeated in two separate locations, at center and 10 cm away from the center. To report the result, average sensitivity obtained from 5 sleeves was evaluated and extrapolated to find the corresponding sensitivity with no attenuation.

Scatter Fraction (SF), Count Rate Performance

Annihilation photons emanated from the patient's body are detected when they hit the PET detectors in a coincidence event. Meanwhile, the events that occur in the detector are classified as random and scatter in addition to the true counts.

The SF of this test measures the sensitivity of the scanner to coincidence events caused by scatter, while the count rate test measures the performance of the PET scanner across variable radioactivity levels. The SF measurement is done at variable activity levels involving negligible system dead time and random events. Scatter was calculated within a radius of 12 cm from center of phantom while scatter photons under the peak was estimated by interpolation between ±2 cm from the center.

Measurement Method

The test phantom consists of a polyethylenated cylinder with an outer diameter of 203 mm, 700 mm length and 0.96 g/cm^3 density. A hole with a diameter of 6.4 mm extends parallel to the central axis of the cylinder at a radial distance of 45 mm. The test phantom was a rod source made of polyethylene or polyethylene coated plastic tube with 800 mm length, the inside diameter was 3.2 mm and the outside diameter was 4.8 mm. This tube was filled with 35 mCi (5.2 mL) ^{18}F and placed in the test phantom through the 6.4 mm diameter hole. To start the test, the highly active source is placed in the FOV of the PET device and many measurements were obtained until the activity in the phantom was quite decayed. Owing to these measurements, true (T), scatter (S), random (R) events are separately counted. Then the rate of scattered counts (SR, equation 1) and the noise equivalent count rate (NECR, equation 2) was calculated with the functions shown below:

$$SR = \frac{SF}{1 - SF} \qquad \text{Eq. (1)}$$

$$NECR = \frac{T^2}{T + S + R} \qquad \text{Eq. (2)}$$

NECR: Noise equivalent count rate, SF: Scatter fraction, T: True, S: Scatter, R: Random, Eq: Equation

Image Quality

The aim of this test is to simulate whole body imaging with hot and cold lesions. Body phantom (IQ) was used with different fillable spheres (Figure 3). The contrast was calculated for both hot and cold spheres. The attenuation and scatter correction accuracy was determined from the uniform background and the residual lung activity.

All corrections were made during image reconstruction with similar imaging parameters in terms of image matrix size, pixel size, slice thickness, reconstruction algorithms, filters and other smoothing applications. VUE point FX with 2 iterations / 28 subsets and 5 mm filter cutoff was employed for image reconstruction in PET/MR, and VUE point FX with 3 iterations / 24 subsets and 5.5 mm filter cutoff in PET/CT. Four classes Dixon method was used for photon attenuation correction in PET/MR.

Image Quality and Calculation Method

Initially, background activity concentration of the body phantom was about 0.14 μCi/cc (±5%). This corresponds to the concentration of typical whole body imaging (10 mCi/70000 cc). Hot lesions were filled with activity ratio 8:1 to that in background while the cold lesions were filled with free water. The phantom with 700 mm linear line was filled with 3.08 mCi ^{18}F that is sufficient for activity concentration equal to the background activity concentration of the body phantom. Two large spheres (28 and 37 mm) were filled with water for imitating cold lesions and the other spheres (10, 13, 17 and 22 mm) were filled with ^{18}F analogous to hot lesions.

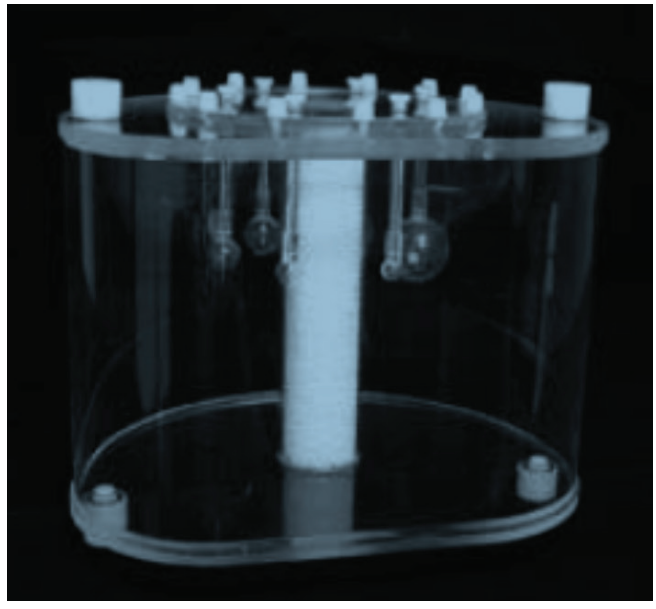

Figure 3. Positron emission tomography body phantom, the middle pipe represents lungs, six fillable spheres with inner diameters of 10, 13, 17, 22, 28 and 37 mm

The analysis was made on transverse sections in which a circular regions of interest (ROI) was drawn as close as possible to the dense inner diameter of every cold and hot sphere. For background, ROIs of the same size of the ROIs drawn around the hot and cold spheres were delineated near the edge of phantom up to 12 background ROIs per sphere (Figure 4).

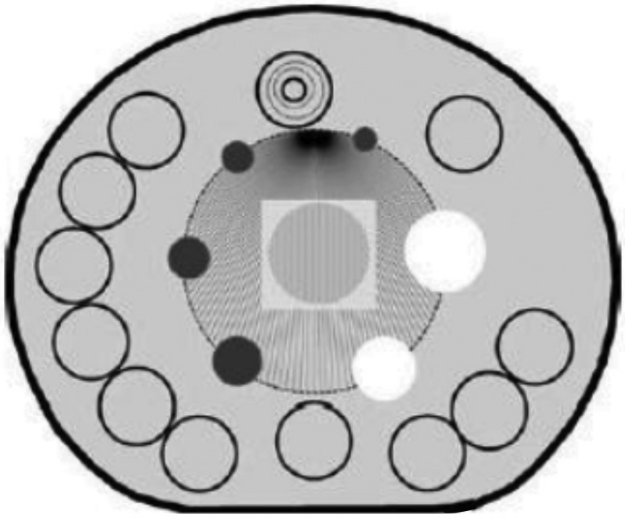

Figure 4. Background regions of interest for image quality analysis

Lesion contrast calculation was performed according to equation (3).

$$\%Q_{H,J} = [(C_{H,J}/C_{B,J}) -1] / [(a_H / a_B)-1] \times 100 \qquad \text{Eq. (3)}$$

$$\%Q_{H,J} = [(C_{H,J}/C_{B,J}) -1] / [(a_H / a_B)-1] \times 100 \qquad \text{Eq. (3)}$$

$C_{H,J}$: j average counts of hot sphere's regions of interest,
$C_{B,J}$: j average counts of background's regions of interest drawn for hot sphere,
a_H: Hot sphere's activity concentration, a_B: Background's activity concentration

Count Loss and Random Event Correction Accuracy

The accuracy of count losses and random correction is measured by comparing the true counts rate, where count losses and random correction are made, to the rate derived from measurements with negligible count losses and random events. The data acquired for the count rate and scatter fraction test was also used for this test.

The line source of the phantom was placed at the closest area to the bed (Figure 5). Body phantom was placed on the tip of the phantom. From the high counting rate to the low rate, subsequent images were acquired with 500,000 counts at certain time intervals. Then, true counts were measured at high and low activity levels. True count rate at low activity levels was extrapolated to determine the amount of deviation (percentage of error) from that at high activity level.

Figure 5. Positioning of polyethylene and body phantom

Results

Spatial Resolution

The measured spatial resolution of PET/MR and PET/CT were shown in a pattern of FWHM and FWTM on transverse and axial dimensions. The deviations in the localization on the three axes (x, y, z) were given in Table 1. In addition, the measurements obtained at 1 cm and 10 cm radial offset from the center is seen in Table 2.

Table 1. Deviations in the position of the sources for spatial resolution measurement in positron emission tomography/magnetic resonance and positron emission tomography/computed tomography equipment

Source no and position	PET/MR			PET/CT		
	Axis deviation (mm)			Axis deviation (mm)		
	x	y	z	x	y	z
1. Center	-0.2	-9.6	-0.5	-1.1	-0.5	0.0
2. X-axis	0.1	-99.4	18	-1.2	0.0	-1.5
3. Y-axis	100.1	18	-0.8	-1.3	-0.7	-0.3

PET/MR: Positron emission tomography/magnetic resonance, PET/CT: Positron emission tomography/computed tomography

Sensitivity

The sensitivity measured at the center of gantry and 10 cm radial offset in PET/MR was 22.2 cps/kBq and 21.74 cps/kBq, respectively. The acceptance limit given by the manufacturer is 21.97 cps/kBq for PET/MR (Figure 6). In comparison to PET/CT, the sensitivity was measured as 5.458 cps/kBq at the center of gantry while the sensitivity at 10 cm from the center was not measured. The limit of acceptance given by the manufacturer is 8.9 cps/kBq.

Scatter Fraction, Dose Rate Performance

Scatter Fraction

The scatter fraction in PET/MR was 43.4% at NECR peak 218 kcps and corresponding activity concentration 17.7 kBq/cc, in which the scatter fraction limit supplied by the manufacturer was 45%. PET/CT system showed less scatter fraction as 39.2% at 72 kcps NECR peak corresponded to activity concentration of 24.3 kBq/cc, while the reference value provided by the manufacturer was 42% (Figure 7, 8).

Table 2. Spatial resolution values in positron emission tomography/magnetic resonance and positron emission tomography/computed tomography

	PET/MR		PET/CT	
	FWHM (mm)	FWTM (mm)	FWHM (mm)	FWTM (mm)
1 cm radius:				
Transverse	4.30	8.62	4.73	9.13
Axial	5.79	11.75	4.93	9.56
10 cm radius:				
Radial	5.79	10.82	5.35	10.08
Transverse	4.40	8.35	4.83	9.55
Axial	7.26	15.15	5.62	11.42

PET/MR: Positron emission tomography/magnetic resonance, PET/CT: Positron emission tomography/computed tomography, FWHM: Full width at half maximum, FWTM: Full width at tenth maximum

Count Loss measurement

In PET/MR, NECR value was measured as 218 kcps at activity concentration of 17.7 kBq/cc. The limit value of NECR was 210 kcps as ecommended by the manufacturer is given as 210 kcps. NECR value in PET/CT was 72.0 kcps at activity concentration of 24.3 kBq/cc. The manufacturer's NECR limit value was given as 68 kcps (Figure 8).

Image Quality

Contrast values of hot spheres with 10, 13, 17, and 22 mm diameter in PET/MR were 56%, 72%, 78% and 85%, respectively, while the provided contrast values from the manufacturer were 30%, 35%, 45% and 55%. Contrast values of background ROIs of the hot spheres were found to be 7.8%, 5.9%, 5.1%, 5.3%, 5.7% and 6%. A threshold value of 10% is given for lung residual activity while the measured value was (1.2%). Contrast value of hot spheres with 10, 13, 17, and 22 mm diameter in PET/CT was found as 53%, 66%, 72% and 79%, respectively. Contrast values provided by the manufacturer are 20%, 30%, 40% and 50%. Contrast values of background ROIs of the hot spheres were 9.5%, 7.6%, 6%, 4.2%, 3.6% and 3%, respectively. A threshold value of 20% is given for the residual activity of lung. The measured value was %13.5 (Figure 9).

Count Loss and Random Event Correction Accuracy

True counts rate at high activity level were obtained from 81 slices of polyethylene phantom and the changes in the maximum and minimum values of true counts at

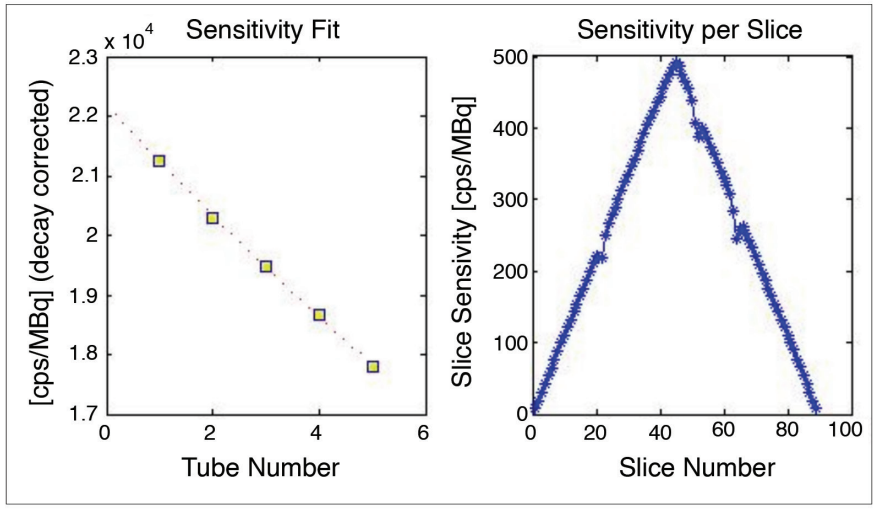

Figure 6. Measurement of sensitivity in positron emission tomography/magnetic resonance. On the left, counts decrease as the rod's thickness increases due to attenuation. On the right, the measured sensitivity changes per section from outside to inside and from inside to outside

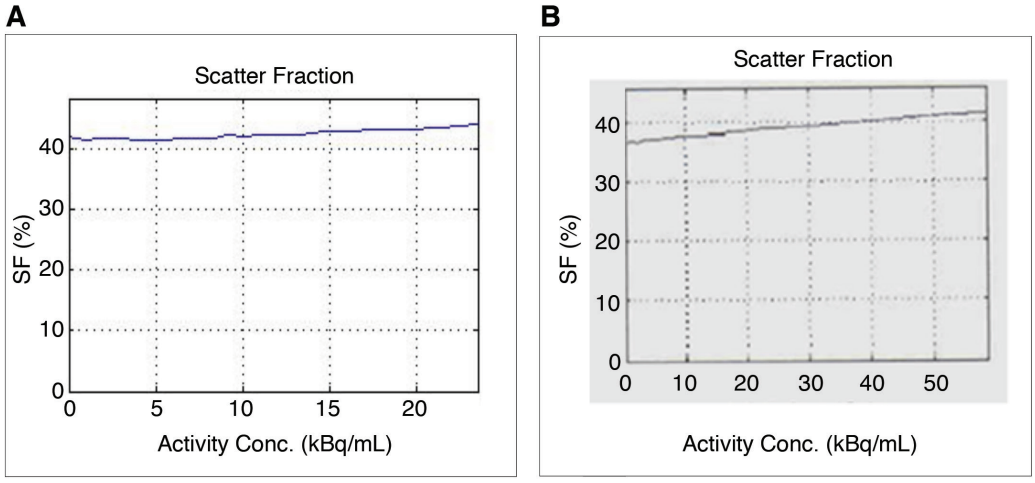

Figure 7. Positron emission tomography/magnetic resonance (A), positron emission tomography/computed tomography (B) measured scatter fraction. *SF: Scatter fraction*

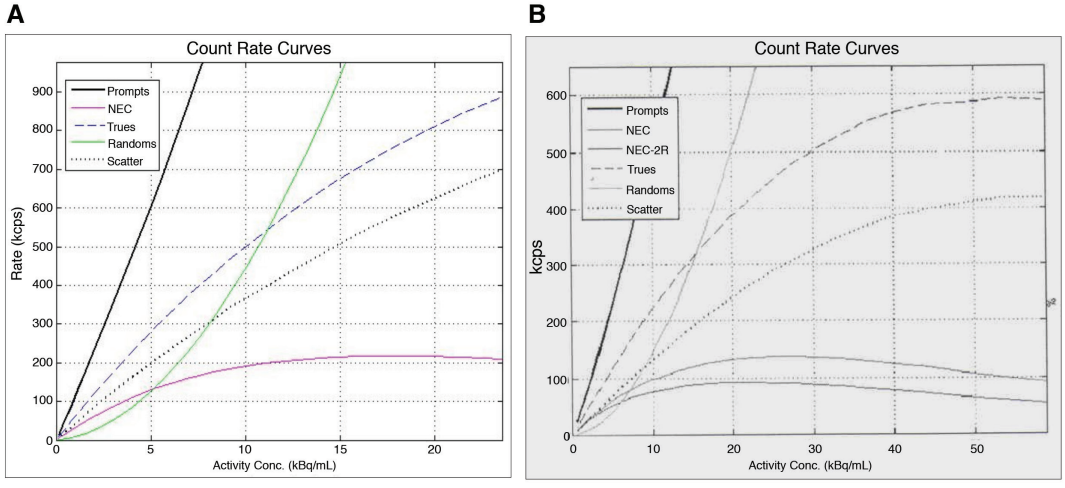

Figure 8. Positron emission tomography/magnetic resonance (A), positron emission tomography/computed tomography (B) measured noise equivalent count rate values

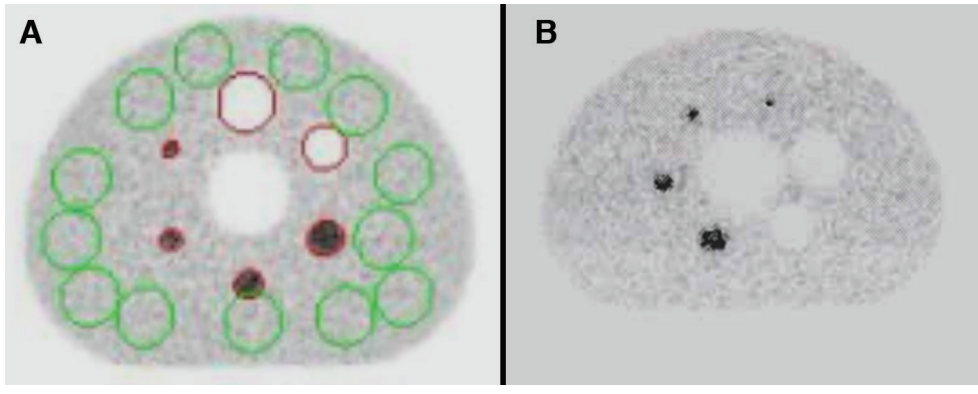

Figure 9. Body phantom image quality. Positron emission tomography/magnetic resonance (A), positron emission tomography/computed tomography (B)

low activity level were analyzed. The true count rate at low level was extrapolated to determine the amount of deviation (percent error) from that at high activity level. The measured percentage error in PET/MR was 3.4% while it was found 3.1% in PET/CT.

Discussion

The endeavor of the present work is to evaluate the performance of PET scanner as a part of two different modalities manufactured by the same vendor. The contrast values of 13 and 22 mm hot spheres in PET/MR was calculated to be 72% and 85%, respectively, while the contrast values in PET/CT for 13 and 22 mm hot lesions were 53% and 78%, respectively. The sensitivity at the center was 22.2 cps/kBq in PET/MR, and 5.48 cps/kBq in PET/CT. In comparison, Yester et al. (10) investigated the performance characteristics of GE PET scanner (Company/ Discovery 710 model) using NEMA tests. The reported spatial resolution in that study was 4.6 mm at 1 cm from the center, and 5.2 mm at 10 cm. Likewise, the average spatial resolution in our study at 1 cm and 10 cm was 4.8 mm and 5.3, respectively. The sensitivity was also reported as 7.1 cps/kBq at the center and the contrast of hot spheres was reported as 70% and 80% for hot spheres of 13 mm and 22 mm diameter. In general, the sensitivity of PET/MR system seems to be higher owing to the fact that PET detectors are functioning with new SiPMT technology. The assembly of SiPMTs is composed of numerous microcells that result in larger detection efficiency, small physical profile, and supply high gain with low operating voltage (20-80 v).

New features of PET gantry including wider axial FOV (25 cm) and less ring diameter in PET/MR improve the scanner sensitivity and spatial resolution compared with the conventional PET/CT gantry. Similarly, Grant et al. (11) published a study involved implementation of NEMA NU 2-2012 protocol to evaluate PET performance in PET/MR (GE SIGNA^{TM} model) including: spatial resolution, NECR, sensitivity, accuracy, and image quality. The scanner showed an average of 4.4, 4.1, and 5.3 mm FWHM for radial, tangential, and axial spatial resolutions, respectively, at 1 cm from the trans-axial FOV center. The peak NECR of 218 kcps and a scatter fraction of 43.6% were achieved at activity concentration of 17.8 kBq/ml. The sensitivity at the center was 23.3 cps/kBq. The maximum relative slice count rate error below peak NECR was 3.3%, and the residual error from attenuation and scatter corrections was 3.6%. The study also mentioned that continuous MR pulsing had either no effect or a minor effect on each measurement.

Additional discrepancy between PET/MR and PET/CT systems originated from the difference in the attenuation correction algorithms (12). The applied attenuation correction in GE Signa PET/MR is atlas based for brain studies and Dixon 4-classes segmentation for the remaining whole body. The MR based attenuation correction of PET/MR is unlike CT based attenuation correction, since it does not directly measure the attenuation coefficients of tissue. Instead, the attenuation is made from information about proton density and relaxation time (fat and water) named by Dixon segmentation. This method has been compared to CT based correction with satisfactory consistence. On the other hand, certain anatomical structures still constitute a challenge to PET/MRI; for example; lung, air, bone and metallic regions like implants. These objects might show quite low MR signal despite their different attenuation properties. However, several studies comparing the efficacy of PET/MR and PET/CT systems in terms of lesion detection stated limitations related to attenuation correction algorithms used in PET/MR. Drzezga et al. (13) performed a study involving twenty-two patients who were subjected to both PET/MR and PET/CT imaging with a standard protocol. The attenuation corrections of PET/MR images were performed using Dixon segmentation and the attenuation correction of PET images was also derived from CT map. As a result, all lesions were detected in PET/MR and PET/CT, and no differences were reported between the two modalities. Wiesmüller et al. (14) reported that 99.2% of the visible lesions in PET/CT were also detected in PET/MR, while 4 patients had extra lesions identified only in PET/MR. There are several experimental trials has been made using NEMA IQ phantom. For instance, Oehmigen et al. (15) evaluated PET/CT and PET/MR images of IQ phantom filled with 8:1 lesion/background ^{18}F concentration ratio. It was determined that images in PET/MR can be acquired at the same level of quality as PET/CT with reducing the activity ratio by 3 times owing to the high sensitivity.

In PET/CT, photon attenuation coefficients are usually derived from the patient's CT images (CT μ map) and PET counts correction is then made pixel by pixel. While in PET/MR where patient's CT images are no longer available, many studies indicated that the algorithms obtained from MR images could be successfully implemented to correct PET/MR images. One of the most relevant studies on this subject was reported by Martinez-Möller et al. (16). Throughout this study, standard uptake values were evaluated in 35 patients with multiple lungs lesions, bones and neck region. They performed attenuation corrections via CT and MR images of the same patients with data derived from CT (4 classes - segmented attenuation map from CT) and they concluded that there was no significant difference between the algorithms operated in PET/MR as compared to PET/CT results. In fact, there is no similarity between annihilations emission in PET and MR signal to be used in the attenuation correction. In addition, MR- image based and CT-based attenuation algorithms for NEMA IQ phantom were compared in which the image quality and contrast were found to increase with the CT-based attenuation correction (17).

Karlberg et al. (18) compared the results of NEMA tests of PET/CT with TOF and Siemens PET/MR without TOF. It was

shown that the sensitivity, NECR values and lesion contrast measurement results were superior in PET/MR when compared to PET/CT. Finally, in the present study, the mean contrast value of five hot lesions in PET/CT was 67.5% while it was 72.7% in PET/MR. The image contrast in PET/MR was superior to PET/CT taking into consideration both systems are incorporating TOF technology. Count loss and random event correction accuracy was also within a close range and acceptable limits.

Conclusion

It was concluded that the sensitivity of PET/MR system is about 4 folds larger than PET/CT, and the contrast of PET/MR was ~ 9% higher than PET/CT, indicating that excellent clinical PET images might be achieved with low administered dose and/or a short acquisition time in PET/MRI acquisition.

Ethics

Ethics Committee Approval: The ethical consent was not working because the study is phantom study.

Informed Consent: The study is phantom study.

Peer-review: Externally peer-reviewed.

Authorship Contributions

Surgical and Medical Practices: M.D., T.T., M.A., H.Ç., H.S.S., N.Y, K.S., Concept: M.D., T.T., M.A., H.Ç., H.S.S., N.Y, K.S., Design: M.D., T.T., M.A., H.Ç., H.S.S., N.Y, K.S., Data Collection or Processing: M.D., T.T., M.A., H.Ç., H.S.S., N.Y, K.S., Analysis or Interpretation: M.D., T.T., M.A., H.Ç., H.S.S., N.Y, K.S., Literature Search: M.D., T.T., M.A., H.Ç., H.S.S., N.Y, K.S., Writing: M.D., T.T., M.A., H.Ç., H.S.S., N.Y, K.S.

Conflict of Interest: No conflict of interest was declared by the authors.

Financial Disclosure: The authors declared that this study received no financial support.

References

1. Torigian DA, Habib Zaidi H, Kwee TC, Saboury B, Udupa JK, Cho ZH, Alavi A. PET/MR Imaging: Technical Aspects and Potential Clinical Applications. Radiology 2013;267:26-44.
2. Roncani E, Cherry SR. Application of silicon photomultipliers to positron emission tomography. Ann Biomed Eng 2011;39:1358-1377.
3. Britvich I, Johnson I, Renker D, Stoykov A, Lorenz E. Characterization of Geiger-mode avalanche photodiodes for medical imaging applications. Nucl Instrum Methods Phys Res A 2007;43:2044-2048.
4. Schaart DR, Seifert S, Vinke R, van Dam HT, Dendooven P, Löhner H, Beekman FJ. LaBr(3):Ce and SiPMs for time-of-flight PET: Achieving 100 ps coincidence resolving time. Phys Med Biol 2011;56:4135-4145.
5. Martinez-Möller A, Nekolla SG. Attenuation correction for PET/MR: problems, novel approaches and practical solutions. Z Med Phys 2012;22:299-310.
6. Martinez-Möller A, Souvatzoglou M, Delso G, Bundschuh RA, Chefd'hotel C, Ziegler SI, Navab N, Schwaiger M, Nekolla SG. Tissue classification as a potential approach for attenuation correction in whole-body PET/MRI: evaluation with PET/CT data. J Nucl Med 2009;50:520-526.
7. National Electrical Manufacturers Association. "NEMA Standards Publication NU 2-2007, Performance measurements of positron emission tomographs". Rosslyn VA 2007;26-33.
8. Sorenson JA, Phelp ME. Physics in Nuclear Medicine. Grune and Stration, Inc, 2003;227-251.
9. National Electrical Manufacturers Association. Performance measurements of position emission tomographs NEMA Standards Publication NU 2-2007. 2007.
10. Yester M, Senan RA, White S. NEMA testing of GE Discovery 710 PET scanner compared to a simplified protocol for routine testing of PET scanners. J Nucl Med 2014;55:2157.
11. Grant AM, Deller TW, Khalighi MM, Maramraju SH, Delso G, Levin CS. NEMA NU 2-2012 performance studies for the SiPM-based ToF-PET component of the GE SIGNA PET/MR system. Med Phys 2016;43:2334.
12. Ziegler S, Jakoby BW, Braun H, Paulus DH, Quick HH. NEMA image quality phantom measurements and attenuation correction in integrated PET/MR hybrid imaging. EJNMMI Phys 2015;2:18.
13. Drzezga A, Souvatzoglou M, Eiber M, Beer AJ, Fürst S, Martinez-Möller A, Nekolla SG, Ziegler S, Ganter C, Rummeny EJ, Schwaiger M. First clinical experience with integrated whole-body PET/MR: comparison to PET/CT in patients with oncologic diagnoses. J Nucl Med 2012;53:845-855.
14. Wiesmüller M, Quick HH, Navalpakkam B, Lell MM, Uder M, Ritt P, Schmidt D, Beck M, Kuwert T, Von Gall CC. Comparison of lesion detection and quantitation of tracer uptake between PET from a simultaneously acquiring whole-body PET/MR hybrid scanner and PET from PET/CT. Eur J Nucl Med Mol Imaging 2013;40:12-21.
15. Oehmigen M, Ziegler S, Jakoby BW, Georgi JC, Paulus DH, Quick HH. Radiotracer Dose Reduction in Integrated PET/MR: Implications from National Electrical Manufacturers Association Phantom Studies. J Nucl Med 2014;55:1361-1367.
16. Martinez-Möller A, Souvatzoglou M, Delso G, Bundschuh RA, Chefd'hotel C, Ziegler SI, Navab N, Schwaiger M, Nekolla SG. Tissue classification as a potential approach for attenuation correction in whole-body PET/MRI. J Nucl Med 2009;50:520-526.
17. Delso G, Fürst S, Jakoby B, Ladebeck R, Ganter C, Nekolla SG, Schwaiger M, Ziegler SI. Performance measurements of the Siemens mMR integrated whole-body PET/MR scanner. J Nucl Med 2011;52:1914-1922.
18. Karlberg AM, Sæther O, Eikenes L, Goa PE. Quantitative comparison of PET Performance-Siemens Biograph mCT and mMR. EJNMMI Phys 2016;3:5.

Original Article
Mol Imaging Radionucl Ther 2018;27:19-24 DOI:10.4274/mirt.51423

Contribution of ^{18}F-FDG PET/CT to Staging of Head and Neck Malignancies

Baş ve Boyun Malignitelerinin Evrelemesinde ^{18}F-FDG PET/BT'nin Katkısı

Yeşim Ceylan[1], Özgür Ömür[2], Filiz Hatipoğlu[3]
[1]*Adıyaman Faculty of Medicine, Training and Research Hospital, Clinic of Nuclear Medicine, Adıyaman, Turkey*
[2]*Ege University Faculty of Medicine, Department of Nuclear Medicine, İzmir, Turkey*
[3]*Bilim Spect Nuclear Medicine Center, İzmir, Turkey*

Abstract

Objectives: Accurate staging of head and neck cancer (HNC) plays an important role in patient management as well as protection of functional characteristics of the head and neck region. Our aim was to investigate the contribution of 2-[^{18}F]-fluoro-2-deoxy-d-glucose (FDG) positron emission tomography/computed tomography (PET/CT) as part of HNC staging to clinical evaluation and treatment planning.

Methods: Clinical records of 138 HNC cases who has undergone ^{18}F-FDG PET/CT imaging were retrospectively reviewed. Sixty-five cases who had accessible clinical follow-up data were included in the study group, and their PET/CT and conventional imaging findings were evaluated.

Results: In the case group with a PET/CT and magnetic resonance imaging (MRI) for evaluation of primary lesion the sensitivity rates for PET/CT and MRI were calculated as 91.3% and 82.6%, the positive predictive values (PPV) as 91.3% and 82.6%, specificity as 71.4% and 42.8%, and the negative predictive value (NPV) as 71.4% and 42.8%, respectively. In terms of metastatic lymph node evaluation, the sensitivity was calculated as 100% and 88.8%, the NPV as 100% and 83.3%, respectively. The PPV and specificity was 100% for both modalities. In the case group with CT for primary lesion evaluation, the sensitivity and PPV were found as 95.2% and 100% for PET/CT, and as 85.7% and 94.7% for CT, respectively. in metastatic lymph node evaluation, the sensitivity was found as 100% for PET/CT and 50% for CT, and the PPV, specificity and NPV were determined as 100% for both methods. PET/CT findings resulted in a change in 'tumor, node, metastasis' staging in 5 cases.

Conclusions: PET/CT in HNC contributes to staging, thus playing a role in treatment planning, especially in patients with locally advanced disease.

Keywords: Head and neck cancer, PET/CT, ^{18}F-FDG

Öz

Amaç: Baş ve boyun kanserlerinde (BBK) doğru evreleme, uygun tedavi modalitesinin seçilmesi ve baş boyun yapılarının işlevsel özelliklerinin korunmasında önemli rol oynamaktadır. Çalışmamızda BBK'lerin evrelendirilmesinde 2-[^{18}F] floro-2-deoksi-d-glukoz (^{18}F-FDG) pozitron emisyon tomografisi/bilgisayarlı tomografi (PET/BT) görüntülemenin klinik değerlendirme ve tedavi planlamasına katkısı araştırıldı.

Yöntem: ^{18}F-FDG PET/BT görüntüleme uygulanan 138 BBK'lı olgunun klinik kayıtları retrospektif olarak incelendi. Klinik izlem verilerine ulaşılabilen 65 olgu çalışma grubuna alındı ve olguların PET/BT ve konvansiyonel görüntüleme bulguları değerlendirildi.

Address for Correspondence: Filiz Hatipoğlu MD, Bilim Spect Nuclear Medicine Center, İzmir, Turkey
Phone: +90 533 378 53 37 E-mail: karagozfiliz@yahoo.com ORCID ID: orcid.org/0000-0002-6893-434X
Received: 20.07.2017 **Accepted:** 08.11.2017

Öz

Bulgular: Primer lezyon değerlendirmede PET/BT ve manyetik rezonans görüntülemesi (MRG) olan olgu grubunda PET/BT ve MRG için sırasıyla sensitivite %91,3, %82,6, pozitif prediktif değer (PPD) %91,3 ve %82,6, spesifite %71,4 ve %42,8 ve negatif prediktif değer (NPD) %71,4 ve %42,8 olarak hesaplandı. Metastatik lenf nodu değerlendirmede ise PET/BT ve MRG için sırasıyla sensitivite %100 ve %88,8, NPD %100 ve %83,3, PPD ve spesifite ise her iki yöntem için de %100 olarak hesaplandı. BT'si olan olgu grubunda primer lezyon değerlendirmede sensitivite PET/BT için %95,2, BT için %85,7, PPD %100 ve %94,7 olarak bulundu. Metastatik lenf nodu değerlendirmede sensitivite PET/BT için %100, BT için %50, PPD, spesifite ve NPD %100 olarak bulundu. PET/BT bulguları 5 olguda 'tümör, nod ve metastaz' evrelemesinde değişikliğe neden oldu.

Sonuç: PET/BT BBK'da evrelemeye katkıda bulunarak özellikle lokal ileri evredeki olgularda tedavi planlamasında önemli rol oynar.

Anahtar kelimeler: Baş ve boyun kanserleri, PET/BT, ^{18}F-FDG

Introduction

Thorough evaluation of patients with head and neck cancer (HNC), which include malignancies originating from the paranasal sinus, nasal-oral cavity, pharynx and larynx, is fundamental in order to apply the most appropriate treatment while optimizing functional and cosmetic outcomes. Ultrasound, computed tomography (CT) and magnetic resonance imaging (MRI) are used prior to selecting treatment modality as well as endoscopic evaluation. CT is especially useful in the evaluation of lung metastasis and local or metastatic bone involvement. However, it is generally insufficient in determining cartilage invasions and in differentiating tissue thickening from tissue damage caused by the tumor (1). MRI is superior to CT in terms of local evaluation of the primary tumor by showing bone marrow involvement (2). Nevertheless, conventional imaging methods are inadequate in small or localized submucosal tumors in determining relapse or residual lesion after radiotherapy (RT) and surgery (3). In addition, the presence of morphologic criteria suggesting lymph node metastasis such as central necrosis, early contrast enhancement, irregular boundary and circular shapes, do not have sufficient specificity in diagnosing metastases. Thus, 2-[^{18}F]-fluoro-2-deoxy-d-glucose (^{18}F-FDG) positron emission tomography (PET)/CT, which provides both metabolic and anatomical information and simultaneously evaluates local tumor and distant metastases, is required for accurate staging (4).

In this study, it was aimed to investigate the contribution of ^{18}F-FDG PET/CT imaging method as part of HNC staging to clinical evaluation and treatment planning.

Materials and Methods

Patient Group

The study protocol was approved by the Ege University Faculty of Medicine, Ethical Committee of Clinical and Laboratory Research Department (Date 24 January 2014, Protocol number: 14-1.1/2). The study was performed in accordance with the ethical standards laid down by Declaration of Helsinki in 1964 and all its subsequent revisions. The clinical records of 138 HNC cases who were referred to the Department of Nuclear Medicine between 2 January 2012 and 1 November 2013 were examined. Our study group consisted of 65 patients who has undergone whole-body PET/CT imaging and whose follow-up data were accessible. ^{18}F-FDG PET/CT imaging was performed for staging in 37 cases and re-staging in 28 cases. Forty-nine (75.3%) patients were male and 16 (24.7%) were female. Their mean age was 68±7.07 years (age interval: 18–89 years). Percentage distribution of the patients in the case group according to primary tumor histopathology is shown in Figure 1.

Patient Preparation and PET/CT Imaging

Before the PET/CT study, detailed clinical information of the patients and informed consent were obtained. All patients fasted for 6 hours. If the blood glucose level was under 200 mg/dL, 7-15 mCi (259-555 MBq) ^{18}F-FDG was administered intravenously. Patients then rested in a quite dark room just prior to the exam. Approximately 45-90 minutes after the injection, image acquisition was performed.

^{18}F-FDG PET/CT imaging was performed by using the Siemens Biograph 16 TruePoint PET/CT scanner (Siemens Medical Solutions, Inc. USA) with a slice thickness of 5 mm. PET/CT data were acquired from the vertex to the proximal thighs in supine position with the arms raised over head, and additional head and neck images were acquired with the arms down. For attenuation correction and anatomic correlation, CT data was obtained from the vertex to the upper thighs (130 keV, 120 mA) with a rotation time of 0,6 sec and a slice thickness of 5 mm, 1 mm/sec bed speed. Immediately after CT data acquisition, PET scanning was performed in 2D mode with a scan duration of 1.8 min per bed. PET data were reconstructed iteratively (matrix size 512x512) with ordered subsets expectation maximization algorithm (3 iteration, 21 subset).

PET/CT data were examined on Syngo MM Workstation. Images were evaluated qualitatively and quantitatively. Two nuclear medicine specialists examined the PET/CT images for qualitative evaluation. According to visual analysis,

the reports were defined as 'abnormal' when ^{18}F-FDG-uptake was greater than background blood pool activities or surrounding normal tissue. For quantitative analysis of PET images, region of interest was drawn around the most intense ^{18}F-FDG uptake and maximum standard uptake value (SUV_{max} corrected for body weight) was calculated.

Data Analysis and Statistics

SPSS package program (Statistical Package for the Social Sciences) version 18.0 (SPSS Inc., Chicago, Illionis, USA) was used for statistical analysis. Mann-Whitney U test was used for evaluation of differences in SUV_{max} between malignant and benign lesions, and McNemar test was used in comparison of the results of conventional methods. P value of <0.05 was considered as significant.

Results

The average SUV_{max} of primary lesions and metastatic lymph nodes in study patients are shown in Table 1. The difference between the SUV_{max} of malignant and benign lesions that were confirmed histopathologically in the primary tumor sites (p=0.013) and lymph nodes (p=0.003) was found to be significant.

Table 1. Correlation of maximum standard uptake value and histopathologic results in the primary lesion area and regional lymph node

Histopathology	Primary tumor mean SUV_{max}	p value	Hypermetabolic lymph node mean SUV_{max}	p value
Malignant	16.2±8.5	0.013	15.7±12.1	0.003
Benign	5.6±4.1		4.7±2.7	
Total	15.6±8.5		11.6±10.4	

SUV_{max}: Maximum standard uptake value

Among 65 patients whose clinical data were examined, MRI was present in 29 cases, CT in 21 cases, and both CT and MRI in 1 case in addition to ^{18}F-FDG PET/CT.

Comparative Evaluation of ^{18}F-FDG PET/CT and MRI Findings

Within the group of patients with MRI (30 cases), 21 had pathological findings in primary lesion localization with MRI and PET/CT. Nineteen of these 21 patients were considered as true positive while the remaining 2 patients were accepted as false positive, according to their clinical follow-ups. Five of the 30 patients were negative on both MRI and PET/CT. According to histopathologic confirmation, two patients were accepted as false negative, one of them had spindle cell carcinoma on the floor of the mouth and the other one had larynx squamous cell carcinoma (Figure 2).

Lesions were observed in the clinical evaluation of two patients who had no pathological findings on MRI (false negative), but an increased metabolic activity was observed in the localization of the primary lesion on PET/CT (true positive). For the other two patients who had pathological findings on MRI and no hypermetabolic lesions on PET/CT, MRI was accepted as false positive according to their clinical follow-up.

In 5 of 14 cases, the pathological lymph node was not defined on MRI or PET/CT as confirmed by histopathologic biopsy (true negative in both examinations). In all the remaining 9 cases with histopathologically proven

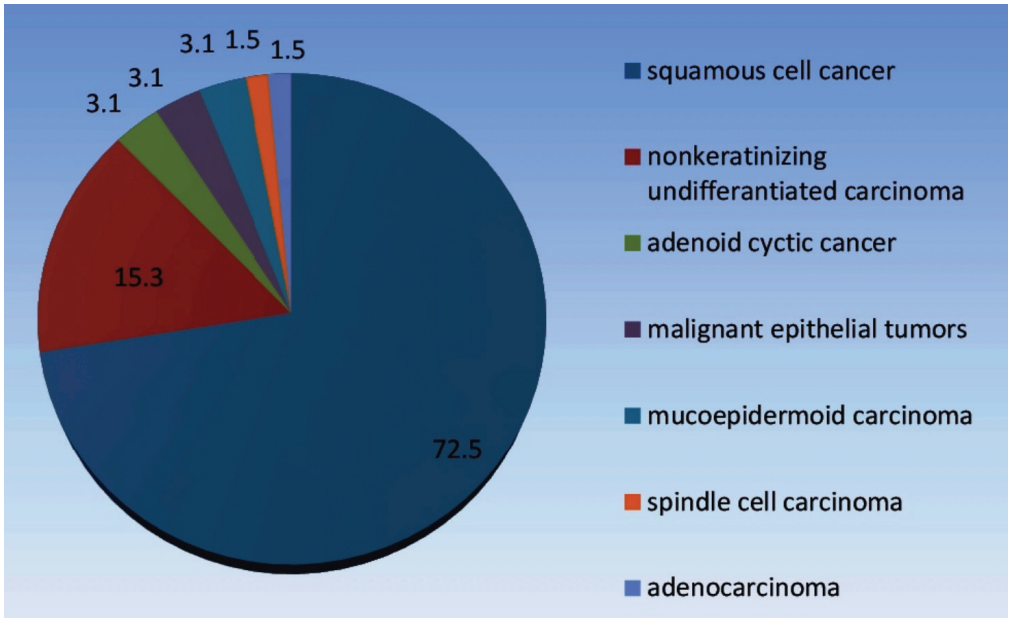

Figure 1. Percentage distribution of the case group according to tumor histopathology

metastatic lymph nodes, hypermetabolic lymph nodes were defined on PET/CT (9 real positives), and in 8 of these patients pathological lymph nodes were demonstrated with MRI (8 true positives) while in 1 patient MRI could not detect the metastatic lymph node (1 false negative). PET/CT did not cause any change in the treatment protocol or in staging of this patient with a T3 tumor.

The sensitivity, specificity, positive predictive value (PPV) and negative predictive value (NPV) in evaluation of primary lesions and metastatic lymph node with MRI and ^{18}F-FDG PET/CT are outlined in Table 2.

Comparative Evaluation of ^{18}F-FDG PET/CT and CT Findings

In the study group, 22 cases had a diagnostic neck CT. In a case with laryngeal carcinoma, despite asymmetrical thickening in the vocal cord, increased ^{18}F-FDG uptake was not observed on PET/CT (false negative). The pathologic lesion was demonstrated in contrast-enhanced CT and then the presence of a tumor was verified histopathologically (true positive).

In another patient who had no local recurrence on PET/CT and no malignant lesion in histological examination, a pathologic finding was detected on contrast-enhanced CT (false positive).

Table 2. Diagnostic competence of positron emission tomography/computed tomography and magnetic resonance imaging in the evaluation of primary tumor and metastatic lymph node

	Primary tumor (n=30)		Metastatic lymph node (n=14)	
	PET/CT	MRI	PET/CT	MRI
Sensitivity	91.3%	82.6%	100%	88.8%
Specificity	71.4%	42.8%	100%	100%
PPV	91.3%	82.6%	100%	100%
NPV	71.4%	42.8%	100%	83.3%

MRI: Magnetic resonance imaging, PET/CT: Positron emission tomography/computed tomography, PPV: Positive predictive value, NPV: Negative predictive value

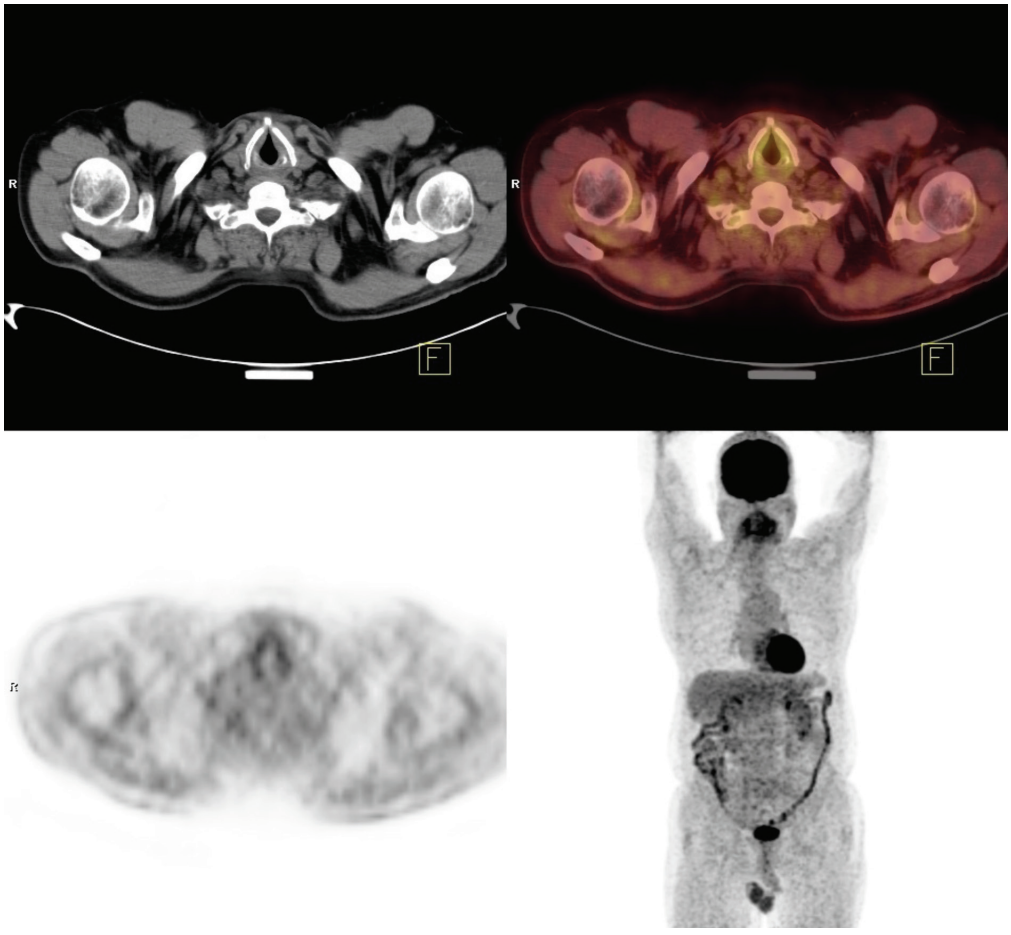

Figure 2. Patient with larynx squamous cell carcinoma. No pathologic findings with ^{18}F-FDG positron emission tomography/computed tomography, left vocal cord histopathology report is compatible with carcinoma *in situ*

Among the case group including 22 patients with neck CT and PET/CT, a metastatic lymph node was not observed on CT or PET/CT in 4 of 10 cases who had pathological confirmation (true negative). In 6 cases with metastatic lymph nodes on pathologic examination, PET/CT defined a pathological hypermetabolic lymph node (6 true positives), whereas CT did not define a metastatic lymph node in 3 of these 6 cases (3 true positives, 3 false negatives).

In the patients with a PET/CT and a contrast-enhanced CT, the results of sensitivity, specificity, PPV and NPV in primary lesion evaluation and metastatic lymph node determination are specified in Table 3.

Contribution of ^{18}F-FDG PET/CT in Staging and Re-staging of All Patients

PET/CT suggested the same disease stage with conventional imaging methods in 27 of 37 cases. However, in five cases who had suspicious findings with conventional methods, PET/CT indicated stage 2 (T2N0M0) disease in 2 patients, stage 4 (T4aNxM0, TxN2bM0) in 2 patients, and stage 3 (T3N1M0) in 1 patient, and it resulted in a change in staging (Table 4). In 25 of 28 cases who had conventional imaging, PET/CT imaging was obtained for re-staging purposes and it did not cause any change in 'tumor, node, metastasis' (TNM) classification.

Table 3. Diagnostic competence of positron emission tomography/computed tomography and contrast-enhanced computed tomography in the evaluation of primary lesion and metastatic lymph node

	Primary tumor (n=22)		Metastatic lymph node (n=10)	
	PET/CT	CT	PET/CT	CT
Sensitivity	95.2%	85.7%	100%	50%
Specificity	100%	-	100%	100%
PPV	100%	95.7%	100%	100%
NPV	50%	-	100%	100%

PET/CT: Positron emission tomography/computed tomography, PPV: Positive predictive value, NPV: Negative predictive value, CT: Computed tomography

Discussion

PET/CT plays a role in the treatment planning of HNCs by leading to a change in TNM classification, in especially locally advanced stage.

HNCs constitute 6% of all malignancies, and they are the 8th leading cause of cancer-related deaths (5). Correct staging is vital in treatment planning of HNCs.

In terms of T staging, PET/CT may be insufficient in determining tumor size, specifying the infiltration boundaries and invasion of the surrounding tissue. The presence of soft tissue, perineural and bone marrow invasion can be evaluated with MRI with a higher accuracy than PET/CT (6). However, recent studies have reported that in 1/3 of patients more accurate results can be obtained with PET/CT in terms of T staging (7). In our study, for evaluation of primary lesion; in the case group with MRI the sensitivity, specificity, PPV and NPV of PET/CT were found higher as compared to MRI; and in the case group with CT, the sensitivity and PPV of PET/CT were found to be higher than CT. However, ^{18}F-FDG PET may not detect early-stage tumors with a small tumor volume, superficial tumors with a depth of less than 4 mm, as well as low stage tumors (such as carcinoma *in situ*) (8,9). In our study group, pathologic ^{18}F-FDG uptake was not observed in tumors of two patients with larynx carcinoma (one with carcinoma in situ) along with another patient with spindle cell carcinoma of the oral cavity.

The presence of ipsilateral, contralateral or bilateral metastatic lymph nodes reduce 5-year survival rate of HNCs by about 50% (10). The presence of occult lymph node metastasis in cases who have been staged as N0 based on scanning techniques is reported to be approximately 25-30%. That is why several authors recommend routine neck dissection in each case (9). It is stated that in identifying metastatic lymph nodes PET/CT is superior to morphological scanning techniques with the advantage of functional information (11,12) in spite of the partial volume effect on the lymph nodes with millimetric sizes. In our study, in 4 of 24 patients (16.6%) who had PET/CT, CT, MRI imaging and histopathologically confirmed nodal metastasis, the hyper-metabolic lymph node was observed with PET/CT although there were no pathologic findings

Table 4. Tumor, node, metastasis staging with ^{18}F-FDG positron emission tomography/computed tomography

Case no	Primary tumor localization	Indication	Conventional imaging	TNM with ^{18}F-FDG PET/CT
12	Oral cavity	Staging	No pathologic findings	T2N0M0 (Stage 2)
31	Oral cavity	Staging	Irregularities on the contour of the tongue	T2N0M0 (Stage 2)
32	Oral cavity	Staging	No pathologic findings	T3N1M0 (Stage 3)
42	Hypopharynx	Staging	Thickening of the posterior wall in the post-cricoid region	T4aNxM0 (Stage 4a)
47	Oral cavity	Staging	No buccal lesion, reactive lymph nodes	TxN2bM0 (Stage 4a)

^{18}F-FDG: 2-[^{18}F]-fluoro-2-deoxy-d-glucose, PET/CT: Positron emission tomography/computed tomography, TNM: Tumor, node, metastasis

with conventional techniques. The false positive results obtained with PET/CT are usually related to reactive lymph nodes. Therefore, it is recommended that the lymph nodes with increased ^{18}F-FDG involvement should be evaluated histopathologically (13). Schwartz et al. (14) reported the sensitivity of PET/CT and CT in detection of nodal metastasis as 96% and 78%, respectively. In our study, the sensitivity of PET/CT, MRI and CT in the evaluation of metastatic lymph nodes was calculated as 100%, 88.8% and 50% respectively.

In our study, the TNM stage according to PET/CT and conventional scanning techniques was the same in 27 of 37 patients. In five patients (13.5%), suspicious findings were identified with conventional techniques and the accurate result was obtained with PET/CT. In a prospective study by Lonneux et al. (15), it was stated that PET/CT may cause changes in treatment planning in 30% of patients with advanced stage head and neck squamous cell carcinoma, in 13% of patients with early stage disease, and in 13.7% of the entire group. PET/CT offers several advantages in planning of surgical treatment as compared to morphological scanning techniques by identifying the resection boundary of the primary lesion as well as the presence of lymph node metastasis (16). In addition, evaluation of distant metastasis with a single scanning technique and detection of a secondary malignancy is possible with PET/CT. The treatment options of surgery, systemic treatment and RT can be evaluated based on PET/CT data with much higher accuracy than conventional techniques and the risks related to an unnecessary radical surgical procedure or to inappropriate treatment can be avoided.

Conclusion

The results of this study indicate that PET/CT provides more accurate staging of HNCs than conventional techniques, and it plays a significant role in treatment planning. PET/CT seems to produce similar results with conventional imaging methods in restaging of head and neck malignancies, due to the limited number of patients in the study group.

Ethics

Ethics Committee Approval: The study was approved by Ege University Faculty of Medicine, Ethical Committee on Clinical and Laboratory Research Department (Protocol number: 14-1.1/2).

Informed Consent: Consent form was filled out by all participants.

Peer-review: Externally peer-reviewed.

Authorship Contributions

Surgical and Medical Practices: Ö.Ö., Concept: Ö.Ö., Design: Ö.Ö., F.H., Data Collection or Processing: Y.C., Analysis or Interpretation: Ö.Ö., F.H., Y.C., Literature Search: Y.C., Writing: F.H., Y.C.

Conflict of Interest: No conflict of interest was declared by the authors.

Financial Disclosure: The authors declared that this study received no financial support.

References

1. Saito N, Nadgir R, Nakahira M, Takahashi M, Uchino A, Kimura F, Truong MT, Sakai O. Posttreatment CT and MR Imaging in Head and Neck Cancer: What the Radiologist Needs to Know. Radiographics 2012;32:1261-1282.
2. Porter BA, Sheilds AF, Olson DO. MRI of Bone Marrow Disorders. Radiol Clin North Am 1986;24:269-289.
3. Brix G, Semmler W, Port R, Schad LR, Layer G, Lorenz WJ. Pharmacokinetic parameters in CNS Gd-DTPA enhanced MR imaging. J Comput Assist Tomogr 1991;15:621-628.
4. Senft A, de Bree R, Hoekstra OS, Kuik DJ, Golding RP, Oyen WJ, Pruim J, van den Hoogen FJ, Roodenburg JL, Leemans CR. Screening for Distant Metastases in Head and Neck Cancer Patients by Chest CT or Whole Body FDG-PET: A Prospective Multicenter Trial. Radiother Oncol 2008;87:221-229.
5. Wei WI, Kwong DL. Current Management Strategy of Nasopharyngeal Carcinoma. Clin Exp Otorhinolaryngol 2010;3:1-12.
6. Wong WL, Chevretton EB, McGurk M, Hussain K, Davis J, Beaney R, Baddeley H, Tierney P, Maisey M. A prospective Study of PET-FDG Imaging for the Assessment of Head and Neck Squamous Cell Carcinoma. Clin Otolaryngol 1997;22:209-214.
7. Mathews A, Jayakar J P, Rosenblat J. The role of FDG-PET and PET/CT in the diagnosis and staging of head and neck cancer. UWOMJ 2011;80:29-31.
8. Hannah A, Scott AM, Tochon-Danguy H, Chan JG, Akhurst T, Berlangieri S, Price D, Smith GJ, Schelleman T, McKay WJ, Sizeland A. Evaluation of 18 F-fluorodeoxyglucose positron emission tomography and computed tomography with histopathologic correlation in the initial staging of head and neck cancer. Ann Surg 2002;236:208-217.
9. Ng SH, Chan SC, Yen TC, Chang JT, Liao CT, Ko SF, Liu FY, Chin SC, Fan KH, Hsu CL. Staging of untreated nasopharyngeal carcinoma with PET/CT: comparison with conventional imaging work-up. Eur J Nucl Med Mol Imaging 2009;36:12-22.
10. Gordin A, Daitzchman M, Israel O. Hybrid Imaging of Head and Neck Malignancies. In: Delbeke D, Israel O, editors. Hybrid PET/CT and SPECT/CT Imaging. New York: Springer 2010;2:137-171.
11. Gordin A, Golz A, Daitzchman M, Keidar Z, Bar-Shalom R, Kuten A, Israel O. Fluorine-18 fluorodeoxyglucose positron emission tomography/computed tomography imaging in patients with carcinoma of the nasopharynx: diagnostic accuracy and impact on clinical management. Int J Radiat Oncol Biol Phys 2007;68:370-376.
12. Teknos TN, Rosenthal EL, Lee D, Taylor R, Marn CS. Positron emission tomography in the evaluation of stage III and IV head and neck cancer. Head Neck 2001;23:1056-1060.
13. Subramaniam RM, Truong M, Peller P, Sakai O, Mercier G. Fluorodeoxyglucose-Positron-Emission Tomography Imaging of Head and Neck Squamous Cell Cancer. Am J Neuroradiol 2010;31:598-604.
14. Schwartz DL, Ford E, Rajendran J, Yueh B, Coltrera MD, Virgin J, Anzai Y, Haynor D, Lewellyn B, Mattes D, Meyer J, Phillips M, Leblanc M, Kinahan P, Krohn K, Eary J, Laramore GE. FDG-PET/CT imaging for preradiotherapy staging of head-and-neck squamous cell carcinoma. Int J Radiat Oncol Biol Phys 2005;61:129-136.
15. Lonneux M, Hamoir M, Reychler H, Maingon P, Duvillard C, Calais G, Bridji B, Digue L, Toubeau M, Greqoire V. Positron emission tomography with [18F]fluorodeoxyglucose improves staging and management in patients with head and neck squamous cell carcinoma: a multicenter prospective study. J Clin Oncol 2010;28:1190-1195.
16. Roh JL, Yeo NK, Kim JS, Lee JH, Cho KJ, Choi SH, Nam SY, Kim SY. Utility of 2-[18F] fluoro-2-deoxy-d-glucose positron emission tomography and positron emission tomography/ computed tomography imaging in the preoperative staging of head and neck squamous cell carcinoma. Oral Oncol 2007;43:887-893.

Interesting Image
Mol Imaging Radionucl Ther 2018;27:25-28 DOI:10.4274/mirt.93685

Sphenoid Bone Fibrous Dysplasia Detected Incidentally on Bone Scintigraphy by the Contribution of SPECT/CT Hybrid Imaging

SPECT/BT Hibrid Görüntülemenin Katkısıyla Kemik Sintigrafisinde Tesadüfen Saptanan Sfenoid Kemik Fibröz Displazisi

Hüseyin Şan[1], Kürşat Okuyucu[2], Ali Ozan Öner[3], Özdeş Emer[2], Alper Özgür Karaçalıoğlu[2]
[1]*Karabük Training and Research Hospital, Clinic of Nuclear Medicine, Karabük, Turkey*
[2]*Gülhane Training and Research Hospital, Clinic of Nuclear Medicine, Ankara, Turkey*
[3]*Afyon Kocatepe University Faculty of Medicine, Department of Nuclear Medicine, Afyon, Turkey*

Abstract

Fibrous dysplasia (FD) is a benign fibroosseous bone disorder. It has poliostotic and monostotic patterns. Monostotic FD is frequently asymptomatic and is usually discovered incidentally by radiologic imaging performed for other reasons. Bone scintigraphy is valuable for identifying disease extent. Craniofacial FD (CFD) is a form of the disease where lesions are limited to contiguous bones of the craniofacial skeleton. We presented a case with monostotic CFD who was detected incidentally on bone scintigraphy single-photon emission computed tomography/computerized tomography while being investigated for inflammatory arthropaties.

Keywords: Craniofacial fibrous dysplasia, technetium-99m-methylene diphosphonate bone scintigraphy, single-photon emission computed tomography/computed tomography

Öz

Fibröz displazi (FD) kemiklerin iyi huylu bir fibroosseöz bozukluğudur. Poliyostatik ve monostatik formları vardır. Monostatik FD sıklıkla asemptomatiktir ve genellikle radyolojik görüntülerde tesadüfen fark edilir. Kemik sintigrafisi hastalığın yayılımını belirlemede değerlidir. Kraniyofasiyal FD (CFD) hastalığın kraniyofasiyal iskeletin kemiklerine sınırlı olduğu bir formudur. Enflamatuvar artropati yönünden araştırılırken tesadüfen kemik sintigrafisinde tek-foton emisyon bilgisayarlı tomografi/bilgisayarlı tomografi ile tespit edilen bir monostatik CFD olgusunu takdim ediyoruz.

Anahtar kelimeler: Kraniyofasiyal fibröz displazi, teknesyum-99m-metilen difosfonat kemik sintigrafisi, tek-foton emisyon bilgisayarlı tomografi/bilgisayarlı tomografi

Address for Correspondence: Kürşat Okuyucu MD, Gülhane Training and Research Hospital, Clinic of Nuclear Medicine, Ankara, Turkey
Phone: +90 312 304 48 08 E-mail: k.okuyucu@yahoo.com ORCID ID: orcid.org/0000-0002-4481-9531
Received: 15.04.2016 **Accepted:** 10.08.2017

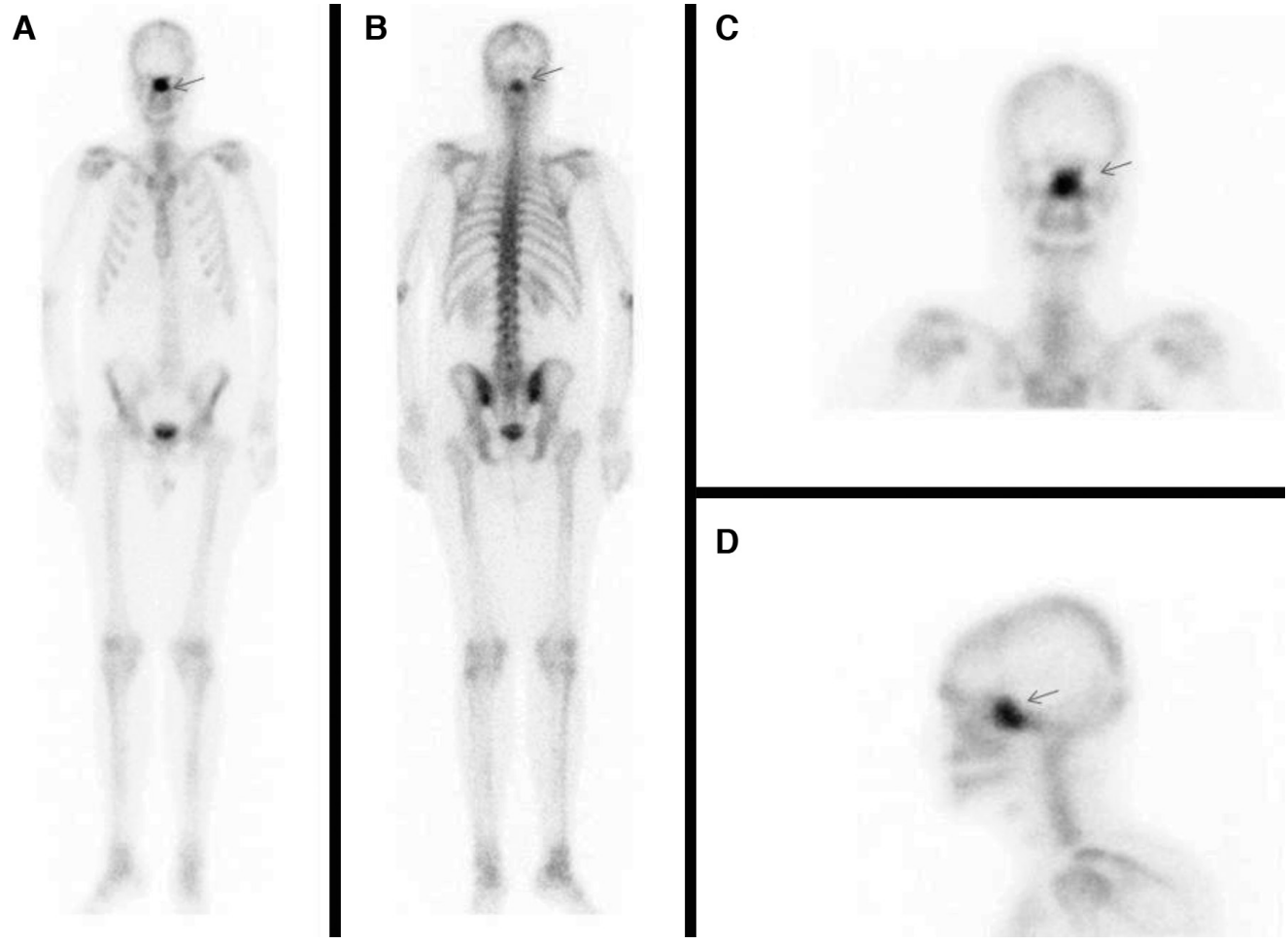

Figure 1. Anterior whole-body (A), posterior whole-body (B), anterior head spot (C), left lateral head spot (D) late static planar images of technetium (Tc)-99m-methylene diphosphonate (MDP) bone scintigraphy showing uptake in the middle facial region (arrows).

Fibrous dysplasia (FD) is a benign disorder of the bone in which there is developmental arrest of all components of normal bone (1). The lesions progressively replace the medullary cavity (2). Long bones, ribs, craniofacial bones and pelvis are the most common sites of skeletal involvement (3). It has been reported that the monostotic form constitute 70% of cases while 30% are polyostotic (4). Craniofacial FD (CFD) is a form of the disease where lesions are limited to contiguous bones of the craniofacial skeleton (5,6). Craniofacial involvement is present in 10-27% of monostotic cases and 50% of polyostotic ones (7,8). CFD without involvement of bones out of the cranium can not be easily described as monostotic because of the potential adjoining involvement of cranial bones (6,9).

A 20-year-old male with back pain was investigated for seronegative spondylarthropathy. In order to demonstrate any inflammatory joint involvement, a three-phase Tc-99m-MDP bone scintigraphy was requested. Although perfusion and blood pool phases were normal, there was intense MDP uptake in the middle facial region on late static phase whole-body images.

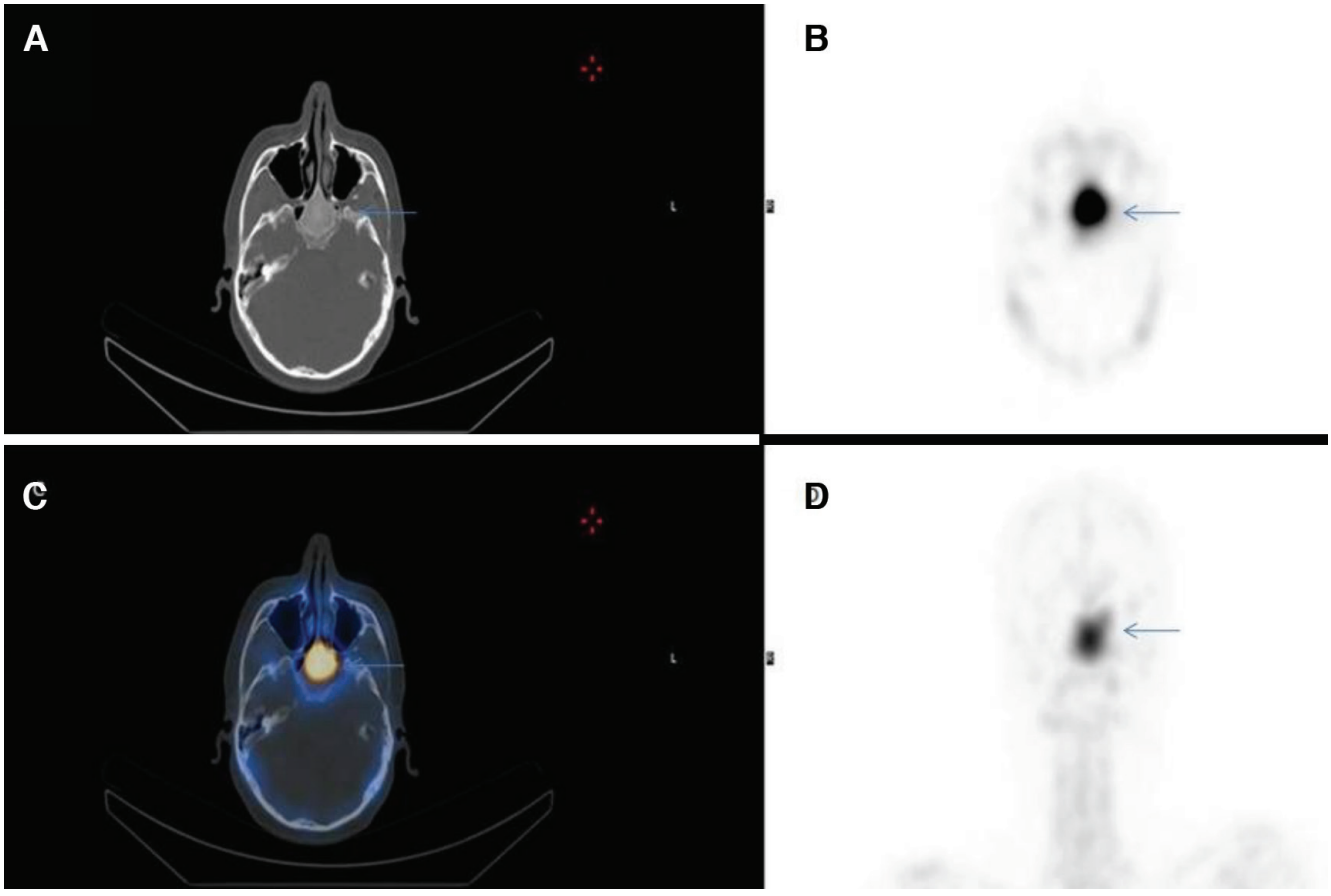

Figure 2. Computerized tomography (CT) (A), single-photon emission CT (SPECT) (B), fusion (C), maximum intensity projection (D) images on SPECT/CT hybrid imaging of Tc-99m-MDP bone scintigraphy that localize and spot the uptake on planar images in the sphenoid bone (arrows).

For the exact localization of this abnormal incidental finding, SPECT/CT hybrid imaging was performed. This accumulation was situated at and confined to a well-marginated, ground-glass opacity in the corpus of the sphenoid bone on CT component (Figure 2). The lesion was resembling a benign bone disorder (suggestive of monostotic FD). Magnetic resonance imaging (MRI) was requested to differentiate it from other benign bone pathologies that confirmed the diagnosis of FD.

CT is the best technique for depicting lesion extent, cortical boundary and homogeneity of the poorly mineralized lesion (10). Well margination, hazy ground-glass opacity and contrast enhancement are characteristic features of FD on CT (10,11). MRI is quite sensitive for detecting FD and provides complementary information to CT (12).

Although bone scintigraphy has low specificity for FD, it has a valuable role on identifying disease extent at initial presentation due to its high sensitivity (10,11). Despite its high capability of lesion detection, determining exact lesion location by this method is problematic especially for contiguous bones of the craniofacial region. CT and MRI are good options to overcome this obstacle easily, by providing accurate anatomical detail. On the other hand, without a whole-body imaging which is not practical by CT or MRI, whether CFD is polyostotic or not can not be clarified. For this reason, existence of any lesion in other parts of the body other than the craniofacial region should be clearly depicted. A whole-body bone scintigraphy at a single session and an additional SPECT/CT, which provides both anatomical and functional data, will be sufficient to elucidate this issue.

Ethics

Informed Consent: Consent form was filled out by all participants.

Peer-review: Externally peer-reviewed.

Authorship Contributions

Surgical and Medical Practices: H.Ş., K.O., Ö.E., A.Ö.K., A.O.Ö., Concept: H.Ş., K.O., Design: H.Ş., K.O., Ö.E., Data Collection or Processing: H.Ş., Analysis or Interpretation: A.Ö.K., Literature Search: A.O.Ö., Writing: H.Ş., K.O.

Conflict of Interest: No conflict of interest was declared by the authors.

Financial Disclosure: The authors declared that this study received no financial support.

References

1. Kumar V, Abbas AK, Aster JC. Robbins & Cotran Pathologic Basis of Disease, 9th ed. 2015;1408.
2. Elgazzar AH. Synopsis of Pathophysiology in Nuclear Medicine. Springer International Publishing 2014;357.
3. Harisankar CN, Bhattacharya A, Bhadada SK, Kamaleshwaran KK, Mittal BR. An interesting case of polyostotic fibrous dysplasia: The "pirate sign" evaluated with Tc-99m methylene diphosphonate single-photon emission computed tomography/ computerized tomography. Indian J Nucl Med 2011;26:40-41.
4. Schlumberger HG. Fibrous dysplasia of single bones (monostatic fibrous dysplasia). Mil Surg 1946;99:504-527.
5. Daves ML, Yardley JH. Fibrous dysplasia of bone. Am J Med Sci 1957;234:590-606.
6. Menon S, Venkatswamy S, Ramu V, Banu K, Ehtaih S, Kashyap VM. Craniofacial fibrous dysplasia: Surgery and literature review. Ann Maxillofac Surg 2013;3:66-71.
7. Harris WH, Dudley HR Jr, Barry RJ. The natural history of fibrous dysplasia: An orthopedic pathological and roentgenographic study. J Bone Joint Surg 1962;44:207-233.
8. Owlia F, Karbassi MH. Craniofacial polyostotic fibrous dysplasia: A rare case. Dent Res J (Isfahan) 2014;11:518-521.
9. Kim DD, Ghali GE, Wright JM, Edwards SP. Surgical treatment of giant fibrous dysplasia of the mandible with concomitant craniofacial involvement. J Oral Maxillofac Surg 2012;70:102-118.
10. Leeds N, Seaman WB. Fibrous dysplasia of the skull and its differential diagnosis. Radiology 1962;78:570-582.
11. Zhibin Y, Quanyong L, Libo C, Jun Z, Hankui L, Jifang Z, Ruisen Z. The role of radionuclide bone scintigraphy in fibrous dysplasia of bone. Clin Nucl Med 2004;29:177-180.
12. Jee WH, Choi KH, Choe BY, Park JM, Shinn KS. Fibrous dysplasia: MR imaging characteristics with radiopathologic correlation. AJR Am J Roentgenol 1996;167:1523-1527.

Interesting Image
Mol Imaging Radionucl Ther 2018;27:29-31 DOI:10.4274/mirt.27247

The Contribution of SPECT/CT in the Diagnosis of Stress Fracture of the Proximal Tibia

Proksimal Tibia Stres Kırığında SPECT/BT'nin Katkısı

Berna Okudan, Nazım Coşkun, Pelin Arıcan
University of Health Sciences, Ankara Numune Training and Research Hospital, Clinic of Nuclear Medicine, Ankara, Turkey

Abstract

Stress fractures are injuries most commonly seen in the lower limbs and are usually caused by repetitive stress. While the distal and middle third of the tibia is the most frequent site for stress fractures (almost 50%), stress fractures of the proximal tibia is relatively rare and could be confused with other types of tibial fractures, thus altering management plans for the clinician. Early diagnosis of stress fractures is also important to avoid complications. Imaging plays an important role in the diagnosis of stress fractures, especially bone scan. Combined with single-photon emission computed tomography/computed tomography (SPECT/CT) it is an important imaging technique for stress fractures in both upper and lower extremities, and is widely preferred over other imaging techniques. In this case, we present the case of a 39-year-old male patient diagnosed with stress fracture of the proximal tibia and demonstrate the contribution of CT scan fused with SPECT imaging in the early diagnosis of stress fracture prior to other imaging modalities.

Keywords: Stress fracture, proximal tibia, bone scintigraphy, single-photon emission computed tomography/computed tomography

Öz

Stres kırıkları çoğunlukla alt ekstremitede görülen ve genellikle tekrarlayan strese bağlı gelişen yaralanmalardır. Tibia orta kesimi ve distali stres kırıklarının en sık görüldüğü bölgeler iken (yaklaşık %50), proksimal tibianın stres kırıkları nispeten nadirdir, diğer kırık türleriyle karıştırılabilir ve bu durum klinisyenin tedavi planını etkileyebilir. Stres kırıklarının erken tanısı komplikasyonları önlemek açısından önemlidir. Görüntüleme yöntemleri, stres kırıklarının teşhisinde önemli bir rol oynamaktadır. Özellikle tek-foton emisyon bilgisayarlı tomografi/bilgisayarlı tomografi (SPECT/BT) ile birleştirilen kemik sintigrafisi hem üst hem de alt ekstremite stres kırıkları için önemli bir görüntüleme tekniğidir ve diğer görüntüleme tekniklerine göre çok daha fazla tercih edilmektedir. Bu yazıda proksimal tibiada stres kırığı tanısı alan 39 yaşındaki bir erkek hastanın hikayesini sunuyor ve stres kırığının erken tanısında SPECT/BT taramasının katkısını gösteriyoruz.

Anahtar kelimeler: Stres kırığı, proksimal tibia, kemik sintigrafisi, tek-foton emisyonlu bilgisayarlı tomografi/bilgisayarlı tomografi

Address for Correspondence: Nazım Coşkun MD, University of Health Sciences, Ankara Numune Training and Research Hospital, Clinic of Nuclear Medicine, Ankara, Turkey
Phone: +90 534 328 84 74 E-mail: nazimcoskun@gmail.com ORCID ID: orcid.org/0000-0002-1458-9392
Received: 25.06.2016 **Accepted:** 15.10.2017

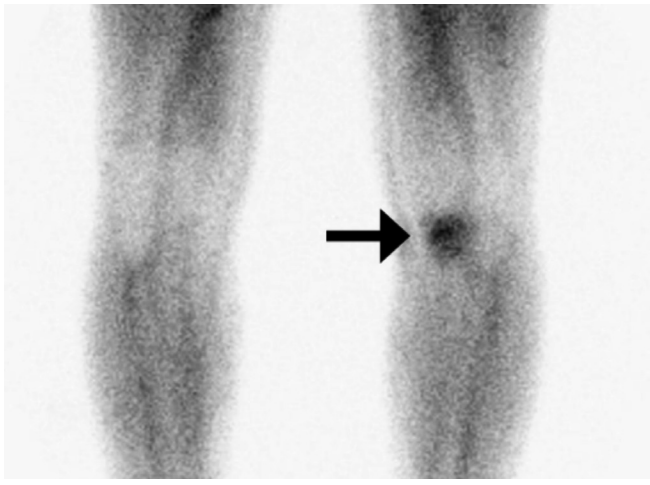

Figure 1. Blood pool phase of 3-phase bone scintigraphy (3-PBS) showing hyperemia in the left knee joint. 3-PBS, revealing the pathologic changes in osseous compartments as early as a few days after the onset of complaints, is a widely used method in the diagnosis of stress fractures.

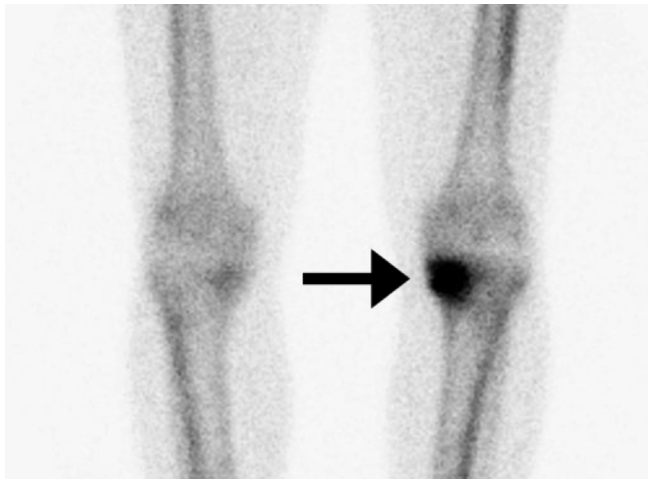

Figure 2. Delayed phase 3-PBS showing increased activity in the left knee joint.

Figure 3. Computed tomography (CT) image from single-photon emission CT (SPECT)/CT fusion study showing a linear fracture in the proximal tibia. While distal and middle third of the tibia are the most frequent sites for stress fractures (almost 50%), stress fractures of the proximal tibia is relatively rare and could be confused with other types of tibial fractures (1). SPECT/CT, which combines the high anatomical resolution of CT with the early-diagnosis capability of SPECT, is an increasingly preferred imaging technique in the diagnosis and follow-up of these patients (2).

Figure 4. Magnetic resonance image confirming the stress fracture line in the proximal tibia.

Ethics

Informed Consent: Consent form was filled out by all participants.

Peer-review: Externally peer-reviewed.

Authorship Contributions

Surgical and Medical Practices: B.O., N.C., Concept: B.O., N.C., Design: B.O., N.C., Data Collection or Processing: B.O., N.C., Analysis or Interpretation: B.O., N.C., Literature Search: P.A., Writing: N.C.

Conflict of Interest: No conflict of interest was declared by the authors.

Financial Disclosure: The authors declared that this study received no financial support.

References

1. Drabicki RR, Greer WJ, DeMeo PJ. Stress Fractures Around the Knee. Clin Sports Med 2006;25:105-115.
2. Huellner MW, Strobel K. Clinical applications of SPECT/CT in imaging the extremities. Eur J Nucl Med Mol Imaging 2014;41(Suppl 1):S50-58.

Interesting Image
Mol Imaging Radionucl Ther 2018;27:32-36 DOI:10.4274/mirt.02419

Unilateral Muscle Artifacts due to Non-compliance During Uptake Phase of ^{18}F-FDG PET/CT in an Oncologic Patient

Bir Onkoloji Hastasında ^{18}F-FDG PET/BT Tutulum Fazı Sırasında Uyumsuzluğa Bağlı Unilateral Kas Artefaktları

William Makis, Emmanuel W. Hudson
Cross Cancer Institute, Department of Diagnostic Imaging, Edmonton, Canada

Abstract

A 49-year-old male patient with a prior history of poor compliance with medical appointments was referred for an ^{18}F-fluoro-2-deoxy-D-glucose (^{18}F-FDG) positron emission tomography/computed tomography (PET/CT) for the staging of a rectal squamous cell carcinoma. The PET/CT showed unilateral diffuse skeletal muscle ^{18}F-FDG uptake as well as bilateral salivary gland uptake artifacts, suggestive of non-compliance with patient preparation instructions. The PET/CT nurse noted that during the ^{18}F-FDG uptake phase, the patient appeared intoxicated, and she found two beer cans hidden in the waste disposal beside his chair just prior to imaging. The patient only admitted to eating a cookie approximately 30 minutes after the injection of ^{18}F-FDG PET/CT and denied consuming alcohol during the uptake phase. We present the imaging findings of non-compliance with patient instructions during the uptake phase of ^{18}F-FDG.

Keywords: Non-compliance, artifact, pitfall, muscle, musculoskeletal, ^{18}F-FDG, PET

Öz

Kırk dokuz yaşında doktor randevularına uyumsuz olduğu bilinen bir erkek hasta rektal skuamöz hücreli karsinom evrelemesi amacıyla ^{18}F-fluoro-2-deoksi-D-glukoz (^{18}F-FDG) pozitron emisyon tomografisi/bilgisayarlı tomografi (PET/BT) için yönlendirilmişti. PET/BT'de unilateral diffüz iskelet kasında ^{18}F-FDG tutulumu, bilateral tükrük bezi artefaktları görüldü, bulguları hastanın hazırlık talimatlarına uyumsuzluğu olarak değerlendirildi. PET/BT hemşiresi ^{18}F-FDG tutulumu sırasında hastanın intoksike görünümde olduğunu farketti ve görüntülemeden önce hastanın iskemlesinin yanındaki çöp kutusunda iki bira şişesi buldu. Hasta ^{18}F-FDG PET/BT enjeksiyonundan 30 dakika sonra bir kurabiye yediğini ancak alkol almadığını belirtti. Burada hazırlık talimatlarına uyumsuz bir hastada ^{18}F-FDG tutulum fazındaki görüntüleme bulgularını sunuyoruz.

Anahtar kelimeler: Uyumsuzluk, artefakt, tuzak, kas, kas-iskelet, ^{18}F-FDG, PET

Address for Correspondence: William Makis MD, Cross Cancer Institute, Department of Diagnostic Imaging, Edmonton, Canada
Phone: +90 780 432 87 60 E-mail: makisw79@yahoo.com ORCID ID: orcid.org/0000-0003-0241-3426
Received: 30.12.2016 **Accepted:** 15.10.2017

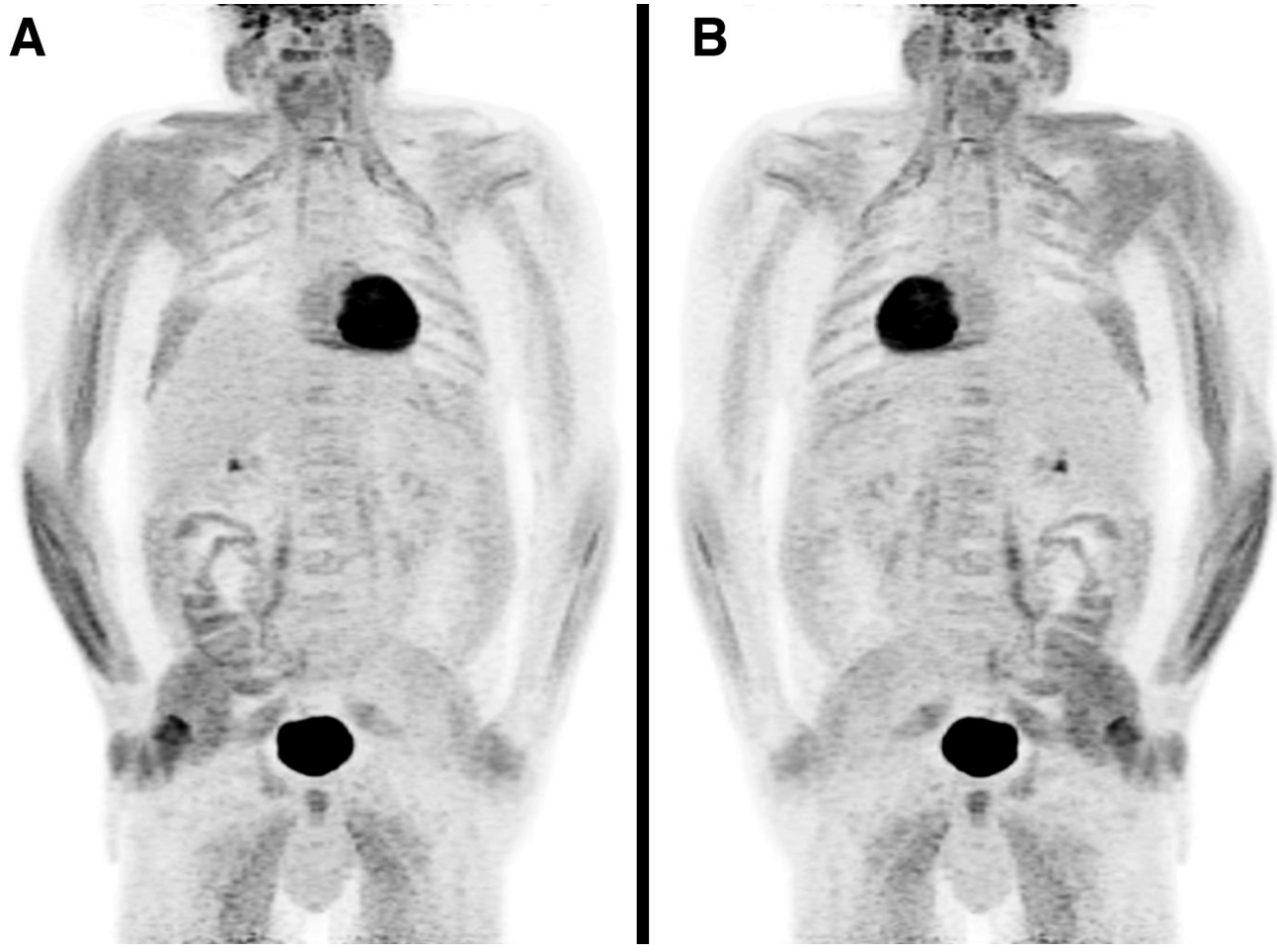

Figure 1. A 49-year-old male patient had ^{18}F-fluoro-2-deoxy-D-glucose (^{18}F-FDG) positron emission tomography/computed tomography (PET/CT) (Biograph-mCT, Siemens, Germany) to stage a rectal squamous cell carcinoma. He was injected with 352 MBq of ^{18}F-FDG and his blood glucose was 6.8 mmol/L just prior to injection. During the 60-minute uptake phase prior to imaging, the nurse observed the patient: he was sitting and leaning on one side, appeared intoxicated and his breath smelled of alcohol. He was constantly moving in his seat. Two beer cans were found in the waste disposal next to his chair just prior to imaging. On questioning, he denied drinking alcohol and only admitted to eating a cookie at approximately 30 minutes after ^{18}F-FDG injection. PET/CT maximum intensity projection images with (A) anterior and (B) posterior views revealed diffuse intense unilateral muscle ^{18}F-FDG uptake artifacts involving the right shoulder, arm, hand, right chest wall and right gluteus muscles.

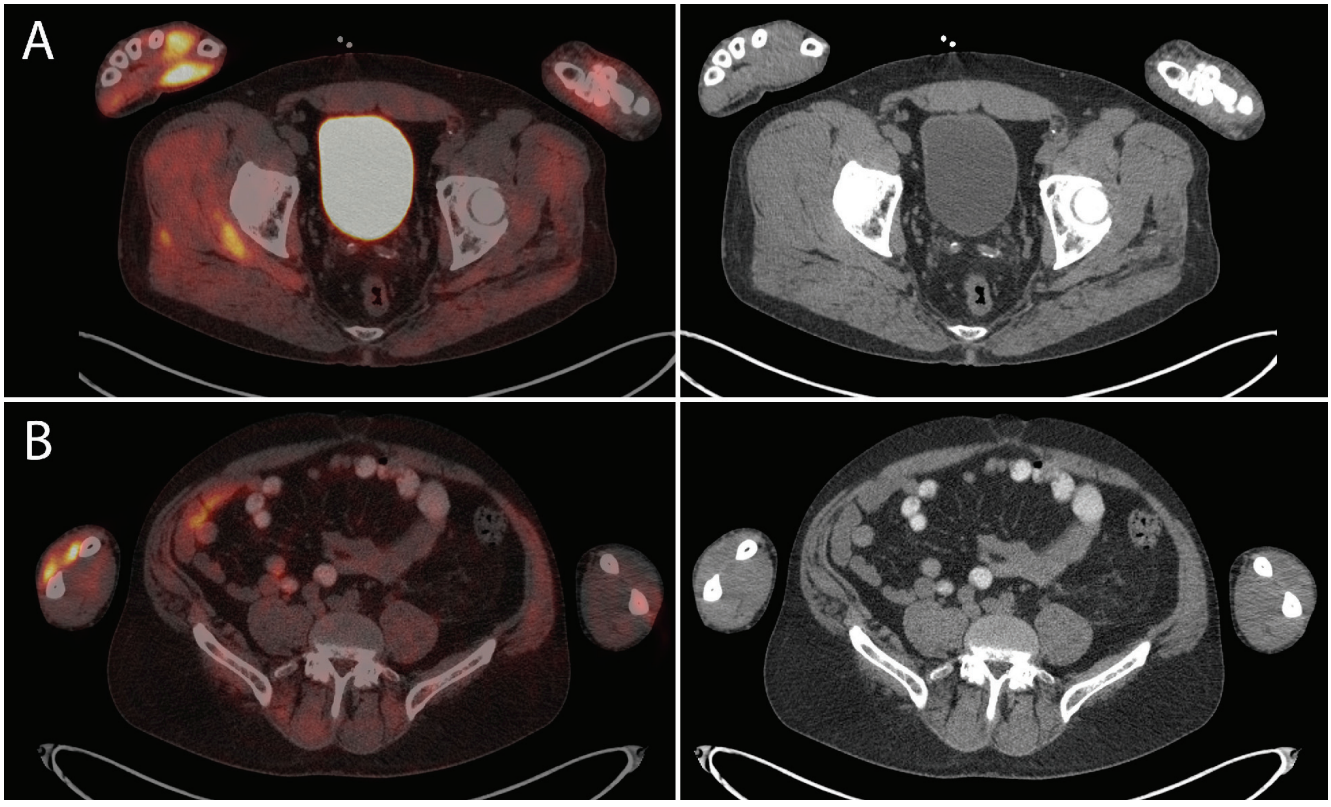

Figure 2. (A) Intense ^{18}F-FDG uptake in the right thenar eminence with maximum standard uptake value (SUV_{max}) 8.8 was the most intensely ^{18}F-FDG avid abnormality in the entire PET/CT study, and was most likely the result of the patient holding beer cans and drinking beer. (B) Right dorsal extensor forearm muscles also showed intense ^{18}F-FDG uptake with SUV_{max} 6.7.

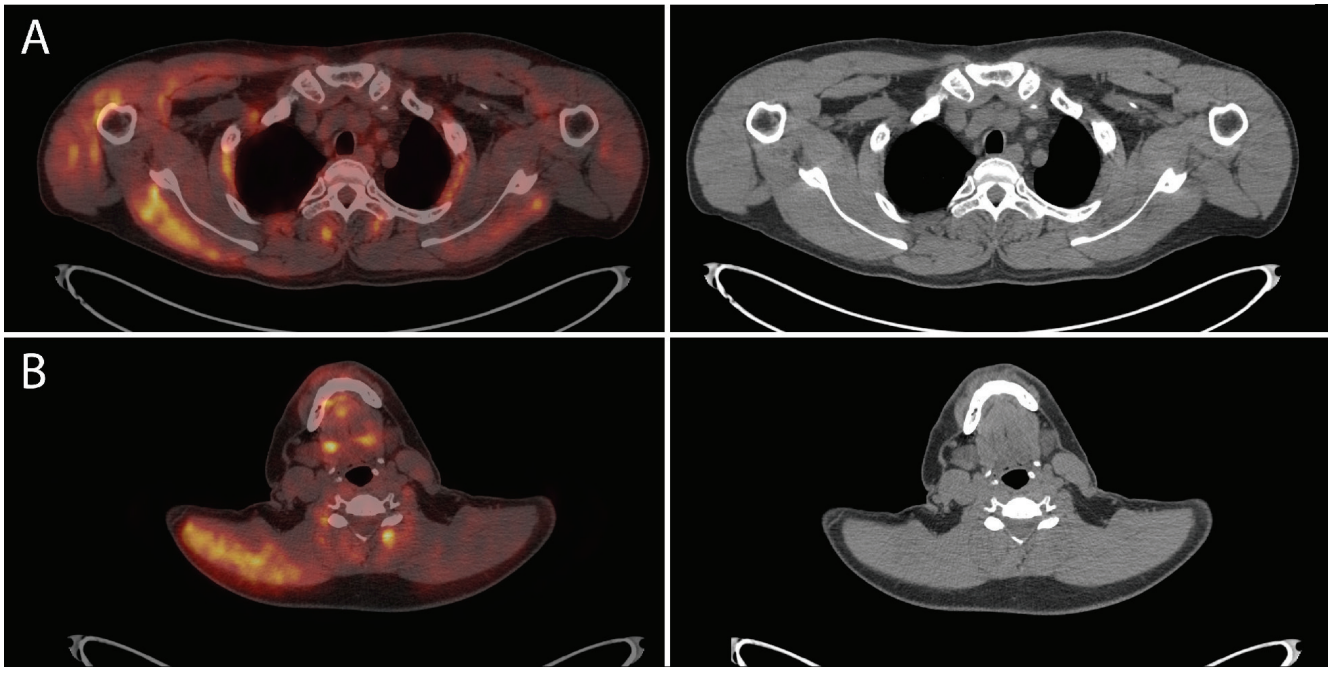

Figure 3. Right biceps muscles showed increased ^{18}F-FDG uptake with SUV_{max} 5.0, (A) right shoulder muscles had SUV_{max} 4.0, (B) right trapezius muscle had SUV_{max} 4.1 and right serratus anterior muscle had SUV_{max} 3.8.

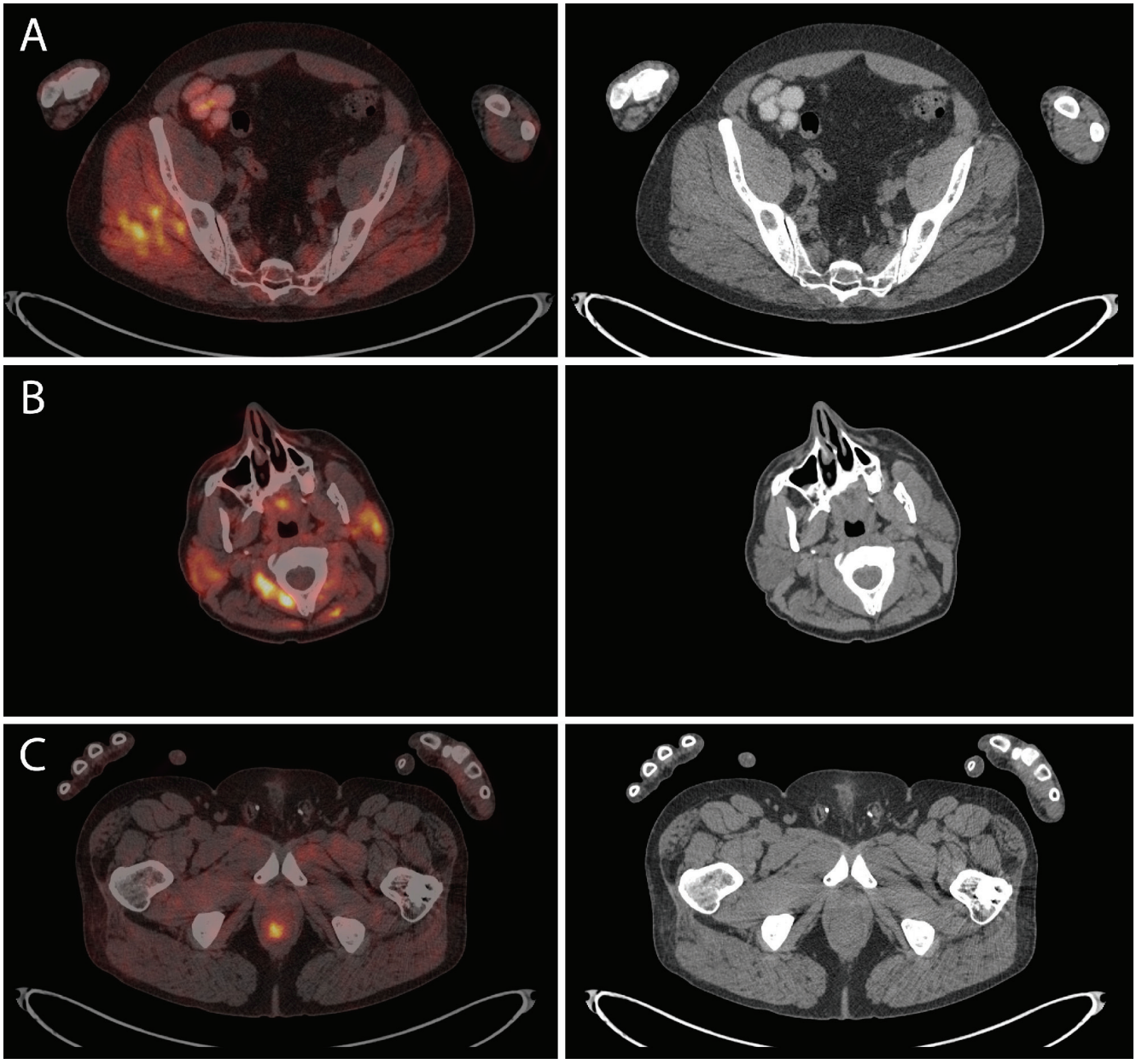

Figure 4. (A) Right gluteal muscles showed increased ^{18}F-FDG uptake with SUV_{max} 5.3, and (B) both parotid glands showed increased ^{18}F-FDG uptake with SUV_{max} 4.7 in the right and SUV_{max} 4.8 in the left, most likely due to alcohol/food consumption. (C) The rectal primary lesion had intense ^{18}F-FDG uptake with SUV_{max} 5.2 and there was no evidence of distant metastases. The ^{18}F-FDG physiologic uptake artifacts from physical activity and movements of the right hand, arm, shoulder and gluteus maximus (as well as drinking and eating), with normal corresponding CT findings, did not interfere with cancer staging. It is important that a patient is relaxed at time of ^{18}F-FDG injection and has avoided vigorous exercise in the hours leading up to the PET/CT. Most authors recommend avoiding physical exercise 24 hours before ^{18}F-FDG administration (1,2,3,4), although vigorous exercise up to 4 days before imaging has been reported to cause muscle ^{18}F-FDG uptake artifacts (5). Diffusely increased ^{18}F-FDG uptake in muscles, as a PET/CT artifact, has been described in the following situations: insulin administration (6), voluntary physical activity such as chewing gum, exercise or sexual activity (4,5,7), involuntary physical activity such as labored breathing or muscle spasms (8), post surgical changes (9,10), post radiation inflammation (11), dermatomyositis (12), infection (10,13,14), or post injection (15). Unilateral intense muscle ^{18}F-FDG uptake is rare and has been described in a few cases such as hemiparesis from stroke (16), in patients with multiple sclerosis (17), due to tracer injections (15) or more commonly in certain head and neck muscles (18). Non-compliance with patient instructions during the uptake phase of ^{18}F-FDG can cause significant artifacts and recent examples in the literature include smartphone use (19), reading a small book and even tapping the foot (20).

Ethics

Informed Consent: All subjects in the study gave written informed consent or the institutional review board waived the need to obtain informed consent.

Peer-review: External and internal peer-reviewed.

Authorship Contributions

Surgical and Medical Practices: W.M., E.W.H., Concept: W.M., Design: W.M., Data Collection or Processing: W.M., E.W.H., Analysis or Interpretation: W.M., E.W.H., Literature Search: W.M., E.W.H., Writing: W.M.

Conflict of Interest: No conflict of interest was declared by the authors.

Financial Disclosure: The authors declared that this study received no financial support.

References

1. Cook G, Wegner EA, Fogelman I. Pitfalls and artifacts in 18FDG PET and PET/CT oncologic imaging. Semin Nucl Med 2004;34:122-133.
2. Rosenbaum SJ, Lind T, Antoch G, Bockisch A. False-positive FDG PET uptake – the role of PET/CT. Eur Radiol 2006;16:1054-1065.
3. Yasuda S, Ide M, Takagi S, Shohtsu A. Elevated F-18 FDG uptake in skeletal muscle. Clin Nucl Med 1998;23:111-112.
4. Choi BW, Kim SH, Kim HW, Won KS, Zeon SK. Hypermetabolism of skeletal muscles following sexual activity: a normal variation. Nucl Med Mol Imaging 2010;44:228-229.
5. Bai X, Wang X, Zhuang H. Long-lasting FDG uptake in the muscles after strenuous exercise. Clin Nucl Med 2015;40:975-976.
6. Blodgett TM, Mehta AS, Mehta AS, Laymon CM, Carney J, Townsend DW. PET/CT artifacts. Clin Imaging 2011;35:49-63.
7. Kawabe J, Higashiyama S, Okamura T, Torii K, Koyama K, Kawamura E, Ishizu H, Inoue Y, Shiomi S. FDG uptake by tongue and muscles of mastication reflecting increased metabolic activity of muscles after chewing gum. Clin Nucl Med 2003;23:220-221.
8. Lin FI, Foster CC, Hagge RJ, Shelton DK. Extensive FDG uptake in accessory muscles of respiration in a patient with shortness of breath. Clin Nucl Med 2009;34:428-430.
9. Costelloe CM, Murphy WA, Chasen BA. Musculoskeletal pitfalls in 18F-FDG PET/CT: pictorial review. AJR Am J Roentgenol 2009;193(Suppl 3):WS1-WS13.
10. Love C, Tomas MB, Tronco GG, Palestro CJ. FDG PET of infection and inflammation. Radiographics 2005;25:1357-1368.
11. Tomita H, Kita T, Hayashi K, Kosuda S. Radiation-induced myositis mimicking chest wall tumor invasion in two patients with lung cancer: a PET/CT study. Clin Nucl Med 2012;37:168-169.
12. Mahmood S, de Llano SRM. 18F-FDG PET detection of unknown primary malignancy in dermatomyositis. Clin Nucl Med 2012;37:e204-e205.
13. Strobel K, Stumpe KD. PET/CT in musculoskeletal infection. Semin Musculoskelet Radiol 2007;11:353-364.
14. Palestro CJ. FDG-PET in musculoskeletal infections. Semin Nucl Med 2013;43:367-376.
15. Nakatani K, Nakamoto Y, Togashi K. Unilateral physiological FDG uptake in teres minor muscle seems well associated with IV tracer injection procedures. Clin Nucl Med 2015;40:62-64.
16. Gupta P, Kota G, Alavi A, Mintz A. Unilateral diffusely increased muscle uptake of F-18 FDG in a patient with hemiparesis due to stroke. Clin Nucl Med 2011;36:1140-1141.
17. Rudroff T, Kindred JH, Koo PJ, Karki R, Hebert JR. Asymmetric glucose uptake in leg muscles of patients with multiple sclerosis during walking detected by [18F]-FDG PET/CT. NeuroRehabilitation 2014;35:813-823.
18. Lin EC. Focal asymmetric longus colli uptake on FDG PET/CT. Clin Nucl Med 2007;32:67-69.
19. Schwartz P Jr, Pinaquy JB. Unilateral forearm muscle 18F-FDG uptake after using a smartphone. Clin Nucl Med 2015;40:e532-e533.
20. Jackson RS, Schlarman TC, Hubble WL, Osman MM. Prevalence and patterns of physiologic muscle uptake detected with whole-body 18F-FDG PET. J Nucl Med Technol 2006;34:29-33.

Interesting Image
Mol Imaging Radionucl Ther 2018;27:37-40 DOI:10.4274/mirt.03371

Inflammatory and Ischemic Post Liver Transplant Complications Mimic Malignancy on ^{18}F-FDG PET/CT

Enflamatuvar ve İskemik Karaciğer Transplantasyonu Komplikasyonları ^{18}F-FDG PET/BT'de Maligniteyi Taklit Eder

William Makis[1], *Anthony Ciarallo*[2], *Stephan Probst*[3]

[1]*Cross Cancer Institute, Department of Diagnostic Imaging, Edmonton, Canada*
[2]*McGill University Health Centre, Department of Nuclear Medicine, Montreal, Canada*
[3]*Jewish General Hospital, Department of Nuclear Medicine, Montreal, Canada*

Abstract

A 65-year-old male patient with a one year history of liver transplantation was referred for an ^{18}F-fluoro-2-deoxy-D-glucose (^{18}F-FDG) positron emission tomography/computed tomography (PET/CT) to rule out post transplant lymphoproliferative disease. Multiple foci of intense abnormal ^{18}F-FDG uptake were seen in the transplanted liver which were concerning for malignancy. Explantation of the liver approximately 1 month following the PET/CT revealed multiple inflammatory and ischemic changes including large bile duct necrosis, acute cholangitis, bile duct obstruction changes and periportal fibrosis, with no evidence of malignancy. We present the ^{18}F-FDG PET/CT image findings of this case.

Keywords: Liver transplant, complications, pitfall, artifact, ^{18}F-fluorodeoxyglucose, positron emission tomography

Öz

Altmış beş yaşında bir erkek hasta karaciğer transplantasyonundan bir yıl sonra post transplant lenfoproliferatif hastalık açısından değerlendirilmek üzere ^{18}F-fluoro-2-deoxy-D-glucose (^{18}F-FDG) pozitron emisyon tomografisi/bilgisayarlı tomografi (PET/BT) için yönlendirildi. Transplante karaciğerde malignite şüphesi uyandıran multipl yoğun ^{18}F-FDG tutulumu saptandı. PET/BT'den 1 ay sonra yapılan karaciğer eksplantasyonunda multipl enflamatuvar ve iskemik değişiklikler, safra kanalı nekrozu, akut kolanjit, safra yolu obstrüksiyonuna bağlı değişiklikler ve periportal fibrozis saptandı, malignite bulgusu görülmedi. Bu olgunun ^{18}F-FDG PET/BT görüntüleme bulgularını sunuyoruz.

Anahtar kelimeler: Karaciğer transplantasyonu, komplikasyon, tuzak, artefakt, ^{18}F-fluorodeoxyglucose, pozitron emisyon tomografisi

Address for Correspondence: William Makis MD, Cross Cancer Institute, Department of Diagnostic Imaging, Edmonton, Canada
Phone: +90 780 432 87 60 E-mail: makisw79@yahoo.com ORCID ID: orcid.org/0000-0003-0241-3426
Received: 31.12.2016 **Accepted:** 15.10.2017

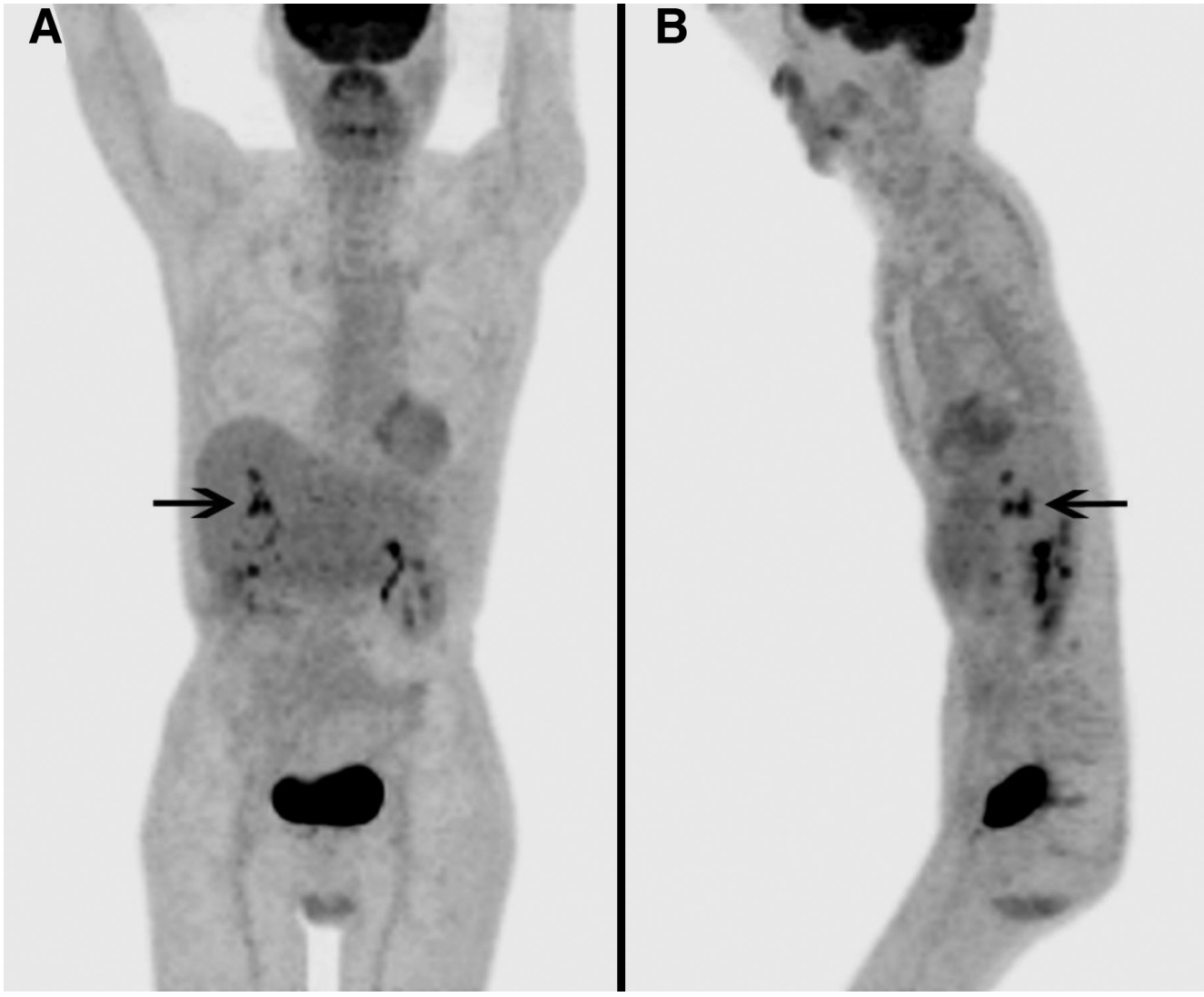

Figure 1. A 65-year-old male had a liver transplant one year prior, for hepatitis B cirrhosis and hepatocellular carcinoma (HCC) with a 3.5 cm lesion in the left lobe and a 4 cm lesion in the right. For several months prior to positron emission tomography/computed tomography (PET/CT), the patient had persistently elevated liver function tests but multiple transjugular biopsies showed no evidence of transplant rejection. Seven endoscopic retrograde cholangiopancreatographies (ERCPs) were performed as the patient developed recurring stenoses and strictures of intrahepatic bile ducts, with failed attempts of cannulation, balloon dilation and stent replacements. The patient tested positive for Epstein-Barr virus and underwent PET/CT to rule out post transplant lymphoproliferative disease (PTLD). Maximum intensity projection images showed multiple foci of intense ^{18}F-FDG uptake in the liver in segments 5, 6, 7 and 8, with maximum standardized uptake value of 9.0, concerning for malignancy.

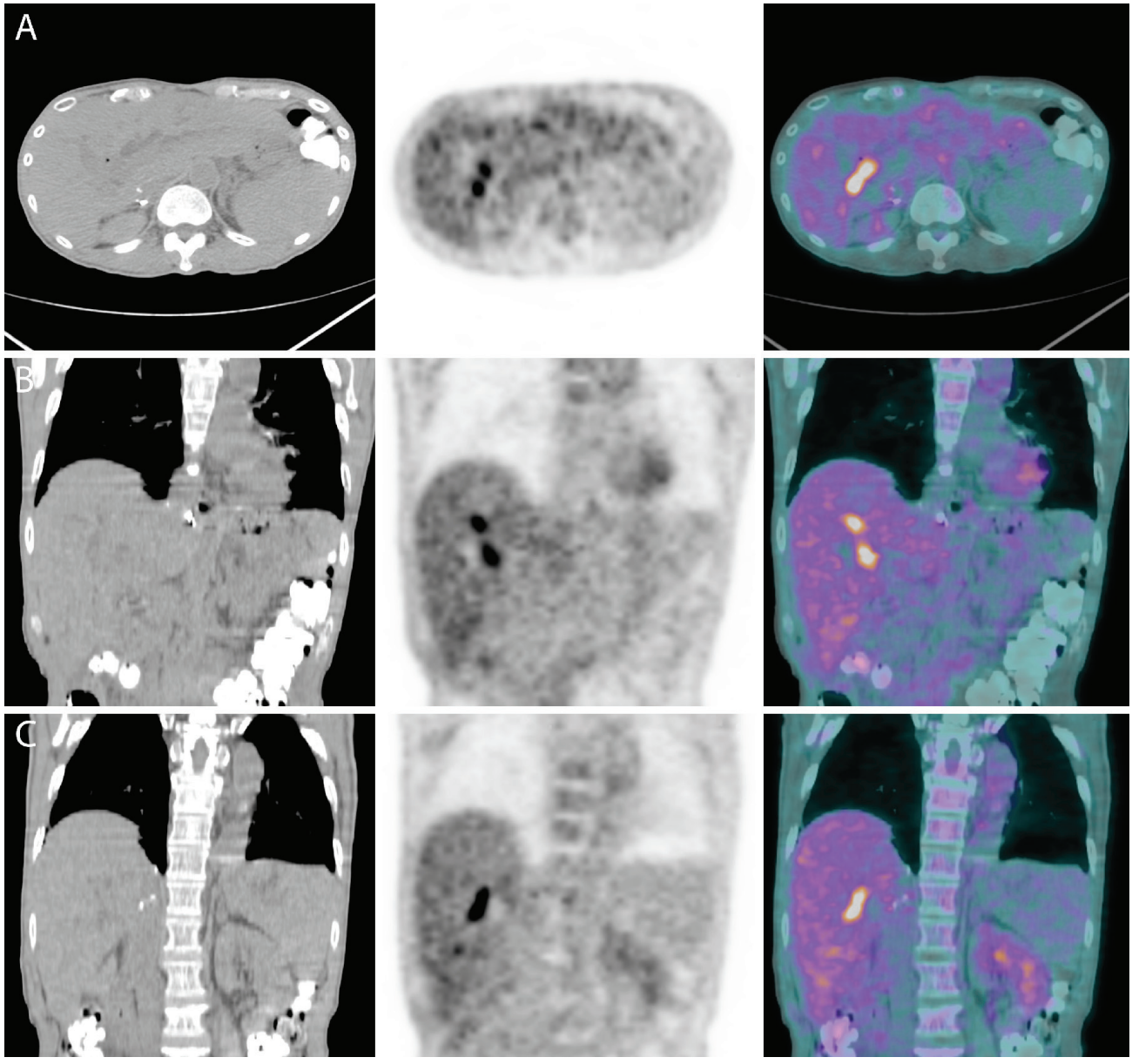

Figure 2. Transaxial and coronal views of the PET/CT fusion images showed multiple foci of intense ^{18}F-FDG uptake in the liver, although no obvious mass lesions were seen on the CT. An ERCP done 1 month after PET/CT showed multiple strictures involving the common hepatic duct and its intrahepatic segments associated with stones, debris and a failed right hepatic biliary stent. The liver was explanted and histopathological evaluation showed a cirrhotic liver weighing 1260 g measuring 20x14.5x7.2 cm. The surface of the liver revealed homogeneous macronodular appearance with absence of infarctions. Ducts of the right and left lobe appeared dilated, and sectioning showed large bile duct necrosis, acute cholangitis, bile duct obstruction changes and periportal fibrosis (stage 2/4). There was no evidence of malignancy within the explanted liver. Liver transplantation is a standard treatment for patients with end stage liver disease. Biliary complications of liver transplantation remain a significant problem with bile leak and stricture rates of ~20%, majority of them being related to biliary anastomosis (1,2). Re-transplantation is required following the development of ischemic type biliary strictures or ischemic cholangiopathy which is defined as intra or extra-hepatic biliary stricture in the presence of a patent hepatic artery (3). The only ^{18}F-FDG positive liver transplant complications reported in the literature are PTLD and recurrent HCC (4,5). ^{18}F-FDG PET/CT is widely used to assess for extrahepatic metastases prior to liver transplantation (6). PET/CT has also been found to be useful as a predictive parameter for evaluation of early HCC recurrence after liver transplantation (7). In light of the increasing use of PET/CT in liver transplant patients, it is important to be aware of lesions that mimick malignancy. In our case, foci of increased ^{18}F-FDG uptake in the transplanted liver were concerning for malignancy but were found to be benign inflammatory and ischemic changes including large bile duct necrosis, acute cholangitis, bile duct obstruction changes and periportal fibrosis. In non-transplanted liver, several non-malignant processes have been described to take up ^{18}F-FDG including: intrahepatic cholestasis (8), acute cholangitis (9,10), sclerosing cholangitis (11), liver abscess (12,13), hepatic pseudotumor (14), and hepatic sarcoidosis (15).

Ethics

Informed Consent: All subjects in the study gave written informed consent or the institutional review board waived the need to obtain informed consent.

Peer-review: Externally peer-reviewed.

Authorship Contributions

Surgical and Medical Practices: W.M., A.C., S.P., Concept: W.M., Design: W.M., Data Collection or Processing: W.M., A.C., S.P., Analysis or Interpretation: W.M., A.C., S.P., Literature Search: W.M., A.C., S.P., Writing: W.M.

Conflict of Interest: No conflict of interest was declared by the authors.

Financial Disclosure: The authors declared that this study received no financial support.

References

1. Patkowski W, Nyckowski P, Zieniewicz K, Pawlak J, Michalowicz B, Kotulski M, Smoter P, Grodzicki M, Skwarek A, Ziolkowski J, Oldakowska-Jedynak U, Niewczas M, Paczek L, Krawczyk M. Biliary tract complications following liver transplantation. Transplant Proc 2003;35:2316-2317.
2. Welling TH, Heidt DG, Englesbe MJ, Magee JC, Sung RS, Campbell DA, Punch JD, Pelletier SJ. Biliary complications following liver transplantation in the model for end-stage liver disease era: effect of donor, recipient, and technical factors. Liver Transpl 2008;14:73-80.
3. Foley DP, Fernandez LA, Leverson G, Anderson M, Mezrich J, Sollinger HW, D'Alessandro A. Biliary complications after liver transplantation from donation after cardiac death donors: an analysis of risk factors and long term outcomes from a single center. Ann Surg 2011;253:817-825.
4. McCormack L, Hany TI, Hubner M, Petrowsky H, Mullhaupt B, Knuth A, Stenner F, Clavien PA. How useful is PET/CT imaging in the management of post-transplant lymphoproliferative disease after liver transplantation? Am J Transplant 2006;6:1731-1736.
5. Takehana CS, Twist CJ, Mosci C, Quon A, Mittra E, Iagaru A. 18F-FDG PET/CT in the management of patients with post-transplant lymphoproliferative disorder. Nuc Med Comm 2014;35:276-281.
6. Mocherla B, Kim J, Roayaie S, Kim S, Machac C, Kostakoglu L. FDG PET/CT imaging to rule out extrahepatic metastases before liver transplantation. Clin Nucl Med 2007;32:947-948.
7. Lee SD, Kim SH, Kim YK, Kim C, Kim SK, Han SS, Park SJ. 18F-FDG PET/CT predicts early tumor recurrence in living donor liver transplantation for hepatocellular carcinoma. Transplant Int 2013;26:50-60.
8. Frohlich A, Diederichs CG, Staib L, Vogel J, Beger HG, Reske SN. Detection of liver metastases from pancreatic cancer using FDG PET. J Nucl Med 1999;40:250-255.
9. Bleeker-Rovers CP, Vos FJ, Wanten GJ, van der Meer JW, Corstens FH, Kullberg BJ, Oyen WJ. 18F-FDG PET in detecting metastatic infectious disease. J Nucl Med 2005;46:2014-2019.
10. Kitajima K, Murakami K, Yamasaki E, Domeki Y, Kaji Y, Morita S, Suganuma N, Sugimura K. Performance of integrated FDG-PET/contrast-enhanced CT in the diagnosis of recurrent uterine cancer: comparison with PET and enhanced CT. Eur J Nucl Med Mol Imaging 2009;36:362-372.
11. Kawamura E, Habu D, Higashiyama S, Tsushima H, Shimonishi Y, Nakayama Y, Enomoto M, Kawabe J, Tamori A, Kawada N, Shiomi S. A case of sclerosing cholangitis with autoimmune pancreatitis evaluated by FDG-PET. Ann Nucl Med 2007;21:223-228.
12. Keidar Z, Gurman-Balbir A, Gaitini D, Israel O. Fever of unknown origin: the role of 18F-FDG PET/CT. J Nucl Med 2008;49:1980-1985.
13. Delbeke D, Martin WH, Sandler MP, Chapman WC, Wright JK Jr, Pinson CW. Evaluation of benign vs malignant hepatic lesions with positron emission tomography. Arch Surg 1998;133:510-516.
14. Kawamura E, Habu D, Tsushima H, Torii K, Kawabe J, Ohsawa M, Shiomi S. A case of hepatic inflammatory pseudotumor identified by FDG-PET. Ann Nucl Med 2006;20:321-323.
15. Guglielmi AN, Kim BY, Bybel B, Slifkin N. False-positive uptake of FDG in hepatic sarcoidosis. Clin Nucl Med 2006;31:175.

Interesting Image
Mol Imaging Radionucl Ther 2018;27:41-47 DOI:10.4274/mirt.07088

Primary Thyroid Lymphoma: External Beam Radiation Therapy Induced Thyroiditis Mimics Residual Disease on Serial ^{18}F-FDG PET/CT Imaging

Primer Tiroid Lenfoması: Eksternal Işın Radyasyon Tedavisi ile İndüklenmiş Tiroidit ^{18}F-FDG PET/BT Rezidü Hastalığı Taklit Eder

William Makis[1], *Anthony Ciarallo*[2], *Stephan Probst*[3]

[1]*Cross Cancer Institute, Department of Diagnostic Imaging, Edmonton, Canada*
[2]*McGill University Health Centre, Department of Nuclear Medicine, Montreal, Canada*
[3]*Jewish General Hospital, Department of Nuclear Medicine, Montreal, Canada*

Abstract

A 67-year-old female patient with no prior history of benign thyroid disease was diagnosed with primary thyroid lymphoma and was staged with ^{18}F-fluoro-2-deoxy-D-glucose (^{18}F-FDG) positron emission tomography/computed tomography (PET/CT). She was treated with chemotherapy and external beam radiation therapy, and a follow-up PET/CT showed significant reduction in the size of the thyroid lymphoma with persistent intense ^{18}F-FDG uptake, which was interpreted as partial response to therapy. However, two subsequent PET/CT studies showed no change in the persistent intense ^{18}F-FDG uptake in the thyroid and a biopsy confirmed the presence of thyroiditis with no evidence of residual lymphoma. Follow-up PET/CTs performed over the subsequent three years showed stable intensely ^{18}F-FDG avid thyroiditis with no evidence of lymphoma recurrence. We present the imaging characteristics of a long term radiation treatment induced thyroiditis mimicking ^{18}F-FDG avid residual disease on PET/CT.

Keywords: Thyroid lymphoma, thyroiditis, pitfall, artifact, ^{18}F-FDG, PET

Öz

İyi huylu tiroid hastalığı anamnezi olmayan 67 yaşında bir kadına primer tiroid lenfoması tanısı konularak ^{18}F-florodeoksiglukoz (^{18}F-FDG) pozitron emisyon tomografisi/bilgisayarlı tomografi (PET/BT) ile evreleme yapılmıştı. Kemoterapi ve eksternal radyasyon tedavisi uygulanması sonrası takip PET/BT'de tiroid lenfomasında anlamlı çap küçülmesi saptanarak, devam eden yoğun ^{18}F-FDG tutulumu tedaviye kısmi cevap olarak değerlendirilmişti. Ne var ki, takip eden iki PET/BT'de tiroiddeki persistan yoğun ^{18}F-FDG tutulumu gerilememiş ve biyopside rezidü lenfoma olmaksızın tiroidit bulunmuştu. Takip eden üç yıl boyunca çekilen PET/BT'lerde stabil yoğun ^{18}F-FDG tutan tiroidit, lenfoma nüksü olmaksızın devam etmiştir. Burada PET/BT'de ^{18}F-FDG tutan rezidüel hastalığı taklit eden uzun dönemli radyasyona bağlı tiroidite bağlı görüntüleme özelliklerini sunuyoruz.

Anahtar kelimeler: Tiroid lenfoma, tiroidit, tuzak, artefakt, ^{18}F-FDG, PET

Address for Correspondence: William Makis MD, Cross Cancer Institute, Department of Diagnostic Imaging, Edmonton, Canada
Phone: +90 780 432 87 60 E-mail: makisw79@yahoo.com ORCID ID: orcid.org/0000-0003-0241-3426
Received: 31.12.2016 **Accepted:** 15.10.2017

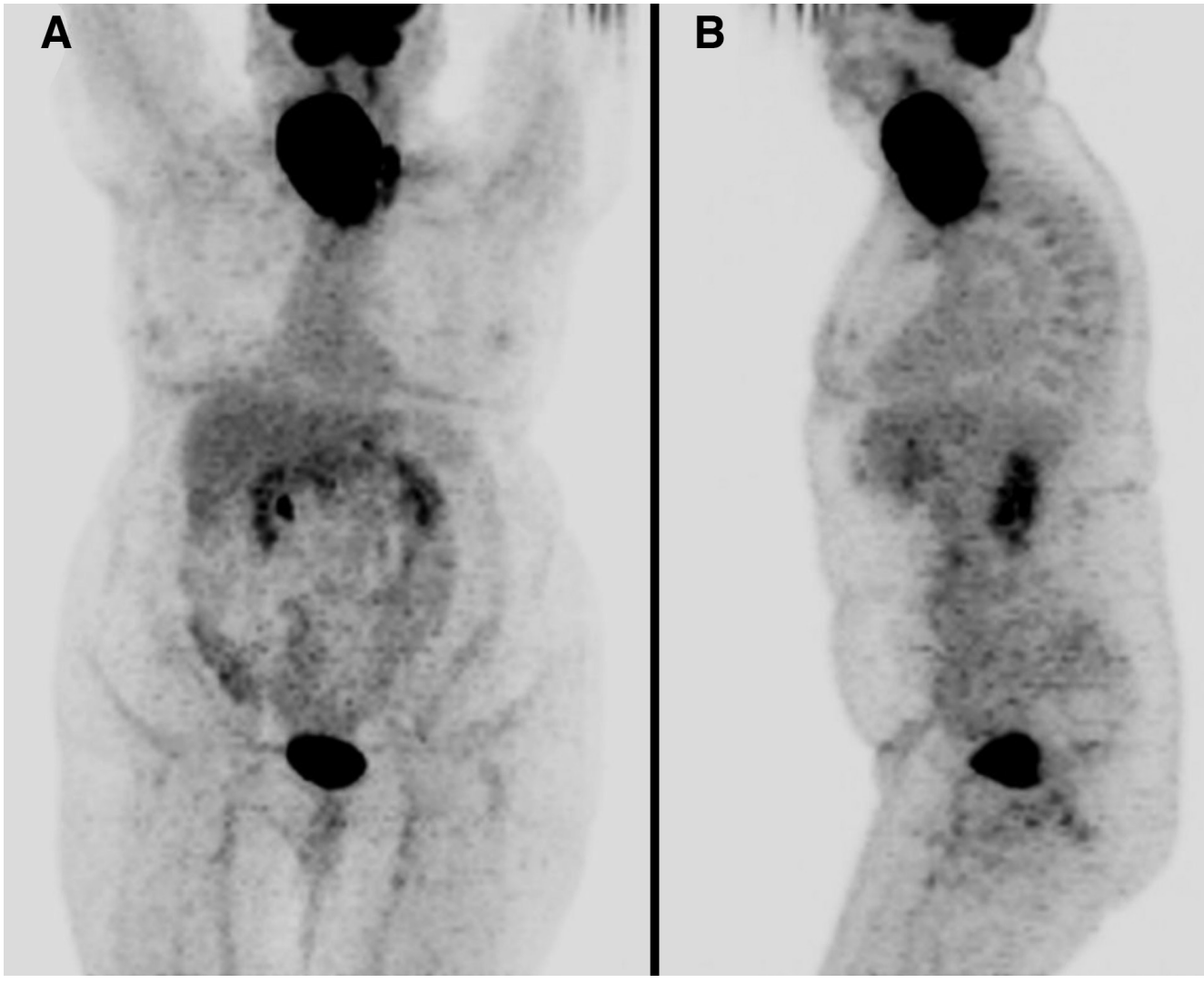

Figure 1. A 67-year-old woman with no prior history of benign thyroid disease presented with a two month history of fevers, night sweats, and rapidly enlarging neck mass. Biopsy of the right thyroid lobe revealed a diffuse large B-cell lymphoma (DLBCL). A staging ^{18}F-fluoro-2-deoxy-D-glucose (^{18}F-FDG) positron emission tomography/computed tomography (PET/CT) (Discovery-ST, GE Healthcare, WI, USA) was performed and maximum intensity projection (MIP) images, (A) anterior and (B) left lateral, showed a large intensely ^{18}F-FDG avid mass in the right neck with no distant metastases.

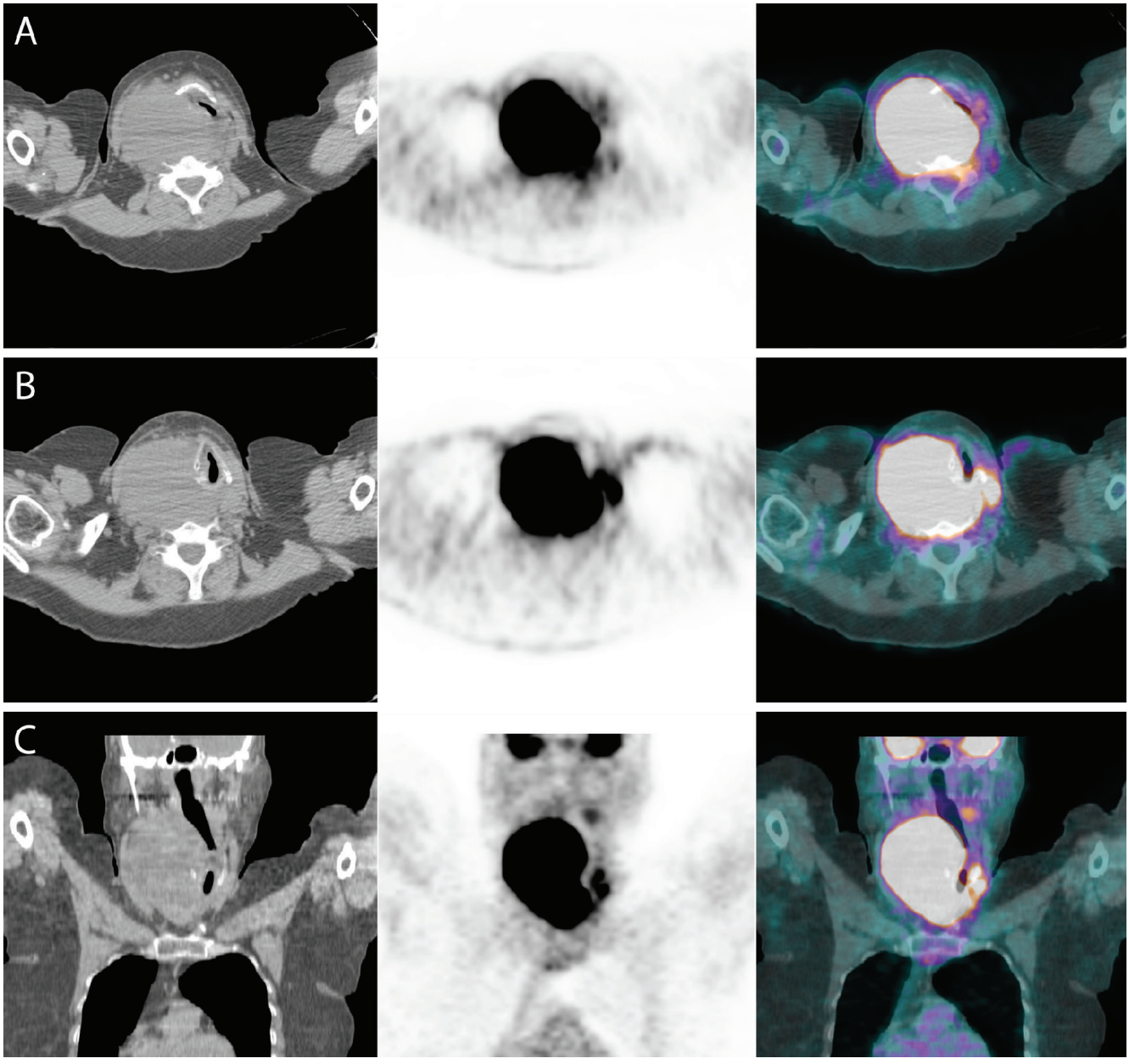

Figure 2. (A, B) Transaxial and (C) coronal views of the neck with CT (left), PET (middle), and PET/CT fusion (right) images show right thyroid DLBCL, measuring 13x9 cm with maximum standardized uptake value (SUV_{max}) 54, compressing the trachea to a narrow slit left of the midline.

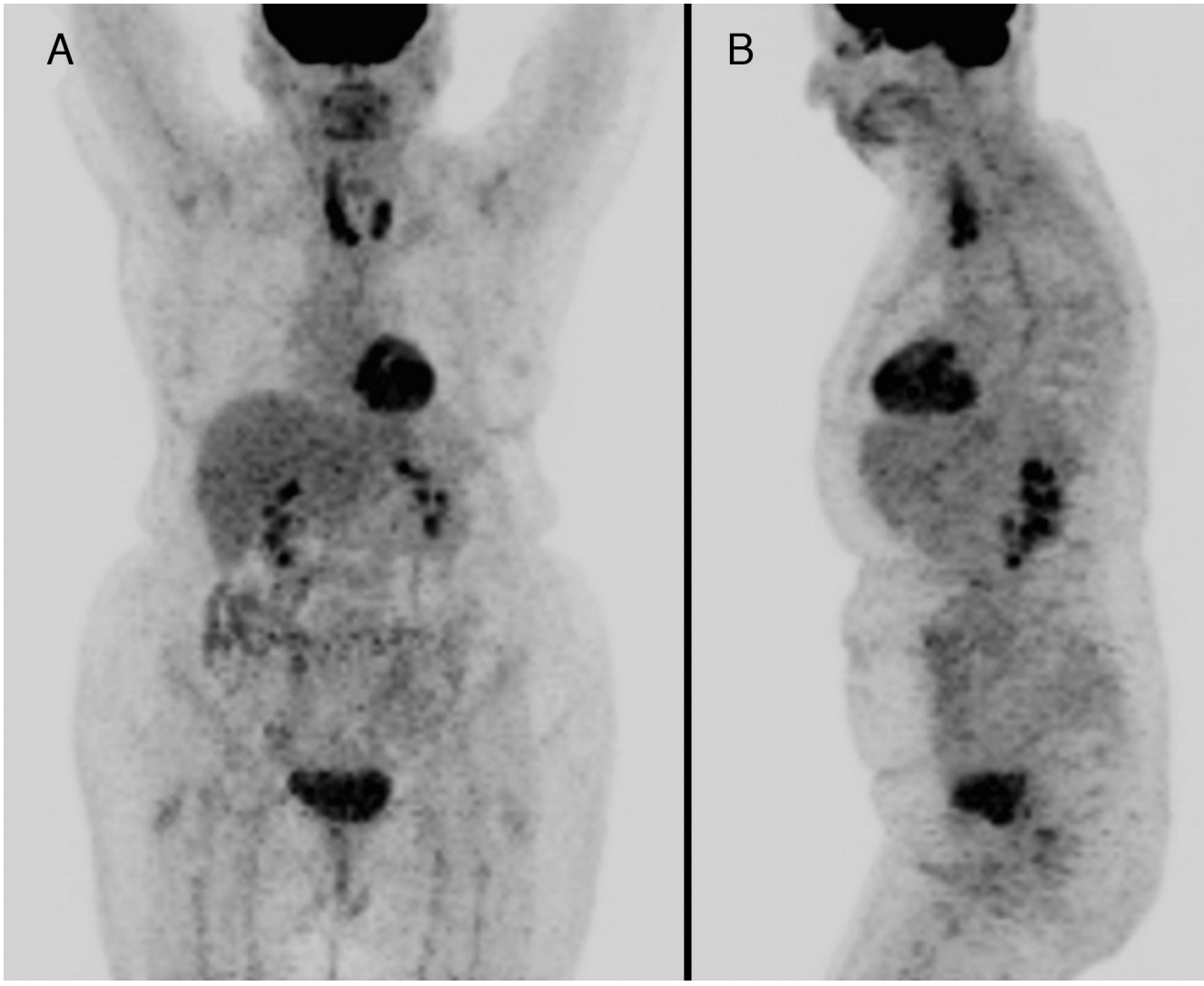

Figure 3. The patient was treated with 3 cycles of CHOP chemotherapy (cyclophosphamide, doxorubicin, vincristine, prednisone) followed by external beam radiation therapy. The first follow-up PET/CT was performed 3 months after the end of radiation therapy and MIP views, (A) anterior and (B) left lateral, show a dramatic reduction in the size of right thyroid DLBCL and resolution of tracheal compression with persistently intense ^{18}F-FDG uptake in both thyroid lobes with SUV_{max} 8.9 on the right. These findings were interpreted as partial response to therapy, however since the patient was asymptomatic, a conservative management approach was taken.

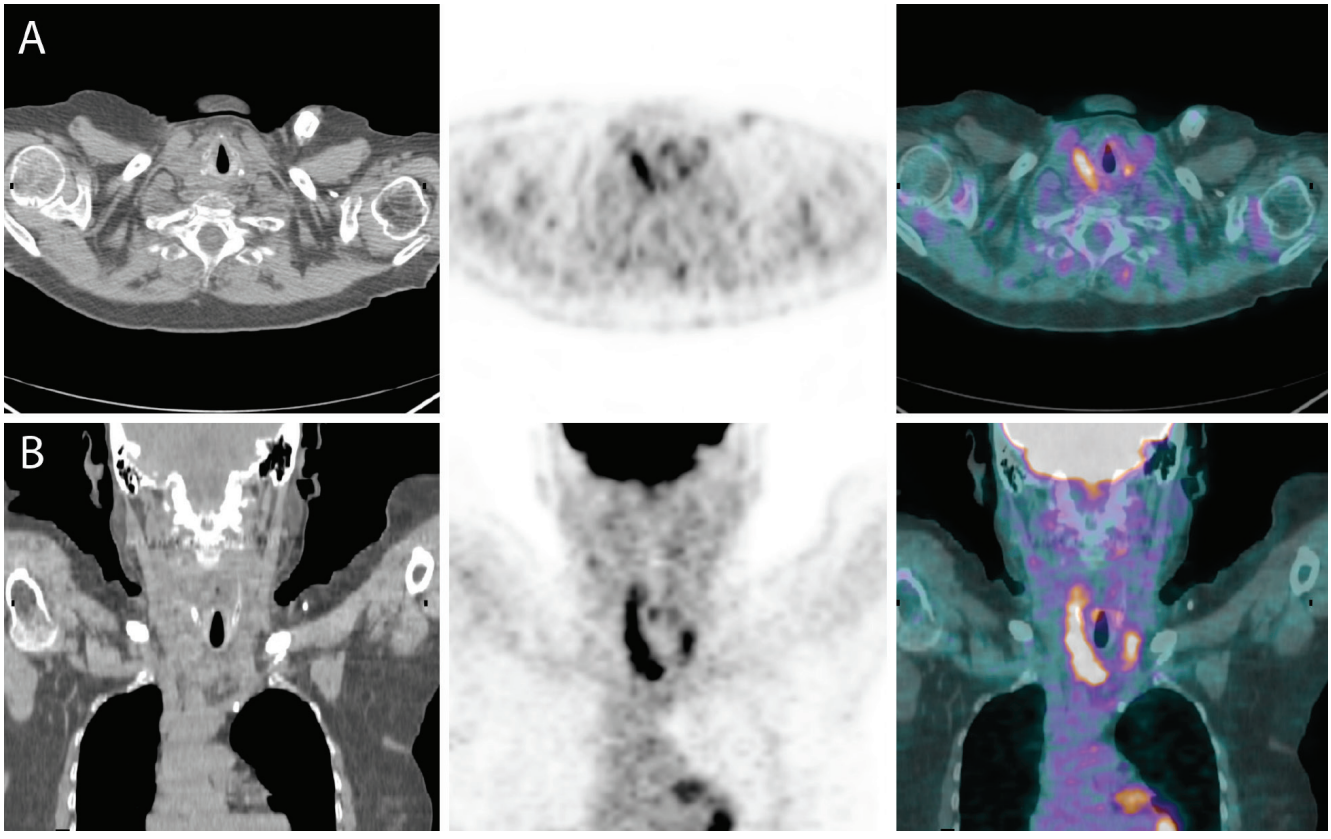

Figure 4. (A) Transaxial and (B) coronal views of the post therapy PET/CT showing apparent partial response to therapy.

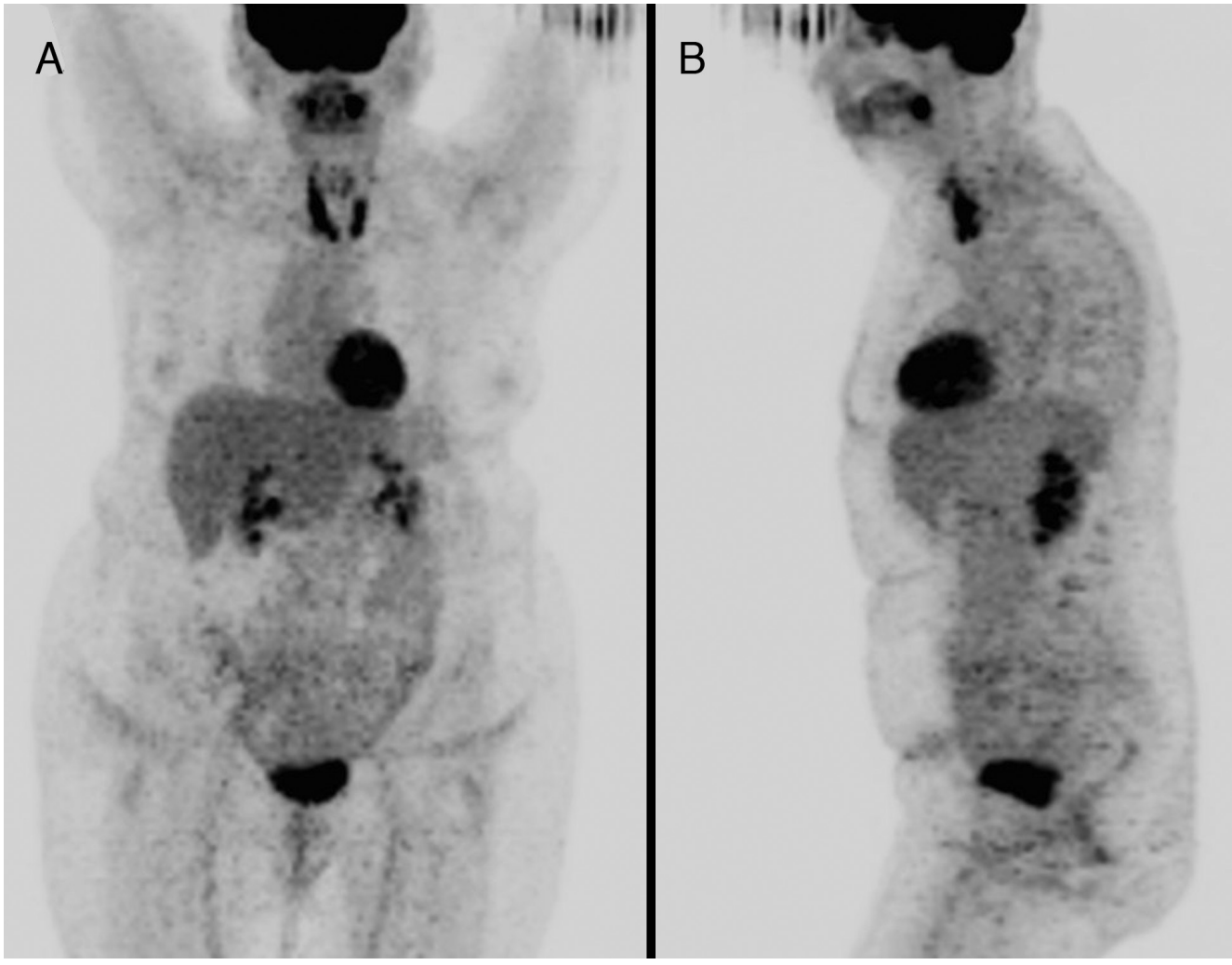

Figure 5. A second follow-up PET/CT was performed one year later. SUV_{max} of right thyroid lobe was 10.2, unchanged according to PET Response Criteria in Solid Tumors (PERCIST 1.0). The pattern of ^{18}F-FDG uptake and distribution in the thyroid gland were also unchanged. Biopsy of both thyroid lobes revealed thyroiditis with no evidence of residual lymphoma. A third follow-up PET/CT was performed 2 years later and SUV_{max} in the right thyroid lobe was 9.5 (unchanged according to PERCIST) with stable pattern of ^{18}F-FDG uptake and distribution, consistent with remission. Primary thyroid lymphoma makes up 1-5% of thyroid malignancies and less than 2% of extranodal lymphomas (1). It is more common in women, and patients present in the seventh decade of life with rapidly enlarging neck mass (1,2,3,4). The use of ^{18}F-FDG PET/CT to stage primary thyroid lymphoma and evaluate response to therapy has been previously reported in the literature (5,6). Recent studies have raised concern about high rate of false positives on PET/CT performed following therapy for thyroid lymphoma, although these have been attributed to Hashimoto's thyroiditis (7,8,9,10,11,12). External beam radiation therapy can produce both inflammatory and proliferative changes in the thyroid gland with increases in macrophage populations (9,10). Studies have shown that ^{18}F-FDG uptake is increased in head and neck soft tissues affected by such inflammatory and proliferative processes and lasts several months after the completion of radiation therapy (11,12). The present case is an example of a long-term post-treatment thyroiditis, which remained intensely ^{18}F-FDG avid but stable on several follow-up PET/CTs spanning three years, which to our knowledge has not been previously reported in the literature.

Ethics

Informed Consent: All subjects in the study gave written informed consent or the institutional review board waived the need to obtain informed consent.

Peer-review: Externally peer-reviewed.

Authorship Contributions

Surgical and Medical Practices: W.M., A.C., S.P., Concept: W.M., Design: W.M., Data Collection or Processing: W.M., A.C., S.P., Analysis or Interpretation: W.M., A.C., S.P., Literature Search: W.M., A.C., S.P., Writing: W.M.

Conflict of Interest: No conflict of interest was declared by the authors.

Financial Disclosure: The authors declared that this study received no financial support.

References

1. Mack LA, Pasieka JL. An evidence-based approach to the treatment of thyroid lymphoma. World J Surg 2007;31:978-986.
2. Graff-Baker A, Roman SA, Thomas DC, Udelsman R, Sosa JA. Prognosis of primary thyroid lymphoma: demographic, clinical and pathologic predictors of survival in 1408 cases. Surgery 2009;146:1105-1115.
3. Graff-Baker A, Sosa JA, Roman SA. Primary thyroid lymphoma: a review of recent developments in diagnosis and histology-driven treatment. Curr Opin Oncol 2010;22:17-22.
4. Onal C, Li YX, Miller RC, Poortmans P, Constantinou N, Weber DC, Atasoy BM, Igdem S, Ozsahin M, Ozyar E. Treatment results and prognostic factors in primary thyroid lymphoma patients: a rare cancer network study. Ann Oncol 2011;22:156-164.
5. Lin EC. FDG PET/CT for assessing therapy response in primary thyroid lymphoma. Clin Nucl Med 2007;32:152-153.
6. Basu S, Li G, Bural G, Alavi A. Fluorodeoxyglucose positron emission tomography (FDG-PET) and PET/Computed tomography imaging characteristics of thyroid lymphoma and their potential clinical utility. Acta Radiol 2009;50:201-204.
7. Nakada K, Kamijo K, Fujimoto N, Sakuma I, Sakurai M. Is FDG PET valuable in monitoring early therapy response in primary thyroid lymphoma? J Nucl Med 2010;51:1611.
8. Kurata S, Ishibashi M, Hiromatsu Y, Kaida H, Miyake I, Uchida M, Hayabuchi N. Diffuse and diffuse-plus-focal uptake in the thyroid gland identified by using FDG-PET: prevalence of thyroid cancer and Hashimoto's thyroiditis. Ann Nucl Med 2007;21:325-330.
9. Hunt JL. Radiation induced thyroid diseases. Pathology Case Reviews 2009;14:224-230.
10. Kubota R, Yamada S, Kubota K, Ishiwata K, Tamahashi N, Ido T. Intratumoral distribution of fluorine-18-fluorodeoxyglucose in vivo: high accumulation in macrophages and granulation tissues studied by microautoradiography. J Nucl Med 1992;33:1972-1980.
11. Yao M, Smith R, Graham MM, Hoffman HT, Tan H, Funk GF, Graham SM, Chang K, Dornfeld KJ, Menda Y, Buatti JM. The role of FDG PET in management of neck metastasis from head-and-neck cancer after definitive radiation treatment. Int J Rad Onc 2005;63:991-999.
12. Andrade RS, Heron DE, Degirmenci B, Filho PA, Branstetter BF, Seethala RR, Ferris RL, Avril N. Posttreatment assessment of response using FDG-PET/CT for patients treated with definitive radiation therapy for head and neck cancers. Int J Rad Onc 2006;65:1315-1322.

Interesting Image
Mol Imaging Radionucl Ther 2018;27:48-51 DOI:10.4274/mirt.25743

Tc-99m MDP Bone SPECT/CT Findings of a Patient Detected with a New Mutation in *LEMD3* Gene: A Case of Osteopoikilosis

LEMD3 Geninde Yeni Mutasyon Saptanan Osteopoikiloz Olgusunda Tc-99m MDP Kemik SPECT/BT Bulguları

Güler Silov[1], *Zeynep Erdoğan*[1], *Murat Erdoğan*[2], *Ayşegül Özdal*[1], *Hümeyra Gençer*[1], *Tayfun Akalın*[3], *Seyhan Karaçavuş*[1]

[1]*University of Health Sciences, Kayseri Training and Research Hospital, Clinic of Nuclear Medicine, Kayseri, Turkey*
[2]*University of Health Sciences, Kayseri Training and Research Hospital, Clinic of Molecular Biology and Genetics, Kayseri, Turkey*
[3]*University of Health Sciences, Kayseri Training and Research Hospital, Clinic of Rheumatology, Kayseri, Turkey*

Abstract

Osteopoikilosis is an inherited condition with autosomal dominant trait resulting in sclerotic foci throughout the skeleton. It has been suggested that loss-of-function mutations of *LEMD3* gene located on 12q14.3 result in osetopoikilosis. A bp heterozygote deletion was detected in our patient at the cytosine nucleotide at position 1105 with molecular genetic analysis. Although this mutation has not been previously described, it was considered to be the most likely cause of the disease in our patient due to frame shift and premature stop codon formation. As in our case, three phase bone scintigraphy and whole body imaging did not reflect the true extent of lesion sites and lesion activity. SPECT/CT images could reflect lesion location and activity more accurately, and could be a good alternative for differential diagnosis of unexplained bone pain and sclerotic lesions in one examination.

Keywords: *LEMD3* gene, osteopoikilosis, Tc-99m MDP, SPECT/CT

Öz

Osteopoikiloz kemik doku boyunca kemik adacıkları ile karakterize, otozomal dominant geçiş gösteren herediter bir hastalıktır. Mevcut literatürde, 12q14.3 üzerinde bulunan *LEMD3* genindeki mutasyonların sebep olduğu gösterilmiştir. Hastamızda yapılan moleküler genetik analizde 'Yeni Nesil Dizi Analizi' 1105. pozisyondaki sitozin nükleotidinde bir bp'lik heterozigot delesyon tespit edilmiştir. Bu mutasyon, daha önceden literatürde tanımlanmamış olmakla birlikte; çerçeve kaymasına neden olması ve erken stop kodon oluşturması sebebiyle yüksek olasılıkla hastalık nedeni olarak değerlendirilmiştir. Ancak üç fazlı kemik sintigrafisi ve tüm vücut taraması, bu olguda olduğu gibi gerçek lezyon sayısı ve lezyon aktivitesini yansıtmamaktadır. SPECT/BT görüntüleme bu açıdan iyi bir seçim olarak görülmektedir.

Anahtar kelimeler: *LEMD3* geni, osteopoikiloz, Tc-99m MDP, SPECT/BT

Address for Correspondence: Güler Silov MD, University of Health Sciences, Kayseri Training and Research Hospital, Clinic of Nuclear Medicine, Kayseri, Turkey
Phone: +90 352 336 88 84 E-mail: gulersilov@yahoo.com ORCID ID: orcid.org/0000-0002-4658-8634
Received: 09.06.2017 **Accepted:** 15.10.2017

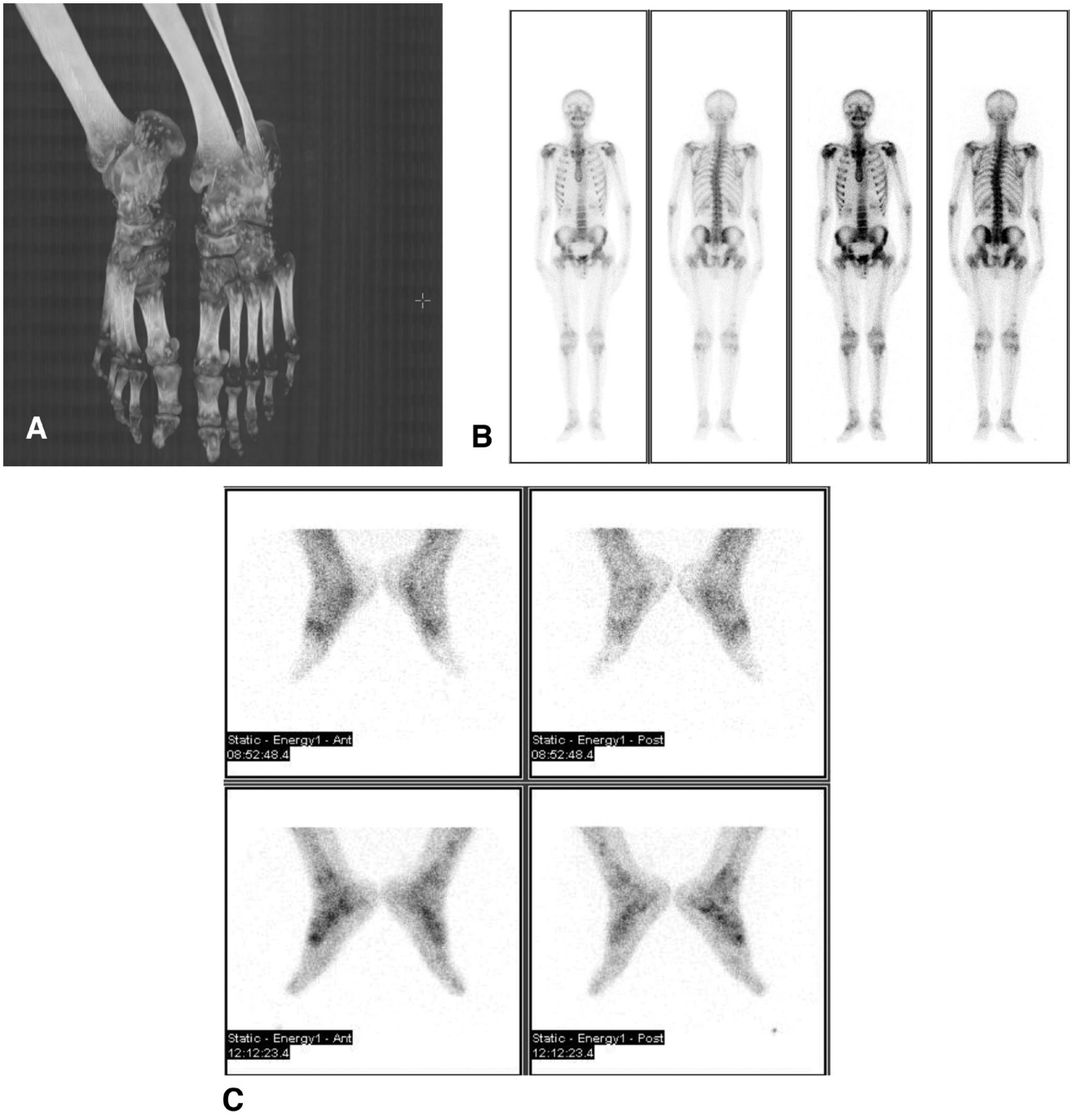

Figure 1. A 20-year-old man was referred to our department with right foot pain. The plain X-ray showed numerous small lesions distributed along the feet (A). A three phase Tc-99m methylene diphosphonate (MDP) bone scan of the foot, whole body scanning along with feet and pelvic-thoracic SPECT/CT were performed. Whole body images showed relative irregularly increased focal MDP uptake on the long bones and pelvic region (B). The late phase static images of feet irregularly increased focal MDP uptake (C).

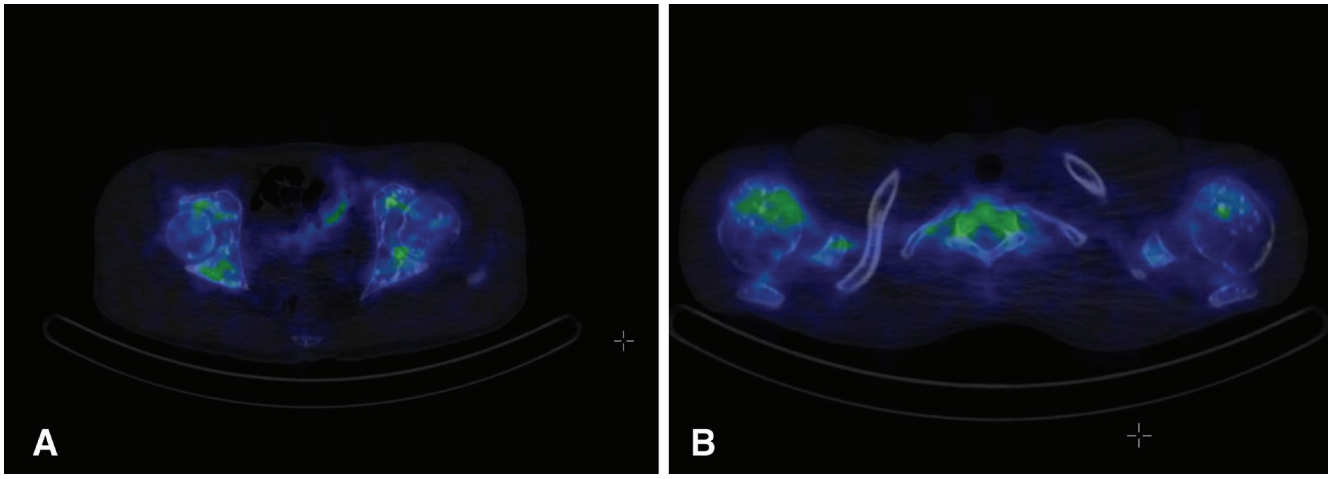

Figure 2. Multiple, sclerotic lesions were detected in thoracic bones, shoulders, and both femur and pelvic bones by CT but radiotracer uptake was observed in some sclerotic lesions on SPECT-CT images (A, B). Laboratory tests were within normal limits except a slightly elevated alkaline phosphatase value of 126 U/L (range: 30-120 U/L).

Osteopoikilosis is an inherited condition with autosomal dominant trait that results in numerous sclerotic foci throughout the skeleton (1). Previous studies have reported that these lesions are symmetric but randomly distributed, with increased concentrations at the carpal and tarsal bones, as well as at the ends of the long bones (2,3). Lesions are reported to be located less in the skull, rib, vertebra, and mandible (1).

Recently, whole-genome linkage analysis of affected individuals resulted in identification of a loss-of-function mutation in gene *LEMD3* at position 12q14.3. *LEMD3* is believed to function in bone morphogenetic protein (BMP) signaling by interacting with the family of SMAD proteins downstream from transforming growth factor-beta (TGF-beta) to regulate bone formation (4,5). It has been reported that *LEMD3* can antagonize both BMP and TGF-beta signaling in human cells (6). Molecular genetic analysis was performed in our patient, and a bp heterozygote deletion was detected in the cytosine nucleotide at position 1105. This mutation has not been previously described in the literature, but is considered to be the most likely cause of the disease due to frame shift and premature stop codon formation.

Histologically, the sclerotic foci correspond to old and inactive remodeling of spongiform lamellar trabeculae with a gross nodular or star-like appearance (7). Sclerotic lesions are classically inactive on whole body scintigraphy (8,9). For this reason, a Tc-99m bone scan is sufficiently diagnostic and usually returns to normal in cases of osteopoikilosis. There have been a few cases reported in the literature of abnormal bone scans in patients with osteopoikilosis (10). In such cases, the pattern of increased uptake is usually symmetric and localized to the distal ends of tubular, carpal, and tarsal bones. This may correspond to active bone remodeling of these multiple foci, which has also been reported in pathologic specimens of osteopoikilosis. As in our patient, localized three phase bone scintigraphy and whole body scanning did not reflect the true extent of lesion site and activity. However, SPECT/CT images could reflect lesion location and activity more accurately, and could be a good alternative for differential diagnosis of unexplained bone pain and sclerotic lesions in one examination.

Ethics

Informed Consent: Consent form was filled out by all participants.

Peer-review: Externally peer-reviewed.

Authorship Contributions

Surgical and Medical Practices: G.S., M.E., T.A., Concept: G.S., Z.E., Design: G.S., A.Ö., Data Collection or Processing: G.S., M.E., T.A., Analysis or Interpretation: G.S., H.G., S.K., Literature Search: G.S., Writing: G.S.

Conflict of Interest: No conflict of interest was declared by the authors.

Financial Disclosure: The authors declared that this study received no financial support.

References

1. Benli IT, Akalin S, Boysan E, Mumcu EF, Kiş M, Türkoğlu D. Epidemiological, clinical and radiological aspects of osteopoikilosis. J Bone Joint Surg Br 1992;74:504-506.
2. Van Hul, Vanhoenacker F, Balemans W, Janssens K, De Schepper AM. Molecular and radiological diagnosis of sclerosing bone dysplasias. Eur J Radiol 2001;40:198-207.
3. Ben-Asher E, Zelzer E, Lancet D. LEMD3: the gene responsible for bone density disorders (osteopoikilosis). Isr Med Assoc J 2005;7:273-274.
4. Korman B, Wei J, Laumann A, Ferguson P, Varga J. Mutation in LEMD3 (Man1) Associated with Osteopoikilosis and Late-Onset Generalized Morphea: A New Buschke-Ollendorf Syndrome Variant. Case Rep Dermatol Med 2016;2016:2483041.
5. Ito Y, Miyazono K. RUNX transcription factors as key targets of TGF-β superfamily signaling. Curr Opin Genet Dev 2003;13:43-47.
6. Pan D, Estevez-Salmeron LD, Stroschein SL, Zhu X, He J, Zhou S, Luo K. The integral inner nuclear membrane protein MAN1 physically interacts with the R-Smad proteins to repress signaling by the transforming growth factor-β superfamily of cytokines. J Biol Chem 2005;280:15992-6001.
7. Lagier R, Mbakop A, Bigler A. Osteopoikilosis: a radiological and pathological study. Skeletal Radiol 1984;11:161-168.
8. de Vernejoul MC, Kornak U. Heritable sclerosing bone disorders: presentation and new molecular mechanisms. Ann N Y Acad Sci 2010;1192:269-277.
9. Tsai SY, Wang SY, Shiau YC, Wu YW. Benign incidental findings of osteopoikilosis on Tc-99m MDP bone SPECT/CT: A case report and literature review. Medicine (Baltimore) 2016;95:e3868.
10. An YS, Yoon JK, Lee MH, Joh CW, Yoon SN. Abnormal bone scan in an adult with osteopoikilosis. Clin Nucl Med 2004;29:856-858.

Interesting Image
Mol Imaging Radionucl Ther 2018;27:52-54 DOI:10.4274/mirt.77044

Inguinal Endometriosis Visualized on I-131 Whole Body Scan

I-131 Tüm Vücut Taramada İnguinal Endometriozis Görünümü

Derya Çayır[1], Mine Araz[1], Mahmut Apaydın[2], Erman Çakal[2]
[1]*University of Health Sciences, Dışkapı Yıldırım Beyazıt Training and Research Hospital, Clinic of Nuclear Medicine, Ankara, Turkey*
[2]*University of Health Sciences, Dışkapı Yıldırım Beyazıt Training and Research Hospital, Clinic of Endocrinology and Metabolism, Ankara, Turkey*

Abstract

We present a rare case with inguinal iodine-131 (I-131) uptake on whole body scan. The patient was suffering from a painful right inguinal mass during menstrual period, which was later sonographically and histopathologically confirmed to be an inguinal focus of endometriosis. Endometriosis is a previously reported site of radioiodine uptake and detection of radioiodine uptake in the inguinal region has also been described. Nevertheless, to the best of our knowledge, this is the first case report of I-131 uptake in an inguinal endometriosis focus. History and physical examination of the patient are both very important in identifying the etiology of the ectopic uptake sites on I-131 whole body scan, and inguinal endometriosis should be kept in mind while reporting inguinal radioiodine uptake on I-131 whole body scan.
Keywords: Endometriosis, whole body imaging, iodine-131

Öz

Bu raporda iyot-131 (I-131) tüm vücut taramada inguinal bölgede tutulum saptanan nadir bir olguyu sunuyoruz. Menstrüel siklus sırasında ağrılı inguinal kitle şikayeti olan hastada, kitlenin daha sonra sonografik ve histopatolojik olarak inguinal endometriozis odağına ait olduğu konfirme edildi. Endometrioziste radyoaktif iyot tutulumu ve inguinal bölgede radyoaktif iyot tutulumunun saptanması daha önce bildirilmiştir; ancak inguinal endometriozis odağında I-131 tutulumu, bildiğimiz kadarıyla, ilk kez bu olguda sunulmaktadır. I-131 tüm vücut taramada ektopik tutulum alanlarının etiyolojisinin çözülmesinde hasta öyküsü ve fizik muayene çok önemli olup, I-131 tüm vücut taramada inguinal bölgede radyoaktif iyot tutulumu raporlanırken inguinal endometriozis de akılda bulundurulmalıdır.
Anahtar kelimeler: Endometriozis, tüm vücut görüntüleme, iyot-131

Address for Correspondence: Derya Çayır MD, University of Health Sciences, Dışkapı Yıldırım Beyazıt Training and Research Hospital, Clinic of Nuclear Medicine, Ankara, Turkey
Phone: +90 535 568 10 66 E-mail: drderyaors@hotmail.com ORCID ID: orcid.org/0000-0002-7756-3210
Received: 27.04.2017 **Accepted:** 15.10.2017

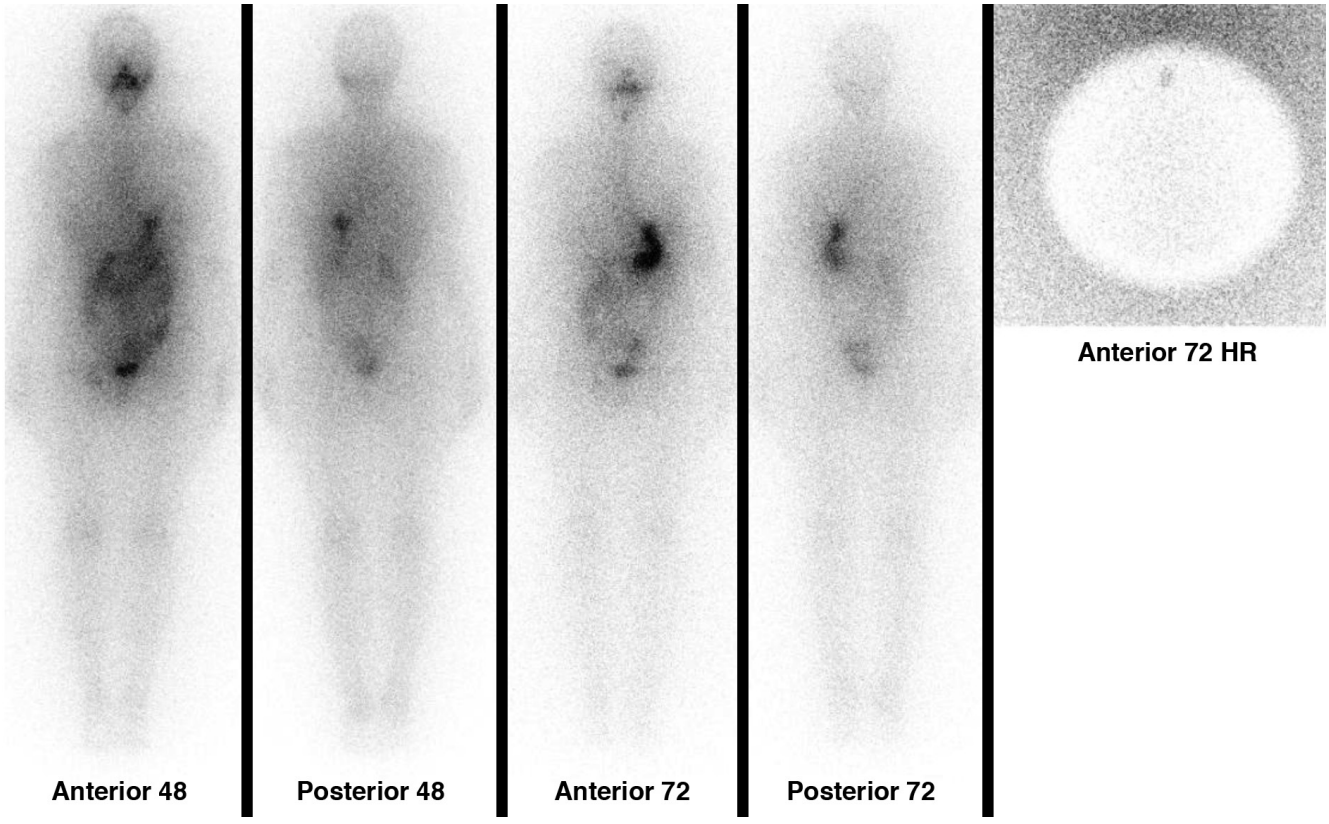

Figure 1. A 35-year-old woman with papillary thyroid carcinoma who had received 50 mCi iodine-131 (I-131) following total thyroidectomy underwent an I-131 whole body scan one year later. While serum levels of thyrotrophin-stimulating hormone was 92.22 mIU/L, thyroglobulin and anti-thyroglobulin antibody levels were 4.61 ng/mL and <0.9 IU/mL, respectively. I-131 whole body images were obtained by using a large field-of-view gamma camera (Siemens e.cam-signature; Siemens, Hoffmann Estates, Illinois, United States of America) in a 256x1024 matrix using a high energy parallel hole collimator and pinhole collimator at 48 and 72 hours. Images showed focal I-131 accumulation on the neck, located in the midline, along with I-131 uptake in the right inguinal region and the suprapubic area (Figure 1). The focal uptake on the neck was interpreted as residual thyroid tissue on the thyroglossal duct, and the suprapubic non-homogenous activity was attributed to uterine activity due to menstrual bleeding. The etiology of the right inguinal uptake was revealed with further evaluation. The patient was also suffering from groin pain during the menstrual period along with a right inguinal mass that enlarged at the same time. Right inguinal superficial ultrasound revealed a hypoechoic solid mass of 25x15 mm located in the neighborhood of femoral artery and multiple accompanying reactive lymph nodes with the largest dimensions measuring 43x8 mm. The Tru-Cut biopsy of the right inguinal palpable mass was performed that revealed endometriosis. Thyroglobulin elevation in our patient was associated with neck uptake and distant metastasis was excluded. Treatment was planned accordingly.

Endometriosis is the existence of endometrium, the layer surrounding the uterine cavity, anywhere in the body other than the uterus. It is mostly located in the intrapelvic region (1). Inguinal (non-cutaneous) endometriosis is a rare presentation of endometriosis, occurring in only 0.6% of women (1,2). Inguinal endometriosis was first reported by Allen in 1896 (3,4,5). Patients with inguinal endometriosis complain of inguinal mass and pain, in particular, acute pain during menstrual cycles (2,6). The mechanism of iodine uptake in endometriosis is not yet clear, and iodine uptake in inguinal endometriosis has not been previously described in the literature. In our case, the scanning was performed during the patient's menstrual cycle. An increase in blood flow to the inguinal endometriosis or presence of inflammation in this area might be the reasons for increased radioiodine uptake. Hyperemia, vasodilation, local edema, and increased capillary permeability may cause increased radioiodine uptake in inflamed areas (7,8). In our case, there were multiple reactive lymph nodes around the inguinal mass. Both increased blood flow and reactive lymph nodes could have led to an increased activity. In conclusion, although it is a well-established technique, one may still confront with unexpected findings on I-131 whole body scan. While reporting radioiodine uptake in the inguinal region, endometriosis should be kept in mind as a rare etiology and the patient should be further evaluated accordingly.

Focal I-131 accumulation on the neck, located in the midline, is detected along with radioiodine uptake in the right inguinal region on I-131 whole body images.

Ethics

Informed Consent: Consent form was filled out by all participants.

Peer-review: Externally peer-reviewed.

Authorship Contributions

Surgical and Medical Practices: D.Ç., M.A., M.A., E.Ç., Concept: D.Ç., Design: D.Ç., M.A., Data Collection or Processing: D.Ç., M.A., Analysis or Interpretation: D.Ç., M.A., Literature Search: D.Ç., Writing: D.Ç.

Conflict of Interest: No conflict of interest was declared by the authors.

Financial Disclosure: The authors declared that this study received no financial support.

References

1. D'Hooghe TM, Hill JA. Endometriosis. In: Berek SJ, Adashi EY, Hillard PA, eds. Novak's Gynecology, 12th ed. Baltimore: Williams&Wilkins;1996;887-915.
2. Bergqvist A. Extragenital endometriosis. Eur J Surg 1992;158:7-12.
3. Tarım E, Bağış T, Tarım A, Kıllıcıdağ EB, Noyan T, Kayaselçuk F. İnguinal endometriozis: bir olgu sunumu. Türkiye Klinikleri J Gynecol Obst 2002;12:184-185.
4. Dwivedi AJ, Agrawal SN, Silva YJ. Abdominal wall endometriomas. Dig Dis Sci 2002;47:456-461.
5. Blanco RG, Parithivel VS, Shah AK, Gumbs MA, Schein M, Gerst PH. Abdominal wall endometriomas. Am J Surg 2003;185:596-598.
6. Kaushik R, Gulati A. Inguinal endometriosis: A case report. J Cytol 2008;25:73-75.
7. Garger YB, Winfeld M, Friedman K, Blum M. In thyroidectomized thyroid cancer patients, false-positive I-131 whole body scans are often caused by inflammation rather than thyroid cancer. J Investig Med High Impact Case Rep 2016;4:2324709616633715.
8. Hannoush ZC, Palacios JD, Kuker RA, Casula S. False Positive Findings on I-131 WBS and SPECT/CT in Patients with History of Thyroid Cancer: Case Series. Case Rep Endocrinol 2017;2017:8568347.